FACULTY OF TECHNOLOGY

Defining hydraulic connections in OL-KR6 area at Olkiluoto by means of interference test and suggestions to the hydrogeological modelling of the area

Jani Junnila

DEGREE PROGRAMME OF GEOSCIENCES

Master of Science thesis

December 2019

FACULTY OF TECHNOLOGY

Defining hydraulic connections in OL-KR6 area at Olkiluoto by means of interference test and suggestions to the hydrogeological modelling of the area

Jani Junnila

Supervisors: Aro, Susanna

Sarala, Pertti

DEGREE PROGRAMME OF GEOSCIENCES

Master of Science thesis

December 2019

TIIVISTELMÄ
OPINNÄYTETYÖSTÄ Oulun yliopisto Teknillinen tiedekunta

Koulutusohjelma (kandidaatintyö, diplomityö) Geotieteiden koulutusohjelma.	Pääaineopintojen ala (lisensiaatintyö)
Tekijä Junnila, Jani	Työn ohjaaja yliopistolla Sarala, P., professori

Työn nimi
Hydraulisten yhteyksien määritys vuorovaikutuskokeen avulla OL-KR6:n alueella Olkiluodossa ja kehitysehdotukset alueen hydrogeologista mallinnusta varten

Opintosuunta	Työn laji	Aika	Sivumäärä
Geotieteiden ko.	Pro Gradu	Joulukuu 2019	117 s. 4 liitettä

Tiivistelmä

Posiva Oy vastaa omistajiensa TVO:n ja Fortumin käytetyn ydinpolttoaineen loppusijoituksesta. Loppusijoitus tullaan toteuttamaan Olkiluodon saarella Eurajoen kunnassa. Työn tavoitteena oli varmentaa Olkiluodon saaren pohjoisosan hydrogeologista mallia vuorovaikutuskokeen avulla. Alueen nykyinen hydrogeologinen malli ei täysin selitä alueella toteutetun OL-KR6:n pitkäaikaispumppauskokeen havaintoja. Työn aikana laadittiin suunnitelma vuorovaikutuskokeesta, jonka tavoitteena oli varmentaa alueen hydrogeologisia yhteyksiä.

Työssä käytettiin erityisesti tätä vuorovaikutuskoetta varten suunniteltua laitteistoa, jossa hyödynnettiin aiemmissa pumppauskokeissa käytettyä kalustoa, sekä osia Posiva Flow Log (PFL) -laitteistosta. Mahdollisia hydraulisia vasteita tarkkailtiin ympäröivien kairareikien painekorkeusdatasta. Lisäksi vuorovaikutuskoetta varten asennettiin uusi painekorkeuden automaattinen seurantapiste eritasopietsometri OL-EP4:lle.

Työssä myös raportoitiin osa OL-KR6:n pitkäaikaispumppauskokeen tuloksista vuosilta 2013–2019. Osa tätä opinnäytetyötä oli olla mukana kenttätöissä ja laitteistoasennuksissa vuorovaikutuskokeen aikana. Painevasteiden analysointi vuorovaikutuskokeen aikana toteutettiin matemaattisesti Posivan aiemmin hyödyntämällä tavalla.

Tärkein työstä saatu tulos oli, että Olkiluodon kallioperän yläosissa, ainakin pohjoisosissa saarta, esiintyy laaja-alaista horisontaalisuuntaista rakoilua. Viitteitä tällaisesta laajasta horisontaalisesta rakoilusta kallioperän yläosissa on jo aiemminkin saatu, mutta tämä opinnäytetyö vahvistaa aiempia tuloksia ja toimii yhtenä uutena merkittävänä lähtötietona Olkiluodon tuleville paikkamalliversioille.

Työn perusteella pohjaveden painekorkeuden luonnollisia korjauskertoimia voidaan mahdollisesti tarkastella uudelleen, sekä voidaan tarkentaa esimerkiksi louheen läjitysalueen ja Korvensuon altaan vaikutuksia Olkiluodon pohjavesisysteemiin. Toisaalta hypoteesia Olkiluodon kallioperän yläosan vaakarakoilun suhteen voidaan todentaa myös Olkiluodon muiden tektonisten vyöhykkeiden alueella toteutettavilla pumppaus- ja vuorovaikutuskokeilla.

Tulevaisuudessa tätä hypoteesia voidaan hyödyntää hydrogeologisessa ja hydrogeokemiallisessa mallinnuksessa. Työn tuloksia voidaan mahdollisesti hyödyntää myös ydinjätteen loppusijoituksen tulevissa turvallisuusperusteluissa. Osaltaan tuloksia voidaan hyödyntää myös myöhemmin, kun pyritään mallintamaan Olkiluodon hydrogeologisten ja hydrogeokemiallisten ominaisuuksien palautumista loppusijoitustilojen sulkemisen jälkeen.

Muita tietoja

ABSTRACT
FOR THESIS

University of Oulu Faculty of Technology

Degree Programme (Bachelor's Thesis, Master's Thesis)	Major Subject (Licentiate Thesis)
Master's Thesis	
Author	**Thesis Supervisor**
Junnila, Jani	Sarala, P., Professor

Title of Thesis

Defining hydraulic connections in OL-KR6 area at Olkiluoto by means of interference test and suggestions to the hydrogeological modelling of the area

Major Subject	Type of Thesis	Submission Date	Number of Pages
Geology	Master's	December 2019	117 p. 4 app.

Abstract

Posiva is responsible for the disposal of spent nuclear fuel of its' owners TVO and Fortum. Final disposal will be carried out at Olkiluoto in Eurajoki. The object of this thesis was to verify the hydraulic connections on the northern parts of the Olkiluoto Island by means of an interference test. The current hydrogeological model of Olkiluoto is not able to explain all of the observations gathered during the long-term pumping test in OL-KR6. During this thesis, an interference test was planned to verify the hydraulic connections in the area.

The equipment used in the interference test was especially designed for this purpose. The equipment incorporated old components from earlier pumping tests together with some components from the Posiva Flow Log (PFL) equipment. Hydraulic responses were observed from the hydraulic head data of the surrounding drillholes. In addition to aforementioned observations, an automatic hydraulic head monitoring system was installed in multilevel piezometer OL-EP4.

Some results gathered from the long-term pumping test on OL-KR6 between 2013 and 2019 were also presented and discussed in this thesis. Part of the thesis was being involved in the field work on the installations during an interference test. Observations of hydraulic responses were anlysed with mathematical methods. These methods have also been used in earlier evaluations of Olkiluoto data by Posiva.

The most remarkable result gathered from this thesis was the hypothesis of a horizontal fracturing at the upper parts of the bedrock, at least on the northern parts of the Olkiluoto Island. Some indications of this kind of horizontal fracturing have also been observed earlier. This thesis verifies these observations.

Based on this thesis, some natural fluctuation corrections could be reviewed. The thesis could also offer some help in the estimation of the effects on the groundwater system caused by Korvensuo reservoir and the rock crushing area. On the other hand, the hypothesis of the horizontal fracture network can be verified in the future in the other tectonic areas on Olkiluoto by means of pumping and interference tests.

In the future, the results of this thesis can be utilised in the hydrogeological and hydrogeochemical modelling. They could also be utilised in future safety assessments of the disposal of nuclear waste, and in modelling the recovery of Olkiluoto's groundwater system to a natural state after the final disposal project has ended and the open volumes in bedrock are closed.

Additional Information

FOREWORD

This thesis was commissioned by Posiva Oy and was done between December 2018 and December 2019. Thesis was funded by Posiva Oy. The purpose of this thesis was to plan an interference test for the drillhole OL-KR6 at Olkiluoto. Based on the results of an interference test the thesis was supposed to give suggestions for the update of the hydrogeological model of the area. Research manager Susanna Aro from Posiva and Professor Pertti Sarala from university of Oulu were supervisors of this thesis. During the project some help was received from other experts from Posiva and hydrogeological experts from Pöyry.

I would like to thank Posiva, especially Susanna Aro for this possibility to do Master's Thesis to Posiva. As for I would like to thank Petri Heikkinen, Jere Komulainen and Aimo Hiironen who made this Thesis possible from technical perspective.

I also received a lot of help from Jere Lahdenperä from Posiva and from Pauliina Aalto and Tiina Vaittinen from Pöyry during the project and therefore I would like to express my gratitute to them. I would also like to thank the PRA-unit from Posiva who helped in the field during the project.

I would also like to thank my parents who have supported my studies throughout the years. I am grateful also for my friends and girlfriend who have been supporting me during this project.

Rauma, 1.12.2019 Jani Junnila

TABLE OF CONTENTS

Appendix 4. GWMS-data from surrounding drillholes of OL-KR6

ABBREVIATIONS

ρ	density of the water
δS	groundwater storage
$\frac{dh}{ds}$	hydraulic gradient
A	cross-sectional area
a	cylindrical flow parameter
ET	evapotranspiration (combined evaporation and transpiration)
G_R	groundwater discharge
g	acceleration of gravity
h	hydraulic head
h_1	hydraulic head far from drillhole
h1, h2	water levels
h_2	hydraulic head in the drillhole
h_p	pressure head
h_{pfl}	hydraulic head (masl)
h_s	hydraulic head of the section far from the drillhole.
K	hydraulic conductivity
K_s	hydraulic conductivity in the s direction
l	distance
P	precipitation
p	pressure water column
p_{abs}	absolute pressure
p_b	atmospheric pressure
Q	flow
Q_{f0}	fracture flow rate
Q_n	fracture flow rate
Q_s	discharge in the s direction
Q_{s2}	predicted flow
q	volumetric flow rate per unit surface area
R	radius of influence
r_0	radius of the drillhole

S_R	runoff
T_{PFL}	transmissivity based on PFL measurements
z	elevation head
Cl	chloride
CTU	central tectonic unit
DIC	dissolved inorganic carbon
DFN	discrete fracture network -model
EC	electrical conductivity
Eh	redox-potential
FDZ	Flutanperä deformation zone
GWMS	groundwater monitoring system
HCO_3	bicarbonate
LDZ	Liikla deformation zone
m.a.s.l	meters above sea level
NTU	northern tectonic unit
^{18}O	oxygen isotope
O_2	oxygen
OL-BFZ	brittle deformation zone
OL-DI	ditch
OL-EP	multilevel piezometer
HZ	hydrogeological zone (site-scale)
HZL	hydrogeological zone (repository-scale)
OL-KR	drillhole
OL-KRB	shorter drillhole for investigation of the upperparts of the bedrock
OL-PP	shallow core drilled hole in bedrock
OL-PVP	groundwater observation tube in overburden
ONKALO®	underground research facility
PAVE	pressurised water sampling equipment
PFL	Posiva flow logging device
PFL DIFF	PFL flow difference measurement
PFL DOPP	PFL double packer pressure probe
POTTI	Posiva's database
SDZ	southern deformation zone

S^{2-}	sulphide
SO_4	sulphate
STU	southern tectonic unit
TDS	total dissolved solids

1 INTRODUCTION

Posiva Oy is responsible for research and development activities related to the final disposal of the spent nuclear fuel of its owners, TVO (Teollisuuden Voima) Plc and Fortum Power and Heat Plc on Olkiluoto in Eurajoki. Posiva Oy was established in 1995. Site investigations related to the final disposal have been carried out on Olkiluoto since the 1980s.

OL-KR6 is a 601-meter-long drillhole located in the northern parts of the Olkiluoto Island. A long-term pumping test took place between 2001 and 2019. During this test, the groundwater quality in the area was monitored both by in-situ measurements and by taking groundwater samples for chemical analysis. Flow measurements have also been performed on a regular basis with the PFL (Posiva Flow Log) device. Posiva has been developing the hydrogeological model of the area based on this groundwater data.

The aim of this long-term pumping test has been to monitor the effects of a long-term pumping on the groundwater environment. This knowledge helps to understand the effects caused by the construction of the ONKALO® underground research facility and the spent nuclear fuel repository.

The hydrogeochemistry results of the OL-KR6, which were discovered during the long-term pumping test were related to the dilution of salinity of the groundwater. This was observed especially in the brackish water zone. Also, the sulphate concentration has decreased over the years.

During the long-term pumping test, it was discovered that some of the observed phenomena cannot be explained by the current hydrogeological model:

- HZ21 intersection on OL-KR6; modelled responses were not seen on the field data
- Possible connection to HZ20A system from the depth of 59 m from OL-KR6
- Continuation of HZL4 towards OL-KR42
- HZ099 intersection in OL-KR6 ("old" vs. new)

- There were noticed some hydraulic responses outside the HZ zones at the upper parts of the bedrock

The results of the pumping test between 2013 and 2019 were used to design a more detailed interference test at the area.

The aim of this thesis was to plan an interference test based on both long-term pumping test results and the current hydrogeological model. The results of this interference test were planned to verify the hydraulic connections on the northern parts of Olkiluoto Island. Another aim of the thesis was to suggest ways to develop the current hydrogeological model of the northern parts of Olkiluoto site. The suggestions that were made were based on the results of the planned and executed interference test.

2 BACKGROUND

2.1 Overview

There are two nuclear companies operating in Finland: TVO Plc (Teollisuuden Voima Oyj) and Fortum Power and Heat Plc (Fortum Power and Heat Oy). There is also one other nuclear company in Finland (Fennovoima Plc) whose nuclear power plant construction has not yet started, but the location has been selected in the northern Finland in the Hanhikivi area of Pyhäjoki, which is located 100 kilometres south of Oulu.

According to the Nuclear Energy Act (11.12.1987/990), a nuclear operating licensee should take care of the nuclear waste generated from its operations, and the amount of nuclear waste should be kept as low as possible.

Posiva Oy is an expert organisation owned by TVO Plc and Fortum Power and Heat Plc. Posiva Oy was established in 1995. It is responsible for research and development of the final disposal of spent nuclear fuel and the disposal of spent nuclear fuel by its owners. Posiva has been constructing an underground research facility called ONKALO since 2004. Posiva's construction license application for a spent nuclear fuel repository was submitted to the Council of State in 2012, and was accepted in November 2015. In the future, ONKALO facilities will be utilised as part of the spent nuclear fuel repository.

The effects of the construction of ONKALO and the repository are monitored by measuring and tracking numerous parameters related to hydrology and hydrogeology, hydrogeochemistry, the environment, rock mechanics and foreign materials. The hydrological and hydrogeological monitoring (to which the long-term pumping test of OL-KR6 was closely related) includes monitoring of: groundwater level, hydraulic head of groundwater, flow conditions of open holes, hydraulic conductivity, precipitation (including snow), seawater level, surface drainage, infiltration, runoff waters in ONKALO and the Korvensuo basin water balance (Vaittinen et al. 2018).

There are a total of 58 deep drillholes on Olkiluoto Island. With some deep drillholes there are also a shorter holes, so called B holes. B holes are used in order to investigate

the upper parts of the bedrock. In addition to deep drillholes, there are groundwater observation tubes in the overburden (OL-PVP holes) and shallow core drilled holes in the bedrock (OL-PP holes). In the OL-PVP holes, there is a perforated section from which groundwater gets to the tube. In the OL-PVP and OL-PP holes, Posiva is investigating the chemical properties of the groundwater yield, hydraulic properties (by means of SLUG-tests), etc. In the OL-KR holes (deep drillholes), Posiva is investigating the chemical properties of the groundwater, water flows in the fractures, the hydraulic head of the hydrogeological zones, etc.

2.2 Geological overview

2.2.1 Groundwater

In this section properties of the groundwater are presented in general. More accurate description of groundwater in Olkiluoto are presented on sections 3.3 & 3.4.

Groundwater is water in a saturated zone in the soil or bedrock, which has (in most cases) infiltrated from rain or snow melt water. Aquifer is a groundwater formation. The water conductivity is relatively high in aquifers (GTK 2019).

Subsurface waters i.e. groundwaters can be divided into two different main categories. The upper one is a vadose zone, i.e. unsaturated zone and the lower one is a phreatic zone, i.e. saturated zone. The unsaturated zone is above the water table where the pore water pressure is less than atmospheric. Generally, there is both air and water in the pore spaces in an unsaturated zone (Fitts 2012).

The boundary between an unsaturated and saturated zone is the water table where the pore water pressure equals atmospheric pressure. The capillary fringe is a zone saturated with water but it is above the water table. Below the water table is the saturated zone where pores are saturated with water and the water pressure is greater than atmospheric (Fitts 2012).

The infiltrating water needs a porous space on the soil or bedrock, in order for groundwater formation to be created. A porous space (open space in a geological

formation) is a prerequisite for groundwater formation (Mälkki 1999). A porous space could be, for example, fractures/fracture zones in the bedrock.

Approximately 0.53% of water on Earth is groundwater (Mälkki 1999). Groundwater occurs as shallow groundwater in the soil or as deep groundwater in the bedrock (Mälkki 1999). This thesis focuses mainly on groundwater in the bedrock.

Most hydrogeological investigations are related to the flowing properties of groundwater: where and how much groundwater is moving. Most of these investigations are related to water supply in general (Fitts 2012). The flow properties of groundwater have been described by Darcy's Law (Fitts 2012).

Darcy's Law can be expressed for one-dimensional flow as follows (Fitts 2012):

$$Q_s = -K_s \frac{dh}{ds} A \quad (1)$$

where

- Q_s= is discharge in the s direction
- K_s= is the hydraulic conductivity in the s direction
- $\frac{dh}{ds}$= is the hydraulic gradient (dimensionless)
- A= cross-sectional area

The constant K_s is a property of geologic medium. Hydraulic conductivity K_s represents how easily the medium transmits water. The higher the K_s the higher amount of transmitted water through the medium. The minus sign is used for hydraulic head decreases in the direction of flow. In this way, if flow is positive in the s direction, Q_s is positive and hydraulic gradient $\frac{dh}{ds}$ is negative (Fitts 2012).

Darcy`s Law is generally valid for granular material where the laminar flow is common, for example in soil. In this way, it is expressed as discharge per cross-sectional area and can be descriebd as follows (Domenico & Schwartz 1990; Fitts 2012):

$$\frac{Q}{A} = q = -K\frac{(h1-h2)}{l} = -K\frac{\delta h}{\delta l} \quad (2)$$

where

- q is the volumetric flow rate per unit surface area, with units of velocity,
- K is a constant of proportionality (hydraulic conductivity),
- Q is flow,
- A is cross-sectional area,
- h1 and h2 are water levels, and
- l is distance.

Equations 1 and 2 are basically the same. Both ways are introduced in order to describe better the hydraulic gradient. The understanding of Darcy's Law helps to understand hydrogeology. There is also a solution for three-dimensional flow (presented e.g. in Fitts (2012)). In this thesis, Darcy's Law itself has not been utilised. It is presented only for background knowledge. Darcy's Law is presented here because it is videly used in Posiva's other hydrogeological analyses and modelling and, in general, aids in understanding different hydrogeological phenomena.

Transmissivity describes of how easily a layer transmits water. Basically it is an integrated parameter of hydraulic conductivity of some specific layer (Fitts 2012). PFL transmissivity can be calculated as follows (Pekkanen & Komulainen 20xx - in prep.):

$$h_f = \frac{h_0 - bh_1}{1-b} \quad (3)$$

$$T_{PFL} = \frac{1}{a}\frac{Q_{f0} - Q_{f1}}{h_1 - h_0} \quad (4)$$

Where

- Q_{f0} & Q_n are the flow rates of fractures
- h_1 is hydraulic head far from drillhole
- T_{PFL} is transmissivity of the fracture

PFL transmissivity (T_{PFL}) is basically specific capacy ($\frac{dQ}{dh}$) in cases where the radius of influence is assumed to be constant (R= 19m) as mentioned in section 7.2 in this thesis. (Pekkanen & Komulainen 20xx - in prep). Pekkanen & Komulainen (20xx - in prep) have described the definition of T_{PFL} values better.

The difficulties of the estimation of groundwater flow are related to the flow in fractured rock. According to Fitts (2012), the difficulties are related to the fact that flow occurs along discrete fractures. The properties of discrete fractures are usually unknown. Usually the location, orientation and width of water-bearing fractures are difficult to determine (Fitts 2012). In this thesis, the aforementioned properties of the fractures are better known due to the huge number of drillholes and investigations in the Olkiluoto area. One uncertainty is that flow in larger fractures could be turbulent as opposed to laminar, which means that Darcy's Law cannot be utilised (Fitts 2012).

The largest groundwater formations in Finland are located on eskers or terminal moraines in the Salpausselkä region (Salonen et al. 2002). The hydraulic conductivity of the crystalline bedrock in Finland is poor in general. For this reason, the largest bedrock groundwaters of Finland are located in the shear zones (Mälkki 1999).

The amount of forming groundwater can be described by the water balance equation (Hiscock 2005):

$$P = ET + S_R + G_R \pm \delta S \quad (5)$$

where

- P is precipitation,
- ET is evapotranspiration (combined evaporation and transpiration)
- S_R is runoff,
- G_R is groundwater discharge and
- δS is change in the amount of water stored in the area during a time period (i.e. groundwater storage).

The water balance equation has been utilised in estimating the water balance of the Korvensuo reservoir at Olkiluoto (Section 3.6). The equation is used to define the amount of water from Korvensuo reservoir that has infiltrated the soil and bedrock. In this thesis, however, the infiltration of Korvensuo reservoir is not taken into account. Due to the fact that, although the reservoir affects the groundwater system, the effects were relatively small during the interference test (because of short time period).

The number of different features affecting the groundwater quality is significant. These features include the amount, composition and dissolving power of infiltrated water, and the structural material of aquifer and biological activity during infiltration. All the features affect differently under different circumstances (Mälkki 1999). It should be remembered that these facts are relating to upper parts of the bedrock and soil and therefore it should be segregated from deep groundwaters in Olkiluoto.

Oxygen plays a key role in groundwater chemistry. The groundwater zone can be either oxidising or reducing, depending on the supply of oxygen in the zone (Mälkki 1999). This feature can vary inside the aquifer. Usually there is less oxygen in the bottom part of the aquifer than in the upper part (Mälkki 1999). The change to anaerobic conditions in groundwater at Olkiluoto is at shallow depths, some indications have been gathered that aerobic waters have intruded to less than 10 m in the history of Olkiluoto (Posiva 2012b).

According to Mälkki (1999), the variation of the oxygen concentration occurs horizontally and usually also vertically in each aquifer. This variation affects ions that are easily oxidised or reduced, such as iron, manganese, nitrite and ammonium.

The chemistry of water changes during infiltration through the soil and bedrock. There is plenty of dissolved matter in the precipitated water. The chemical properties of the precipitated water begin to change during infiltration. The mineral matter starts to dissolve in the water, pH begins to increase and the oxygen in the water disappears in biologically active zones (Mälkki 1999). In Olkiluoto this occurs in the overburden and shallow depths in the bedrock (Posiva 2012b).

Oxygen and carbon dioxide dissolve in the precipitated water. The water, which contains a large amount of carbon dioxide, is a major cause of the chemical weathering of silicates

(Mälkki 1999). During the weathering of silicates, calcium-, magnesium- and iron cations, among others, are released. The dissolved metals form, for example, bicarbonates (Mälkki 1999). This weathering of silicates take place in Olkiluoto at shallow depths (Posiva 2012b). In this thesis, however, the chemical properties of groundwater are not under investigation.

There is a high consumption of oxygen in the aquifers in coastal areas. For this reason, there are usually low amounts of oxygen in the groundwater. The coastal aquifers are vulnerable to seawater intrusions. When water conductivity in the shore area is high, the balance between saline and fresh water is based mainly on the difference in water densities. In this case, the saline water is under the fresh water and the contact is "soft" because of diffusion. (Mälkki 1999)

The aforementioned balance may be disturbed as a consequence of an excessively large water intake/pumping rate. This causes seawater intrusion into the fresh water environment. In the OL-KR6 case, this might be possible during the interference test but, during the long-term pumping test, there were no observations of seawater connections (Reijonen et al. 2015)

The chemical properties of the groundwater in Finland commonly can be described as mildly acidic and soft. The concentration of salinity in Finnish groundwater is low and it is usually mildly corrosive to the metal plumbing systems. Dissolved organic contents such as iron- and manganese concentrations in the groundwater in Finland are usually low. They are most common to the groundwaters of glacifluvial formations (Mälkki 1999).

However it should be remembered that aforementioned facts concern shallow groundwaters in Finland. This thesis is strongly relatet to deep groundwaters in Olkiluoto and therefore these kind of general facts needs to be segregated from deep groundwater which are presented later in this thesis.

2.2.2 Geology

The bedrock of Finland is part of the Fennoscandian shield, one of the oldest areas on the Eurasian continent (Nurmi et al. 1998). The major phases of development in our bedrock took place 2,800–2,700 and 1,900–1,800 million years ago. The northern and eastern parts of Finland belong to 3,100–2,500 million-year-old Archaean bedrock and the southern and western parts belong to 1,900–1,800 million-year-old Paleoproterozoic bedrock (Nurmi et al. 1998).

Only very small parts of the Finnish bedrock are younger than 1,800 million years. The most significant younger formations are Rapakivi granites which are 1,650–1,450 million years old and are located mainly in the southern parts of Finland. A typical feature of bedrock in southern Finland is also the occurrence of diabase veins, which are the same age as Rapakivi granites (1,650–1,450 million years) (Nurmi et al. 1998).

Most Finnish bedrock (97 %) has been covered by different soil types or water systems (lakes, rivers, etc.). The general composition of Finnish soil is that the bottom of the soil consists of glacial formations like moraines and eskers. Above the glacial formations there can be deep water formations (clays, silts). Shallow water formations (which are younger than deep water formations) are above them. The uppermost layers of Finnish soil consist of the sludge layers of lakes or peat formations of mires. The thickness of Finnish soil is approximately 8.6 metres (Salonen et al. 2002).

Most Finnish soil originates from the latest glacial period: Weichelian Ice Age. Weichelian Ice Age started 115,000 years ago and had different stages. Late Weichelian glaciation (the last part) ended approximately 10,000 years ago (Salonen et al. 2002). For instance, Salpausselkä terminal moraines are the Late Weichelian formations.

3 OLKILUOTO SITE

Olkiluoto is a rather large island (12 km^2) on the Baltic Sea coast and is separated from the mainland by a narrow strait. The island is in the Finnish municipality of Eurajoki, between Rauma and Pori. The two operating nuclear power plants and a third nuclear plant (which is under construction) are located in the western part of the island (Figure 1). Near the operating nuclear power plants is also a VLJ repository for low and intermediate level waste. The repository for spent nuclear fuel will be constructed in the central and eastern parts of the Olkiluoto Island.

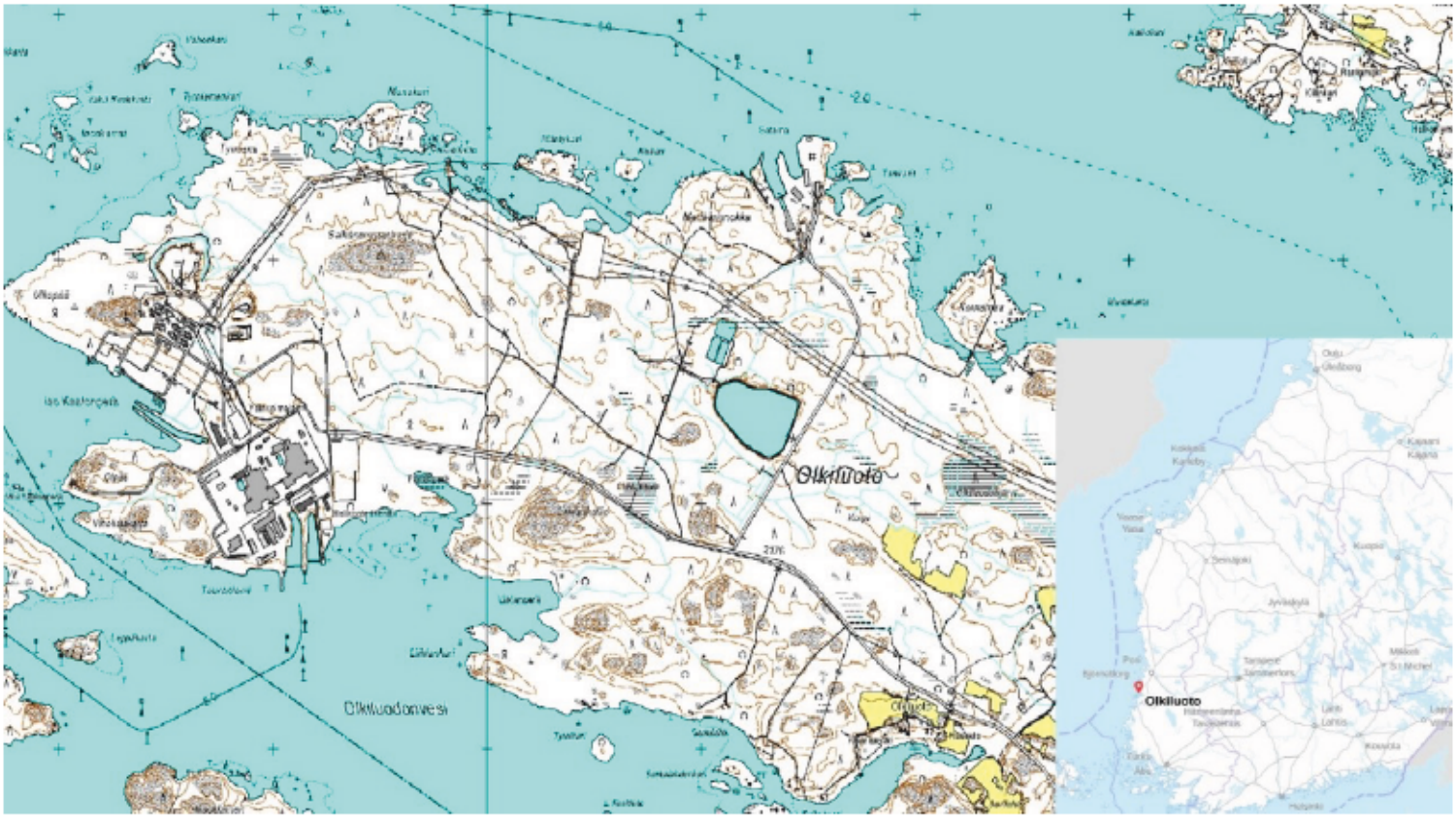

Figure 1. Map of the Olkiluoto area. The operating nuclear power plants are on the western (left) side of the map. ONKALO is located in the middle of the island, a little south of Korvensuo reservoir.Olkiluoto map © Posiva. Finland map © National Land Survey of Finland

There are many different areas on Olkiluoto Island, related to the nuclear power plant activities in the island, the construction of the spent nuclear fuel repository and other industrial activities. There are several landfill sites and excavated rock crushing areas, as well as the Korvensuo reservoir and sedimentation pools located in the central parts of

the island. Olkiluoto harbour is located on the northern coast. There is also a Natura 2000 site on the island, which is an old forest called Liiklansuo.

3.1 Geology

Geological investigations and research at Olkiluoto have been done using outcrops, drillholes, tunnel mapping in ONKALO, geophysical and seismic measurements. The paleoproteroic bedrock of Olkiluoto consists of varied migmatite supracrustal rocks that have undergone high-grade metamorphosis: migmatised meta-pelites, meta-arenites and pyroclastic metavulcanites. These rocks are intruded by granitic-tonalitic stones, granitic pegmatoids, and diabase dikes. At some point, there were ductile deformations in the area and, in the different phases of this deformation, the rocks of Olkiluoto were metamorphosed simultaneously (Aaltonen et al. 2016).

According to Aaltonen et al. (2016) the geological model of Olkiluoto can be divided into five different thematic sub-models. These sub-models are the lithological model, the ductile deformation model, the alteration model, the brittle deformation model and the statistical model of fracturing (integrated DFN-model). The lithological model describes the geometry and lithological properties of site-scale rock domains on Olkiluoto in general. The ductile deformation model describes the products of polyphase ductile formation. The alteration model mainly describes the products of hydrothermal alteration and processes, which have transformed the physical and chemical properties of the rock material.

There are two main lithological units at the Olkiluoto site: a diatexite unit and a veined gneiss unit. It has been detected that both the main units contain small amounts of TGG gneisses, mafic gneisses and mica gneisses. There are also granitic pegmatoids and diabase dikes in the both main units. Those previously mentioned rock types occur as individual lithological objects in the two main units (Aaltonen et al. 2016).

The geometry and properties of the structures produced at the Olkiluoto site during the different phases of brittle- and semi-brittle deformation are presented in the brittle deformation model (Aaltonen et al. 2016). The Discrete Fracture Network (DFN)

describes the geometric, mechanical, hydraulic and transport properties of the bedrock fractures that are constrained quantitatively from site characterisation data (Hartley et al. 2018).

There are some signs of different stages of deformation on Olkiluoto. Olkiluoto can be divided into different tectonic units based on these signs of deformation (Aaltonen et al., 2016). OL-KR6 is located in the NTU (Northern Tectonic Unit) area. Other tectonic units according to Aaltonen et al. (2016) are the Selkänummi Deformation Zone (SDZ), Central Tectonic Unit (CTU1, CTU2, CTU3, which are the subunits of CTU), Flutanperä Deformation Zone (FDZ), Liikla Deformation Zone (LDZ) and Southern Tectonic Unit (STU, with four subunits: STU1, STU2, STU3 and STU4) (Figure 2). These tectonic units relate to the groundwater flow because the units act as a limiting factor for groundwater flow due to the orientation of fractures (Vaittinen et al. 20XX - in prep.).

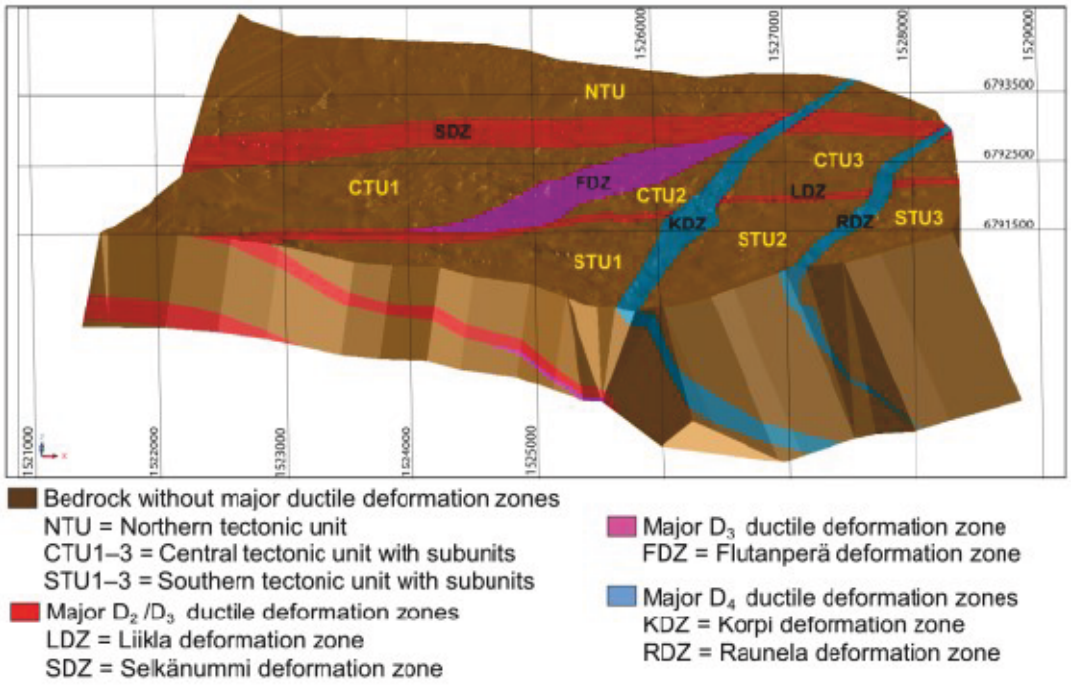

Figure 2. The major ductile deformation zones and tectonic units modelled as 3D (except STU4). View is from the south. The figure is from Aaltonen et al. (2016); Pentti & Vaittinen (2018). Figure is published with Posiva's permission.

The characteristic feature of NTU is the occurrence of E-W-striking planar structural elements that have a statistical maximum of 166/44°. The D_2 deformation phase was a site-scale event (took place approximately 1.86 Ga ago) and affected the whole area of

Olkiluoto Island. There are often some remains of the D_2 deformation phase in the NTU. The coplanar products of the D_3 (later phase of deformation compared to D_2) deformation and fold structures are overprinting traces of the D_2 deformation in places. The overprinting coplanar products of D_3 deformation and fold structures usually have SE-dipping axial surfaces. The intensity of D_3 deformation is lower in the northern parts of NTU than in the southern parts. The intensity of deformation seems to decrease gradually from the southern parts of NTU to the northern parts (Aaltonen et al. 2016).

There are modelled brittle deformation zones (OL-BFZ) on Olkiluoto. These zones are either fracture or brittle deformation zones. The OL-BFZ structures can be divided into two categories. One is site-scale and the other is repository-scale. This division is based on the lateral extent of different OL-BFZ zones. If the OL-BFZ-zone extends less than 1,000 m, it is systematically classified as a repository-scale zone. The repository-scale zones are usually based on one or a few drillhole interceptions. Their orientation is mainly based on the orientation of the slickenside fractures in the interfered core zones. Their actual extent is generally uncertain. (Posiva 2012b; Aaltonen et al. 2016)

Compared to the repository-scale the site-scale zones extend laterally over 1,000 metres and the extent is defined by several drillhole intersections (Posiva 2012b; Aaltonen et al. 2016). Repository-scale zones can also be defined by several drillhole intersections or geophysical and topographic data. (Aaltonen et al. 2016)

3.2 Surficial geology

Olkiluoto Island is relatively flat and is approximately 5 metres above sea level (Lahdenperä et al. 2005). The overburden on Olkiluoto has been studied through test pits, geophysical surveys and some core samples. Other useful sources of information have been installation of groundwater tubes and the overburden information gained from deep drillhole locations.

The most common soil types on Olkiluoto are fine-textured and sandy till. In addition, there is gravelly till, peat and clay (Posiva 2012b). The overburden on Olkiluoto is the thickest in the western parts of the island (Mönkkönen et al. 2017). The average thickness

of the overburden at Olkiluoto is 2–5 metres, but in some places the thickness can be reached up to 14 m (Posiva, 2012b). According to Lahdenperä et al. (2005), the investigated test pits in the Olkiluoto area generally consist of sandy till, which also contains clay, sandy gravel and weathered layers.

The weatherability of rocks has an effect on the geochemical composition of till. Other elements affecting geochemical composition of till are the flow direction of the continental ice sheet and type and amount of re-deposited drift (Salonen et al. 2002). In the Olkiluoto area, till can contain more stones or it can be more compact, which usually occurs in deeper horizons. There have also been some indications of fine-grained glaciolacustrine sediments in the Olkiluoto area (Lahdenperä et al. 2005).

3.3 Hydrogeology

Olkiluoto can be classified as a separate hydrological unit in which surface water flows directly to the sea (Posiva 2012b). There are many different catchments (drainage basins) on Olkiluoto, which are defined based on ground topography and flow directions of water in trenches (Posiva 2012b). The constructed areas also affect the catchments as well as infiltration of groundwaters.

The hydrogeological site-scale concept of the Olkiluoto site is based on connecting the geological, geophysical and hydrogeological research data (Vaittinen et al. 2011), for instance spatial information on the interpreted tectonic units, OL-BFZs with drillhole-to-drillhole connections mostly based on geophysical connections, and high fracture transmissivities and hydraulic connections.

The HZ structure model is based on the hypothesis that the rock mass is strongly channelled, and because of that most of the groundwater flows along hydrogeologically essential deformation zones (Figure 2.). In this hypothesis, only a minor part of groundwater flows along fractures within sparsely fractured rock between HZ structures. The hydrogeological model of Olkiluoto consists of 16 site-scale hydrogeological zones: HZ001, -HZ008, -HZ19A, -HZ19B, -HZ19C, -HZ20A, -HZ20B, -HZ21, -HZ21B, -HZ039, -HZ099, -BFZ100, -HZ146, -HZ056, -BFZ045 and OL-BFZ300 (Figure 4) (Vaittinen et al. 20xx - in prep.).

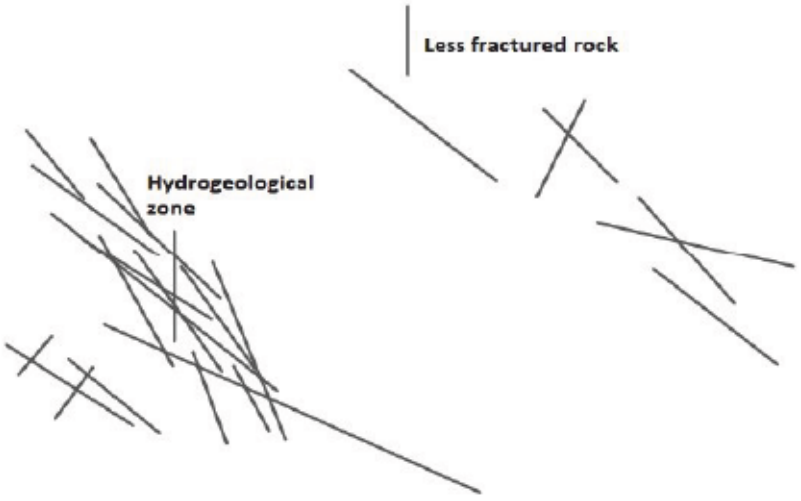

Figure 3. The difference between the hydrogeological zone and less fractured rock. Most of the groundwater flow occurs in the hydrogeological zone. Figure is modified after Vaittinen et al. 20xx - in prep.

For the HZ zones (site-scale) there are determined two different drillhole intersections: zone intersection and hydrogeological influence zone. These determined drillhole sections are corresponding geological data for OL-BFZs, where there are core and geological influence zone (Vaittinen et al. 20XX - in prep.).

Figure 4. Site-scale hydrogeological zones in Olkiluoto according to Vaittinen et al. (20XX – in prep.). Figure is from above.

According to aforementioned site-scale hydrogeological zones, there are also modelled HZL-zones on Olkiluoto (Vaittinen et al. 20xx - in prep.). The HZL- zones are repository-scale hydrogeological zones. HZL-zones can be 1) hydraulic connections between two or more drillholes 2) hydraulic connections between ONKALO and certain drillholes or hydraulic connections between two or more drillholes. There are a total of 16 repository-scale hydrogeological zones on Olkiluoto. These zones are: HZL1–12, OL-BFZ130B, OL-BFZ084, OL-BFZ297 and OL-BFZ346.

Thirteen of the site-scale hydrogeological zones are mostly based on hydraulic properties and the continuity of the interpreted hydraulic connections. Three of the zones are based on the geological conditions (Vaittinen et al. 20xx - in prep.). In addition to the site-scale features, some of the hydraulic connections are determined as local-scale features. These local-scale features are difficult to model in the NTU area (Vaittinen et al. 2011) where OL-KR6 is located. In the NTU area, the drillholes are further from each other, and for this reason the interpretation of the monitored head observations is uncertain.

3.4 Hydrogeochemistry

There is a layered structure in the groundwater chemistry of Olkiluoto. Posiva (2012) identified four types of reference groundwater by age. These are brine reference, glacial reference, Littorina reference (including Baltic Sea water, which is basically a diluted version of Littorina sea water) and meteoritic water. These reference types of groundwater control the groundwater compositions on Olkiluoto by mixing with each other.

During the last hundreds of thousands of years the hydrogeological and hydrogeochemical environment of Olkiluoto site has been formed. This evolution is nowadays seen as clear distribution of different water types. Different water types are characterised by salinity, chemistry and isotope composition. The baseline groundwater composition is depth related (chemistry varies with depth) due to these old phases of development. Indications of different infiltrated water sources are gathered from salinity variation, anion composition and stable isotope signature. Reactions and mixing of different initial water types during the different phases of geological history of the Olkiluoto site are formed the current baseline groundwaters. In present day are identified four types of baseline samples: infiltrated meteoric water, Littorina sea water, glacial meltwater and original brine. (Posiva 2012b)

In the upper parts of bedrock (0–40 metres) is fresh groundwater (TDS (total dissolved solids) <1g/l). At depths of 40 to 430 metres, there is brackish groundwater (1< TDS< 10g/l). At depths greater than 300 metres, there is saline (10< TDS< 100g/l) or brine (>100 mg/l) groundwater. Chloride is the dominant anion in deep bedrock groundwaters. Other dissolved matter in bedrock groundwater varies according to depth (Davis 1964; Posiva 2012b).

According to Posiva (2012b) there are three groups of fresh and brackish groundwater on Olkiluoto. This division is based on characteristic anion contents. One groundwater type is fresh-brackish HCO_3-type groundwater (rich in bicarbonate), another is brackish SO_4-type groundwater (rich in SO_4), which occurs at depths of 100 to 300 metres, and the third type is brackish Cl-type groundwater, which occurs at between 100 and 450 m. In deeper parts the groundwater is saline or brine.

Posiva (2012) estimated that groundwater on Olkiluoto results from at least two types and six different sources of water. The two types of water are from modern and relic sources. Water types from modern sources are meteoric water and sea water from the Gulf of Bothnia and Korvensuo reservoir. Water types from relic sources are Littorina sea water, glacial meltwater and brine.

According to Vuorio et al. (2018), the most important processes affecting the chemical composition of groundwater are the mixing of different groundwater types, water-rock interaction, microbial processes at interfaces between different groundwater types, as well as in the overburden, and weathering. Weathering during infiltration is the main process increasing the amount of solutes in shallow groundwater.

Nowadays the redox conditions on Olkiluoto are anoxic except for some shallow infiltrating groundwater. There are two natural metastable interfaces in the groundwater on Olkiluoto. The upper one is located in the overburden or in very shallow bedrock. At this interface, the conditions change from oxic to non-oxic. The other interface is located approximately at depths of 250–350 metres and contains transition from SO_4-rich groundwater into more saline SO_4-poor groundwater with higher dissolved gas concentrations (e.g. H_2, CH_4 and other hydrocarbons). This results in elevated levels of dissolved sulphide as a microbially-mediated reaction product (Pastina & Hellä 2010).

3.5 ONKALO®

The construction of ONKALO started in July 2004. The excavation of the vehicle access tunnel was finished in 2012. Since then, Posiva has been excavating and constructing demonstration areas, vehicle connections and technical rooms (Vaittinen et al. 2018). These excavations are continuing at the moment in central tunnels.

The effects of ONKALO are notable on the groundwater conditions at Olkiluoto. There has been a large volume of open tunnels since 2004, which create a constant disturbance to the surrounding groundwaters of ONKALO (Rämä 2011). The large number of open tunnels with inflow create suction, change the hydraulic heads of the surrounding areas and the flow directions.

The total inflow of ONKALO has been measured since 2004, usually once a month. Since 2008, the leakage of ONKALO has been based on the sum of the flows of the measuring weirs from the access tunnel and the leakage in the vertical shafts (Vaittinen et al. 2018). This is done in order to have leakage results from every different parts of the tunnel.

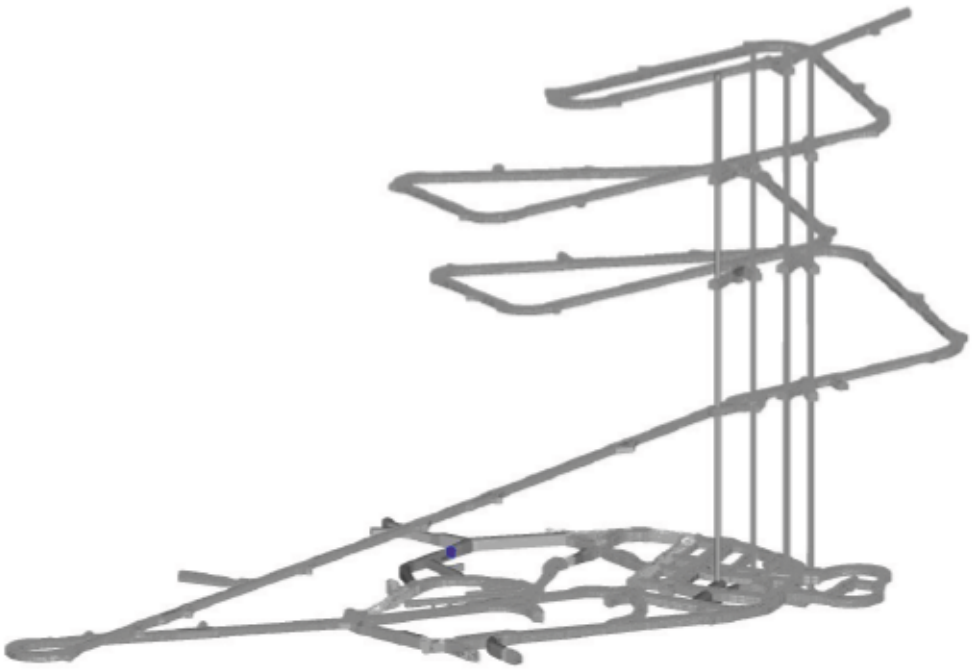

Figure 5. ONKALO layout and excavated spaces nowadays. Figure is from the west. There are acces tunnel, 4 shafts, and part of the technical spaces at the bottom.

The total measured leakage to ONKALO has varied by approximately 25–40 L/min in the last couple of years (Vaittinen et al. 2018). In that time, there have been some technical problems, which have affected to total inflow results of ONKALO, for instance if there has been ongoing drilling during the leakage measurement. Water used in the drilling process can disturb the total leakage measurement in this case the uncertainities are reported together with the results. However, it is important to understand that the real leakage to ONKALO is not varying as much as the measured leakage.

3.6 Korvensuo reservoir

Korvensuo reservoir is located between ONKALO and the investigation drillhole OL-KR6 in the northern part of Olkiluoto (Figure 1.). It is used to supply water to the power plant and flushing water for drilling operations and for the ONKALO construction project. Water to Korvensuo reservoir is pumped from Eurajoki river (Vaittinen et al. 2018).

The water balance of Korvensuo reservoir affects the groundwater conditions nearby (Vaittinen et al. 2018). The more water in the Korvensuo reservoir (higher water table and hydraulic gradient), the more infiltration. The surrounding groundwater conditions also affect the infiltration process (Vaittinen et al. 2018). The higher the groundwater level, the lower the hydraulic gradient. A lower hydraulic gradient decreases the amount of infiltration, because hydraulic gradient is a driving force for groundwater flow.

There have been many indications (based on the chemical and isotopic data) that water infiltrating from Korvensuo reservoir has had an influence on the current groundwater compositions at the site, especially areas near the Korvensuo reservoir (e.g. Penttinen et al. 2011 & Penttinen et al. 2013).

The effects of Korvensuo reservoir are seen in the groundwater of OL-PVP12 (overburden tube 20 m from the reservoir), OL-PVP30 (overburden tube 100 m from the reservoir) and OL-PP3 (shallow bedrock drillhole 65 m from the reservoir). There are clearly higher oxygen-18 and deuterium values in water than in the other shallow groundwater holes (Penttinen et al. 2011). Stable isotope oxygen-18 can be utilised when determining the origin of groundwater (Posiva 2012b).

The effects of Korvensuo reservoir have also been observed at shallow depths on the northern side of the reservoir. There are also some observations that some of the water of Korvensuo reservoir is infiltrating to ONKALO (e.g. Penttinen et al. 2011). These implications are based on the isotopic compositions of some ONKALO samples from shallow depths.

However, the water from Korvensuo reservoir that has infiltrated to the groundwater system nearby has not been taken into account in this thesis. This is due to short pumping periods, and the fact that the distance between OL-KR6 and Korvensuo reservoir is hundreds of metres, which decreases the effects of infiltrated water on the interference test.

4 OL-KR6 AREA

4.1 Overview

OL-KR6 is a 601-meter-long drillhole located in the northern parts of Olkiluoto Island. OL-KR6 is a deep, open drillhole on Olkiluoto Island, which has been a part of Posiva´s monitoring program and site investigations. A long-term pumping test took place between 2001 and 2019.

For the Olkiluoto area, Posiva has created/developed a geological (Section 3.1) and hydrogeological (HZ) (Section 3.3) model. Usually geological structures and hydrogeological connections modelled as HZ's are related to each other, for example in cases where BFZ influence zones are highly transmissive.

The classification of different HZs and OL-BFZs is presented in Sections 3.1 and 3.3. The focus of this thesis is to confirm hydraulic connections (modelled as HZ's) in the area around OL-KR6. This is done by means of an interference test (Section 7).

4.2 Intersecting structures

4.2.1 Geology

OL-BFZ021 is a site-scale structure, which intersects OL-KR6 at a depth of 468–471 m. It is a thrust fault, which dips on average 20° towards the SE. OL-BFZ021 and OL-BFZ099 are considered as two layers of a single structure. OL-BFZ021 is as geologically well-pronounced as OL-BFZ099. These layers combine into a single zone in the central part of the site volume (Aaltonen et al. 2010).

The geological similarity of OL-BFZ021 and OL-BFZ099 appears in certain details of the structures (Aaltonen et al. 2010). These details are, for example, that the fault core is well-developed and characterised by abundant fracturing, clay-filled fractures and slickensides, alteration and varying amounts of incohesive fault breccia and crushed rock (Aaltonen et al. 2010).

According to Aaltonen et al. (2010), the thickness of the fault core of OL-BFZ021 varies between 1 and 8 metres with an average thickness of 4 metres. Fault breccia is the most common type of fault rock (Aaltonen et al. 2010). The ductile and semi-ductile precursors are overprinted by welded fractures, cohesive breccias and younger fractures, which indicate that there have been some recurrent movements within the brittle regime (Aaltonen et al. 2010).

According to Aaltonen et al. (2010), OL-BFZ041 is a repository-scale structure. The intersection depth of OL-BFZ041A related to OL-KR6 is estimated to be 10.9–11.8 m. The fractures of this structure are either clay- or grain-filled. The fractures are also slickensides, weathered and porous. Some of the fracture coatings are rusty.

OL-BFZ049 is a repository-scale structure, which intersects OL-KR6 at a depth of 506.9–508.8 m. Structure is in the VGN (veined gneiss). OL-BFZ049 is densely fractured, and there is also some random fracturing with fractures parallel to and cross-cutting the foliation. There is also some small-scale welded fracturing. Typically, this is older microfracturing and -breakage. The graphite coatings can be seen on the slickensides. The core sample has been split due to drilling (Aaltonen et al. 2010).

According to Aaltonen et al. (2010), OL-BFZ099 is a site-scale thrust fault and intersects OL-KR6 at a depth of 162.8–164.8 m. The dip of this fault is approximately 40 degrees towards the SE. The zone is geologically well-identified and characterised by abundant fracturing, clay-filled fractures and slickensides. Typically, in OL-BFZ099, there is also some hydrothermal fracture-controlled/pervasive illitisation and kaolinisation and variable amounts of fault breccia which is incohesive. There is also some crushed rock. The average thickness of the fault core is 5 metres and the thickness varies from 1 to 13 metres. The fault rock can be either fault breccia or fault gouge. The most common type of fault rock in this structure is fault breccia.

According to Aaltonen et al. (2010), OL-BFZ108 intersects OL-KR6 at a depth of 366.7–367.0 m and is a short fault in mica-rich gneiss. In this structure is some old welded small-scale microfracturing-breccia and some graphite on the younger slickensides parallel to the foliation. There is a gouge with large amounts of graphite in the bottom part of the

OL-BFZ108 structure, as well as some in-situ sheared rock fragments in the bottom part of OL-BFZ108.

4.2.2 Hydrogeology

In the current model (Vaittinen et al. 20XX - in prep.), the intersecting structures of OL-KR6 are HZ001, HZ005, HZ21, HZ21B, HZ056, HZ099, HZL4, HZ21 and HZ21B which are related to each other, and the SE part of HZ099 and HZ21 correspond to each other. In the northern part of the island, they form two splayed zones in which the hydrogeological model is similar to the geological one. Zones HZ21, HZ99 and HZ001 are all located within the NTU (Vaittinen et al. 2011). The hydrogeological model of the OL-KR6 area is presented in Figure 6.

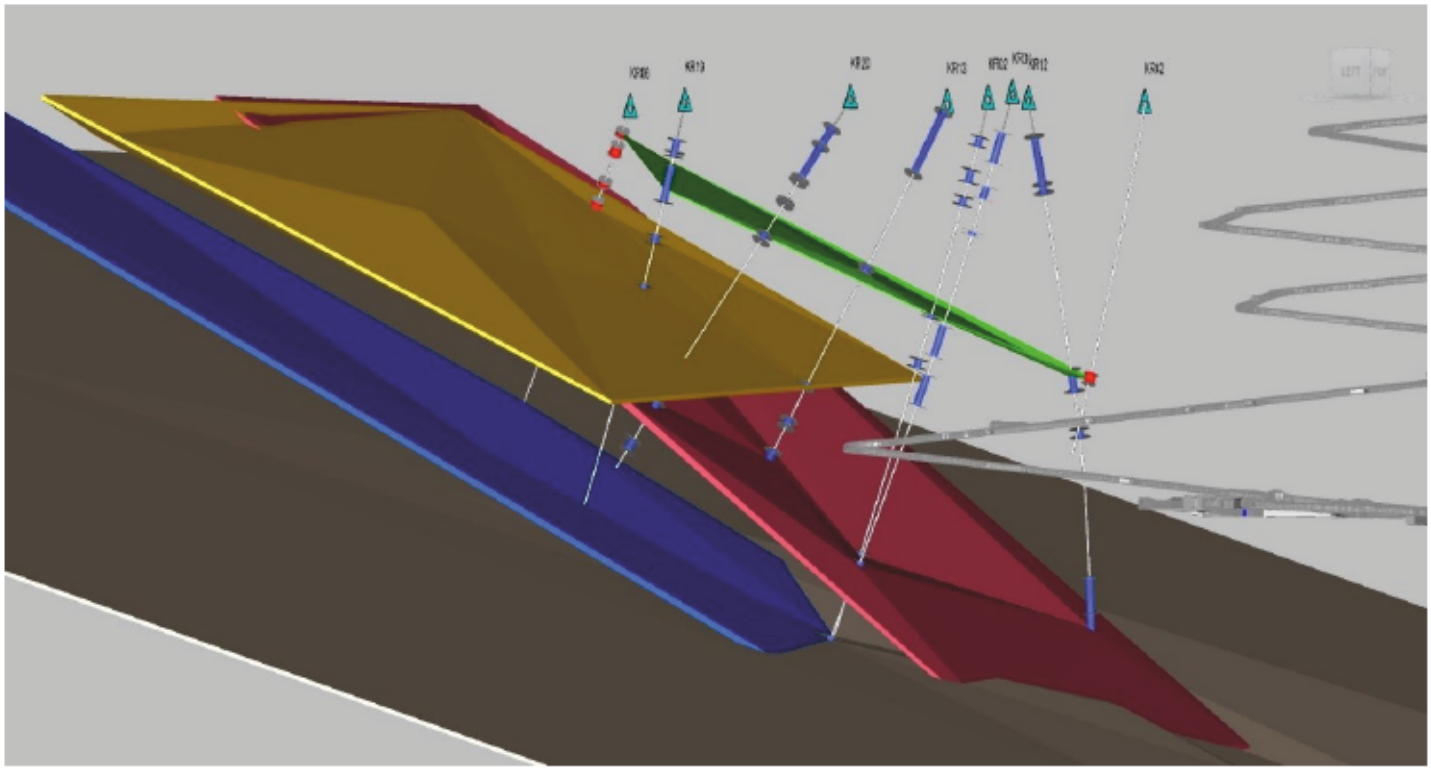

Figure 6. The most notable hydrogeological structures (HZL4 is green; HZ001 yellow; HZ099 red; HZ21B blue and HZ21 grey) of the OL-KR6 area according to Vaittinen et al. (20XX - in prep.). The view of the figure is from the southwest. Also shown are drillholes, (and their packer sections) which are involved in the interference test and part of ONKALO. The figure is not to scale.

According to Vaittinen et al. (2011), the interpretation of zone HZ021 is strongly based on the geological properties of the zone and the results of geophysical measurements. The transmissivity of the HZ021 intersections varies by several orders of magnitude (Vaittinen et al. 20XX - in prep.). In the HZ021 zone, there is intensive fracturing. For the aforementioned reasons, HZ021 could be a major route for deep saline groundwater and for radionuclides from repository level to the biosphere (Ahokas et al. 2007). It is modelled to intersect OL-KR6 at a drillhole section 473.6–477.9 m (Vaittinen et al. 20XX - in prep.). The average orientation of HZ21 is 162/20° (Vaittinen et al. 20XX - in prep.).

Zone HZ21B connects the observed high-fracture transmissivities in drillholes OL-KR4, OL-KR6 and OL-KR12. A hydraulic connection between drillholes OL-KR5 (now plugged/filled) and KR19 (Posiva 2012b) has also been detected. Zone HZ21B is modelled to intersect OL-KR6 at a drillhole length section of 393–400m (Vaittinen et al. 20XX - in prep.). 157/30° is the average orientation of HZ21B zone.There is little data on its continuation and most of its drillhole intersections are common to zone HZ21.

Zone HZ099 is based on the geological brittle fault zone OL-BFZ099. HZ099 is the central part of OL-BFZ099 and was modelled as a hydrogeological zone based on its moderate fracture transmissivities. The hydrogeological properties of HZ099 are similar to zone HZ20 (Vaittinen et al. 2011). Zone HZ099 intersects OL-KR6 in a drillhole length section of 162.2–164.2 m (Vaittinen et al. 20XX - in prep.). The average orientation of HZ099 is 169/38° (Vaittinen et al. 20XX - in prep.).

Zone HZ001 is located in the northern parts of the island. Hydrogeological zone HZ001 connects the drillhole sections with an anomalous low head. A head analysis of Olkiluoto has been carried out on fresh water heads (i.e. baseline heads) that are as representative as possible, for the selected drillholes used in the monitoring programme, to identify and determine any disturbances in groundwater conditions caused by ONKALO (Ahokas et al. 2007).

HZ001 zone was extended towards the east in 2008. This was done based on the differences in the geological and hydrogeological properties of the tectonic units and the lack of pressure responses (Vaittinen et al. 2011). Zone HZ001 intersects OL-KR6 at a

drillhole length section of 134.6–136.7 m (Vaittinen et al. 20XX - in prep.). Average orientation of the HZ001 is 165/28° (Vaittinen et al. 20XX - in prep.).

HZL4 zone is modelled above the site-scale zones on OL-KR6 close to surface. The average orientation of the zone is 162/27°. It is modelled based on the direct responses, observed during the long-term pumping test on OL-KR6. It is modelled to intersect OL-KR6 at depth of 32.6–34.6 m. It includes two modelled brittle fault zones OL-BFZ009a (intersecting OL-KR2 and -KR13) and OL-BFZ041b (intersecting OL-KR12 and OL-KR42) (Vaittinen et al. 20XX - in prep.).

5 INVESTIGATION EQUIPMENT AND METHODS USED BY POSIVA

5.1 Hydrology and hydrogeology

5.1.1 Monitored parameters of the OMO programme

Posiva has set an Olkiluoto monitoring programme (OMO) to monitore and evaluate the effects of undergroung constructions to the Olkiluoto bedrock and surface environment. The programme for the period before the repository operation was published in 2012 (Posiva 2012a). This programme will be used until the repository operation, and it includes many different areas of research, each of which have their own targets.

According to Posiva (2012a), the monitored parameters related to hydrology or hydrogeology include sea water level, runoff, precipitation (including snow), infiltration, ground frost, groundwater table level, flow conditions in open drillholes, groundwater flow across drillholes, hydraulic conductivity and transmissivity, hydraulic head/pressure responses, water balance at ONKALO and water balance in the Korvensuo reservoir. Hydrogeological monitoring has been done, for example, in deep drillholes, multilevel piezometers, shallow-core drilled holes in bedrock, groundwater observation tubes in the overburden and percussion-drilled holes (Posiva 2012a).

5.1.2 Posiva Flow Log dirrefence flow meter (PFL DIFF)

When designing the PFL device, the aim was to detect water-conductive fractures in deep drillholes (Öhberg 2006). Water-conductive sections and fractures are identified by means of PFL DIFF (Pekkanen et al. 2016). Hydraulic properties (transmissivity and hydraulic head) and water flow balance in the drillhole are the second objective for PFL DIFF measurements (Pekkanen et al. 2016).

According to Öhberg (2006), the PFL device differs from traditional types of drillhole flowmeters by measuring the flow rate in or out of selected sections of the hole instead of measuring the total cumulative flow rate along the hole. The device detects incremental

changes of flow along the hole in isolated sections. Normally these incremental changes in flow rate are small and can easily be missed using traditional types of flow metres.

Principle of the PFL equipment have been discussed on many different reports (e.g. Komulainen (2014); Pekkanen et al. (2016); Pekkanen & Komulainen (20xx) - in prep. etc.) The most recent Posiva working report (Pekkanen & Komulainen, 20xx - in prep.) is utilised in this thesis in order to have the latest information related to the equipment.

There are rubber sealing disks at the top and bottom of the PFL DIFF probe, which are used as packers to isolate the flow of water in the test section. In this way, it is possible to isolate the water of the test section from the rest of the drillhole. The flow inside the test section is directed through the flow sensor. The flow guide consists of a bypass pipe, the aforementioned packers and a test section. Flow along the drillhole is directed around the test section. This direction is done by means of the bypass pipe. Water flows through the bypass pipe and is discharged at either the upper or lower end of the probe. It is important to notice that, depending on pressure conditions around and in the measured drillhole section, the direction of the measured flow can be either from the bedrock to the drillhole or from the drillhole to the bedrock. In the same way, the flow along the drillhole can be either downward or upward (Pekkanen et al. (2016); Pekkanen & Komulainen 20xx – in prep.).

Usually there are two separate measurements of two different section lengths (2 m and 0.5 m) used in PFL measurements. The longer section length (2 m) is used first to give a general picture of flow anomalies. The larger section is also used to measure larger fractured zones (< 2 m), and the smaller section is used to separate flow anomalies, which are close to each other. Two different section lengths also help to confirm that a flow anomaly is real and not caused by a leak at the packers (rubber disks) (Pekkanen et al. (2016); Pekkanen & Komulainen 20xx – in prep.).

The PFL DIFF measurement is based on the operation of thermistors. There are three different thermistors in the flow sensor. The central one is used both as a heating element and to register temperature changes. Two different side thermistors are detecting the effects (thermal pulse) caused by the heating of the central thermistor. Flow rate is

measured by monitoring heat transients after constant heating in the central thermistor. This is called the thermal dilution method. First the central thermistor is heated constantly, then the power is cut off and the flow rate is measured by monitoring transient thermal dilution. When exceeding a certain limit, another constant power heating period is started. After constant heating is switched off, the operation is the same as after the first heating (Pekkanen et al. (2016); Pekkanen & Komulainen 20xx – in prep.).

In addition to measuring the flow, the PFL device also measures the following parameters: single-point resistance (SPR), electric conductivity (EC) of the groundwater, temperature of the groundwater and prevailing pressure in the drillhole. The EC electrode is located at the top of the flow sensor. The water going to or coming from the flow sensor goes through the electrode, the setup of which was modified in 2015 to prevent the test-section water for mixing with the surrounding drillhole water in the electrode by guiding the fracture water along a pre-determined route. In this way, possible distortion of the measured fracture-specific EC value can be prevented (Pekkanen et al. (2016); Pekkanen & Komulainen 20xx – in prep.).

The flow is measured when the device is not moving. There is a waiting time after transferring the device. The waiting time can be adjusted depending on the prevailing drillhole conditions. After the waiting time, the thermal pulse is launched. The measurement period after the thermal pulse is usually 100 s each time the PFL probe has moved a distance equal to the test-section length and 10 s in every other location. The measurement time and the waiting time are adjustable. Longer measurements than 100 s are used to identify the direction of the smallest flows (Pekkanen et al. (2016); Pekkanen & Komulainen 20xx – in prep.).

In general, the flow rate measurement range is 30 mL/h–300,000 mL/h, but the PFL DIFF probes have been calibrated in a laboratory for a different flow range of 6 mL/h–300,000 mL/h. Usually the natural conditions in the field raise the lower limit to approximately 30 mL/h, but in some drillholes even 30 mL/h cannot be reached. This can be caused by drilling debris in the drillhole water, gas bubbles or high flow rates along the drillhole ($\geq$ 1 800,000 mL/h). Limits on practical measurements are calculated for each set of data if the disturbances during the measurements are significant. The aforementioned

measurement range (30 mL/h–300,000 mL/h) is based on practical experience and is usually valid except in the situations described above (Pekkanen et al. (2016); Pekkanen & Komulainen 20xx – in prep.).

Flow along the hole can also be measured with a PFL DIFF probe. This is done by removing the lower rubber disks, thus guiding the entire flow along the drillhole through the flow sensor. This kind of setup should be less sensitive to disturbances caused by roughness of the drillhole wall and loose rock material. The relative accuracy of this setup is the same as using the PFL DIFF setup. In some cases (flow rate > 300,000 mL/h), a special flow divider is needed in front of the flow sensor. The shape of the flow divider resembles a torpedo. The flow divider divides the flow along the hole into and past the flow sensor. The main objective of the flow divider is to keep the flow rate through the flow sensor below 300,000 mL/h. The accuracy of flow rate decreases when the flow divider is used, but is does enable the measurement of higher flows. The measurement accuracy of using the flow divider is approx. ± 20 % of the measured value. The PFL DIFF along the hole setup has limitations similar to conventional flowmeters. When flow along the drillhole is high, a small change in flow rate may not be detected (Pekkanen et al. (2016); Pekkanen & Komulainen 20xx – in prep.).

5.1.3 Posiva Flow Log double packer pressure probe (PFL DOPP)

PFL DOPP is PFL double packer pressure probe used to measure pressure in a selected drillhole section (Pekkanen & Komulainen 20xx – in prep.). The measurement drillhole section is isolated from other fractures by two inflatable packers. The PFL pressure sensor measures the total pressure in the test section (between the packers) and atmospheric pressure (Pekkanen & Komulainen 20xx – in prep.). The calculation of the hydraulic head of the test section is presented in Equation 8.

Same pressure probe used in PFL DIFF measurement is also utilised in the PFL DOPP measurement. The difference is that there is no flow guide and double packer is replacing the flow guide. Total pressure (hydrostatic + atmospheric pressure) is measured by means of flow sensor, which measures flow along a drillhole. The flow along a drillhole is guided through tubes inside both packers (Pekkanen & Komulainen 20xx – in prep.).

The results of PFL DOPP measurement show the hydraulic head of the measurement section. These results can also be evaluated based on PFL DIFF measurements, which are done under two different pressure conditions. Pressure measuring with the double packer pressure probe is so slow that it cannot be done in all detected fractures (Pekkanen & Komulainen 20xx – in prep.).

The PFL DOPP measurement elaborates the results of PFL DIFF measurement, and is used in situations where evaluation of the hydraulic head based on PFL DIFF is difficult or when very high accuracy is needed. Problems in obtaining good hydraulic head values can be caused by very small flow values or if the hydraulic head value is very low (Pekkanen & Komulainen 20xx – in prep.).

5.1.4 Multi-packer system

Nowadays, most drillholes located at Olkiluoto are packed using the multi-packer system (Figure 4). The aim of using this system is to isolate interesting parts of the drillholes into their own sections (Öhberg 2006). An isolated section can be based on e.g. monitoring hydraulic head in HZ structures or a need to take groundwater samples from certain drillhole section. Usually the hydraulic head and representative hydrogeochemistry samples are the most important monitored results from the isolated sections. The multi-packer system consists of inflatable rubber-coated packers connected to each other by extension rods (Öhberg 2006). The pressure hoses diameter is 8/6 mm and it connects all the packers together (Voipio et al. 2004). The pressure hose is made of polyamide.

According to Öhberg (2006), the principle of the multi-packer system is simple (Figure 4). The inflatable rubber-coated packers are installed at the desired depth. During the installation of the packers, the pressure hose is filled with fresh water. When the inflatable rubber-coated packers are at the desired depth, the amount of fresh water in the pressure hose is increased, causing overpressure, which expands the rubber-coated packers against the drillhole wall. The expanded packers then isolate the desired packed-off sections.

There are also measuring hoses in each packed-off section. The diameter of a measuring hose is usually 8/6 mm. A measuring hose from each single packed-off section is led to the ground surface. The slim measuring hoses are connected to a tube of larger diameter

(28/23 mm) (Öhberg 2006). This connection takes place approximately at a depth of 35 metres below the ground surface (Alhonmäki-Aaltonen. 1999. according to Öhberg 2006).

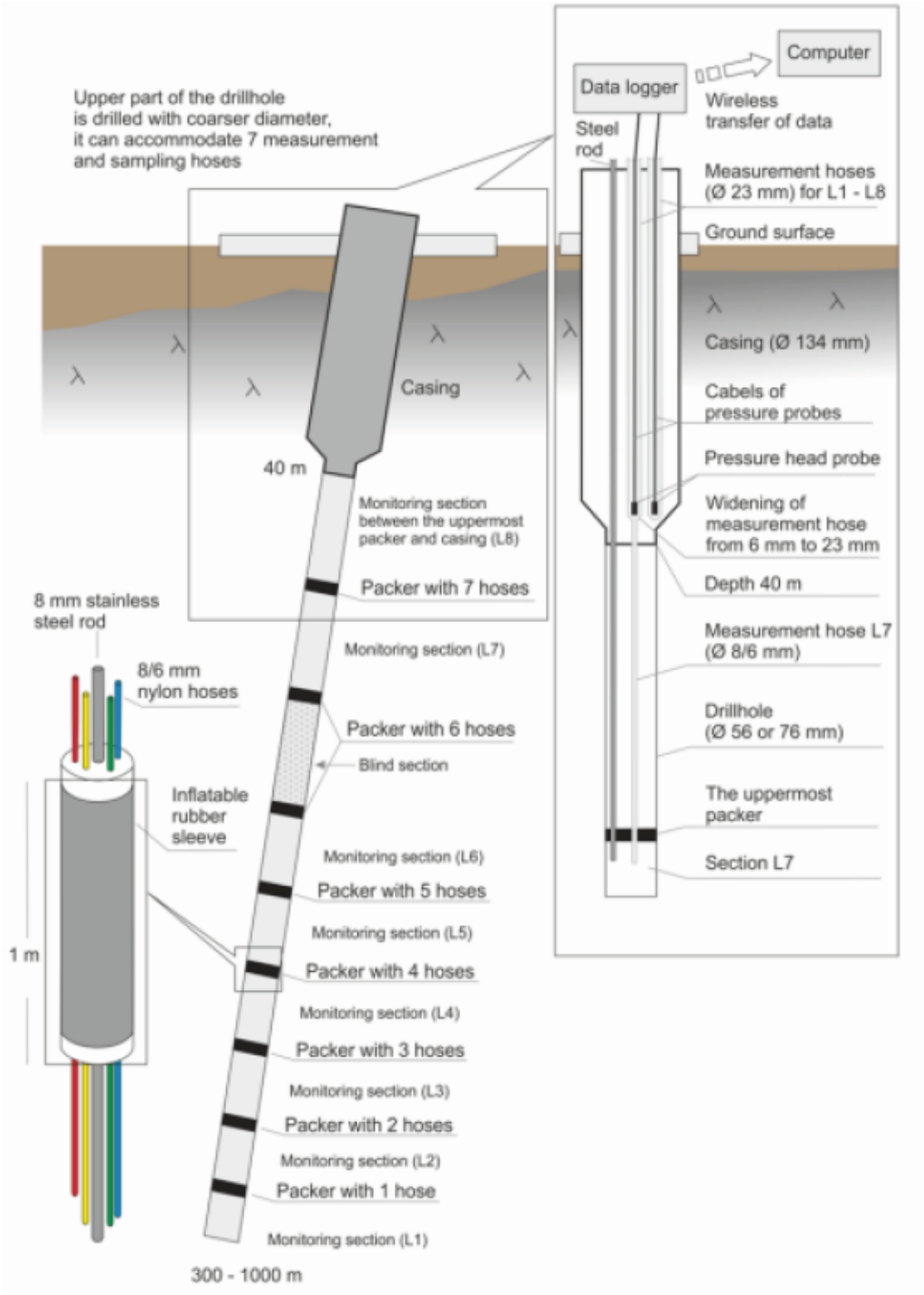

Figure 6. Principle of the multi-packer system. Figure was originally presented by Pentti & Vaittinen (2018). Figure is published with Posiva's permission.

The number of measured packed-off sections is considered per hole and is limited because measuring hoses need space and space is limited in the drillhole. Usually there are more packers in the drillhole than are needed in the measured packed-off sections. More packers are used to prevent the connections of different measured packed-off sections along the drillhole. Due to the large number of packers, there are several "blind" sections in the drillhole, which do not belong to the hydraulic head monitoring (Öhberg 2006).

The measuring hoses in the upper part of a drillhole have a larger diameter, so that the standard pressure probes can be installed into the hose to measure the pressure caused by the water column above the pressure probe. The other reason is that a slim membrane pump for the groundwater sampling needs to be installed in the measuring hose (Öhberg 2006).

In the saline water sections, the installation of inflated rubber-coated packers differs a little. If there is saline water in the drillhole section, the measuring hoses are filled with fresh water before the inflation of the packers. This is because the water table in each measuring hose is directly linked to the fresh water head (Öhberg 2006).

5.1.5 GWMS

Posiva has been using a GWMS (GroundWater Monitoring System) for monitoring a hydraulic head in deep drillholes equipped with the multipacker system since 2000 (Öhberg 2006). The GWMS system consists of pressure probes installed in measuring hoses to depths between 15–38 m (Pentti & Vaittinen 2018). The probes measure the water table above them, and are connected to a logging device, which collects data from the pressure probes and transfers it to the monitoring unit by GSM modem (Pentti & Vaittinen 2018). From the monitoring unit, the data is transferred to POTTI, which is a database for all the research data produced by Posiva.

The pressure sensors are calibrated on a regular basis. In the calibration, the rejection limit for the probe is 23–45 cm of the measuring range depending on the probe (Pentti & Vaittinen 2018). The error limit for measurement is only a few centimetres, which is based on practical experience.

The hydraulic head data from GWMS is corrected by subtracting natural effects (natural fluctuation of groundwater table and sea level, tides and atmospheric pressure) from the data. This is done in order to have more reliable and less disturbed hydraulic head data which eases the observation of hydraulic responses. The correction is done by mathematical equations, which are presented by Pentti & Vaittinen (2018). Nowadays, the correction of tide effect is based on a mathematic value presented by Van Camp & Vauterin (2005). Basically, it is an estimated value of the variation of the vertical tidal power at the Olkiluoto site (Pentti 2019). The calculation of tidal effect is discussed more accurately by Pentti & Vaittinen (2018). Corrections to the GWMS-data presented in the thesis are made by Pöyry.

The correction of sea level is based on sea level measurements done by the Meteorological Institute at the Rauma harbour mareograph (Pentti 2019). The natural fluctuation correction factor is based on groundwater table data collected by Posiva from different observation points over the years (Pentti & Vaittinen 2018; Pentti 2019). Nowadays this correction factor is based on the natural fluctuation data from 11 shallow holes and from five different EP L4 sections data (Pentti 2019). The principle of calculating the hydraulic head is presented in Section 7.4.1 (Equations 8 & 9).

Due to the salinity variation (Section 3.4) of groundwater at Olkiluoto, there are some uncertainties in the observed head levels between different drillholes. The pressure hose is filled with fresh water before the installation of the pressure probes to get standardised observations of hydraulic head between different drillholes. During groundwater sampling (Section 5.2.3), the measuring hose is filled up with groundwater from the depth of the measuring section, i.e. with fracture-specific groundwater from fractures in the measuring section. For this reason, the measuring hose needs to be filled with fresh water again to be able to follow the representative *in situ* fresh water head values after groundwater sampling.

5.2 Hydrogeochemistry

5.2.1 Monitored parameters of the OMO programme

Monitoring of hydrogeochemistry on Olkiluoto is based on laboratory analysis of samples taken from surface water as well as shallow and deep groundwater. The areas of research related to hydrogeochemistry include the chemistry of groundwater (salinity, anions, cations, isotopes etc.), microbial studies and dissolved gases in groundwater. (Posiva 2012a)

There are three different groundwater sampling methods, which Posiva has been using over the years: the double packer system, membrane pump (in multi-packered drillholes) and PAVE equipment (pressurised water sampling equipment) (Öhberg 2006). Also the PFL equipment has been used for the taking of water samples.

Some farctors must be taken into account when selecting the desired sampling method. One is conditions in the drillhole (open or a multi-packered) and another is the aim of the investigation (Öhberg 2006), which can influence the choice of sampling method.

In addition to above-mentioned groundwater sampling locations, groundwater samples can be taken example from from measuring weirs or from leaking fractures at ONKALO. Samples can also be collected from the ditches near ONKALO and the nearby rock crushing area. Ditch samples are related to the surface environment monitoring (Posiva 2012a).

A membrane pump called a Vesitin pump has been used in the multi-packered drillholes (Öhberg 2006). Most of the sampling methods have been used in open drillholes. Before the development of the PAVE equipment, Posiva used the double packer system and a membrane pump to sample from open drillholes (Öhberg 2006). As a simplified way, PAVE equipment is used in open drillholes when sampling includes analyses of dissolved gases or microbes. If there is no need to analyse anything other than the chemistry of groundwater, the double packer system is still used, as it was for example in upper parts of the OL-KR6 drillhole in autumn 2018.

5.2.2 Pressurised sampling with PAVE equipment

The PAVE equipment enables groundwater sampling with in-situ pressure from deep drillholes. It also makes it possible to study dissolved gases and microbes. PAVE equipment consists of different parts, one of which is the wire-line system, which consists of one or two inflatable rubber packers, the PAVE unit and membrane pump. Another part is the field monitoring system, which measures continuosly Eh, pH, O_2, temperature and EC from the groundwater pumped to the surface.

A winch cable is used to lower and lift the part of the equipment placed at the drillhole. The sampling section is isolated from the rest of the drillhole by two inflatable rubber packers (Öhberg 2006). For example, PAVE sampling from OL-KR6 was done in an isolated section at a depth of 422–425 metres on January, 2019. The diameter of a drillhole must be 56–76 mm and its maximum length can be 1,500 metres (Öhberg 2006).

There is a pre-pumping period prior to the sampling. During the pre-pumping period, groundwater is passed by the pressure vessels so that inner parts of the pressure vessels will not be contaminated by microbial biofilms, drilling debris or other fine material. The pre-pumping period is finished and sampling period begun when the monitored on-line parameters have been stabilised (Öhberg 2006). The parameters included in on-line monitoring are pH, electrical conductivity (EC), redox potential (Eh) and oxygen (O_2).

Before starting the sampling period, the water in the sampling section and measuring hose must change at least three times and the analysed tracer (sodium fluorescein), used in drilling water, concentration must be < 5 µg/l (Öhberg 2006). This is called the pre-pumping period, which stops when the monitored online parameters have been stabilised. Sodium fluorescein is a tracer element, which is dissolved in water and used as a tracer by Posiva. Tracer is used to detect the water used for construction activites, drillings etc. from the representative natural groundwater (from fractures). The chemical quality of groundwater is considered representative when the concentration of sodium fluorescein is < 5 µg/l. Once the on-line parameters have settled down, water of the sampling section has changed three times and the chemical quality of a groundwater is representative, the sampling can start.

A water sample is collected in a pressure vessel of the PAVE equipment above the upper packer. The volume of the pressure vessel varies depending on the scale of the investigation, and is either 150 ml or 250 ml. The PAVE equipment allows the combination of 1–3 different-sized pressure vessels to be used at the same time. Groundwater is pumped to the surface with a membrane pump. The membrane pump is attached to the other instrumentation, and is used either with a combination of a nitrogen gas and water or only with water (Öhberg 2006).

The pressure vessels are filled with groundwater during the sampling period. When the hydraulic pressure increases in the pressure hose for the packers, it opens the pressure-regulated control valve. When this valve is opened, it allows groundwater to flow through the pressure vessels, causing compression of back-pressure gases in a pressure compartment due to the piston moving downwards. In this way, groundwater at in-situ pressure fills the sample compartment, and is pumped through the pressure vessel for hours/days in order to get samples with good quality. The valve is closed when the pressure from the pressure hose is released, then the PAVE equipment with the pressurised water samples are lifted up to the ground. The pressure vessels are closed and removed from the PAVE unit and sent to the laboratories for analyses (Öhberg 2006).

5.2.3 Field monitoring system (Kennosto)

The field monitoring system called Kennosto is located at the ground surface. All the groundwater sampling systems can be connected to the field monitoring system, which consists of two separated units, the electric unit and measuring unit. The measuring unit consists of flow-through cells with electrodes and the circulating water pump (Posiva 2018).

The electric unit consists of transmitters, data acquisition equipment and the couplings needed to control the pumping (Posiva 2018.). It is important to protect the field measuring unit from the effects of weather (rain, cold, etc.), so the field measuring unit is placed in a sheltered place above the drillhole (Öhberg 2006). The measuring results from the electrodes of the flow-through cells are recorded in a datalogger from which the data is transferred throughout the GSM network to POTTI (Posiva 2018).

Kennosto is used to control groundwater pumping and to follow groundwater quality continuously during pumping (Posiva 2018.). In practice, Kennosto measures pH, EC, O_2 (ppb), Eh and temperature from pumped groundwater by means of electrodes installed in the flow-through cells. The results of pH- and EC measurements are verified by occasional field measurements with a portable pH and EC measurement gauge (Posiva 2018).

In addition to the above-mentioned measurements, the yield of the measurement section can be measured by means of Kennosto (Posiva 2018). In most cases, first the water is pumped and collected to the Kennosto for three minutes after that the water is pumped to measurement sensors or out of Kennosto for one minute. When taking a sample for measurement, the valve on the outer side of Kennosto must be opened, after which the pumped groundwater exits from Kennosto (Posiva 2018). The groundwater sample is then put in a special sample container (for laboratory samples) or in a measuring dish with scale (for yield, pH, EC field measurements).

6 LONG-TERM PUMPING TEST IN OL-KR6

A long-term groundwater pumping test started on 22 March, 2001 at Olkiluoto in drillhole OL-KR6. The aim was to monitor the effects of long-term pumping from OL-KR6 on groundwater conditions (Reijonen et al. 2015). OL-KR6 is a 601-meter-long drillhole drilled towards NNE (35.9º) at an angle of 50º and is located in the northern parts of Olkiluoto Island (Reijonen et al. 2015). The long-term pumping test on OL-KR6 was stopped on 18 February, 2019 at 11:30 a.m.

The pumping test is a widely used method to investigate the properties of groundwater flow in a certain area (Fitts 2012). Usually the tests are transient unlike in this case. The basic principle of a pumping test is simple and remains the same, whether the test is transient or long-term. Basically, a well or drillhole is pumped at a constant rate for a specified time (Fitts 2012), usually varying from hours to weeks, in this case, years. The head changes caused by pumping are monitored at the pumping well/drillhole and at nearby non-pumping observation points (Fitts 2012). Observation points can be, for example, piezometers, wells or drillholes.

In the case of OL-KR6, the long-term pumping test has been a way to understand the hydrogeological and hydrogeochemical processes at the Olkiluoto site. It began in the investigation phase of ONKALO (2001–2004), continued in the construction phase ONKALO (2004–2012) (Reijonen et al. 2015), and then until spring 2019.

The continuous pumping of OL-KR6 can also be seen as a model of how the underground openings at ONKALO and at the underground disposal facility will affect the hydrogeological and hydrogeochemical conditions on Olkiluoto (Reijonen et al. 2015). Experiences of this test can be utilised when estimating the development of the hydrogeological and hydrogeochemical conditions during the operational period of the final repository.

During long-term pumping, one of the test targets has been to record the pumping rate, and another has been to monitor the quality of the groundwater by regular sampling and

in-situ analyses. In-situ EC measurements, flow rate measurements and chemical analyses of the groundwater have been conducted regularly (Reijonen et al. 2015).

During the long-term pumping test, thousands of cubic metres of groundwater has been pumped from OL-KR6. The amount of groundwater pumped from the drillhole by the end of 2012 was approximately 85,000 m^3 according to (Reijonen et al. 2015). The pumping rate varied between 10 and 25 l/min in the period 2001–2012 (Reijonen et al. 2015). The total amount of pumped water from OL-KR6 during long-term pumping test was approximately a little over 120 000 m^3.

The large groundwater pumping volume from OL-KR6 also helps to understand the effects of ONKALO on groundwater conditions (Reijonen et al. 2015). After stopping the long-term pumping test at OL-KR6 in spring 2019, it has been possible to monitor how fast and in what way the initial groundwater conditions return to their natural state.

An uncertainty related to this thesis is that, because the long-term pumping test has been going on for 18 years (2001–2019), the groundwater conditions in the area may have changed. Another question whether the time between stopping the long-term pumping test and starting the interference test was long enough for the stabilization of the natural conditions. For the aforementioned reasons, PFL DIFF measurement (principles of PFL DIFF presented in Section 5.1.2.) was done in OL-KR6 before starting the interference test. This measurement should indicate whether the transmissivities or flow conditions of the groundwater have changed.

6.1 Results and the observed changes in hydrogeology and hydrogeochemistry near OL-KR6

6.1.1 Hydrogeology

The results of the OL-KR6 long-term pumping test from 2001–2013 are presented by Reijonen et al. (2015). The results from 2014–2019 are presented in figure 8 where pumping is represented by a red line. The amount of pumping was approximately 21–21.5 l /min until February 2016. After that, it was 20.5 l/min. Interruptions (value of pumping rate zero) in pumping were caused by different disturbances like power outages.

The water table (blue line) presented in figure 8 is given as meters from the ground surface. A value of zero in the water table means that it was not measured for some reason. There is a clear sign of seasonal variance in the water table. In late summer, the groundwater table level effected by pumping is lower (approximately 9–10 metres from the ground surface) and in winter/spring it is clearly higher (only 6.5–7.5 metres). Breaks in pumping are recorded as zero in Figure 8. These breaks at OL-KR6 can be seen in GWMS data from other drillholes.

For instance, between 7 and 10 December 2018, there was no power at OL-KR6 and pumping stopped. This caused some disturbance (pressure increased) to GWMS data from OL-KR19, and also some minor disturbance to GWMS data from OL-KR20. This information was used when planning an interference test near OL-KR6 (Section 7.3).

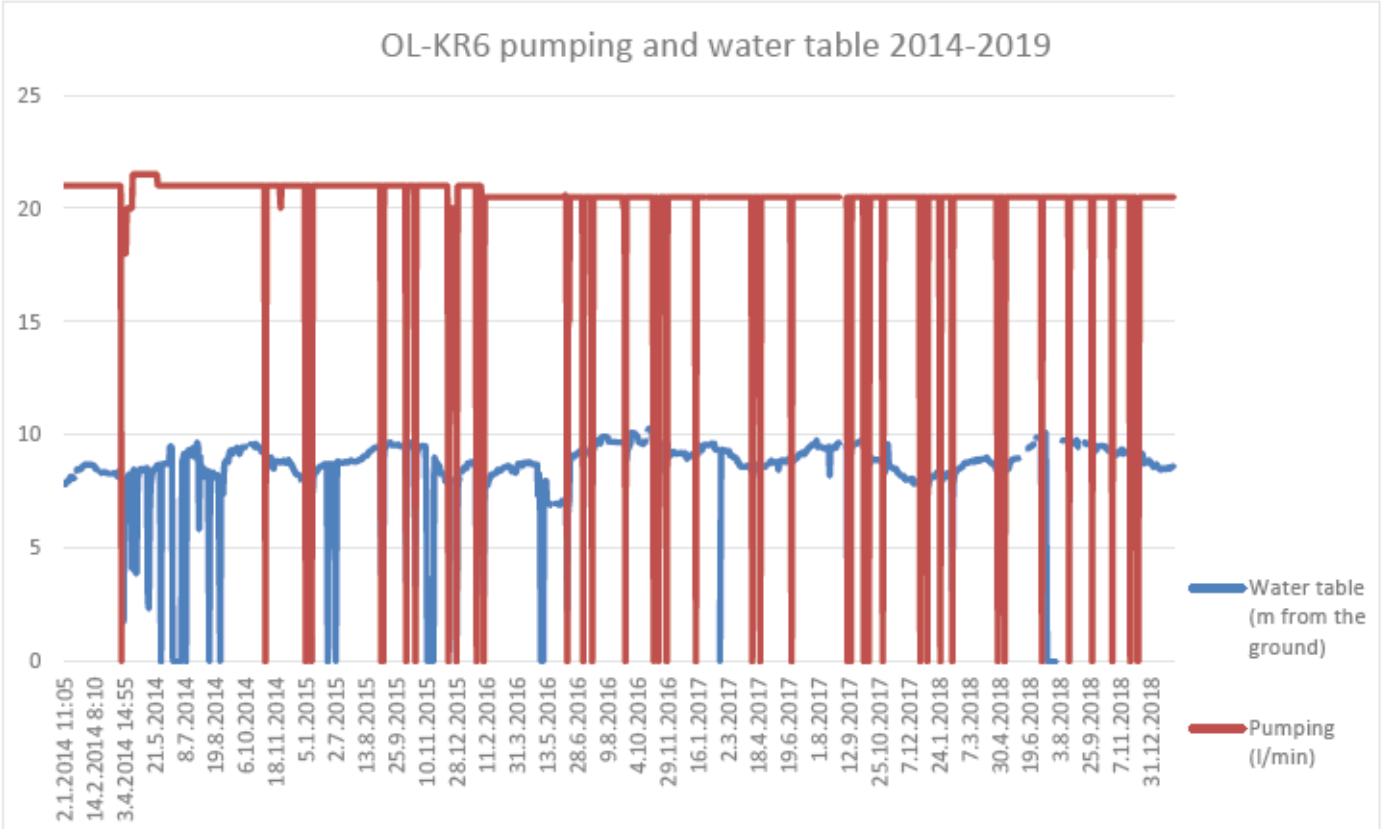

Figure 8. OL-KR6 water table and pumping rate during a long-term pumping test. Possible breaks in pumping are shown as a value of zero (red line).

Development of fracture-specific flow values and changes in flow conditions during the long-term pumping test will be presented later in a separate working report. However, it can be said that dominant fracture-specific flows are located approximately at depth of

30 metres (Posiva 2019). There seems to be no major changes in fracture-specific flows at any depth. The new electrode setup of the PFL device was established in 2014 after which EC values have stabilised more compared to earlier results gained before 2014. (Posiva 2019).

Uncertainity related to the T_{PFL} values (section 3.3.) of OL-KR6 is that the values were measured/ calculated only in 2000. After that, the values could not be calculated because of the long-term pumping test (only one head state). In addition to that, the values had only been reported in Posiva's working report 2012-99 (Ahokas et al. 2012). Transmissivities were defined in 1999 and 2000 and, between these measures, the drillhole was extended. The extension of OL-KR6 hindered the assessment of the most representative T_{PFL} values. In the report it had been evaluated that the highest T_{PFL} value is always the most represantitive value in OL-KR6's case (Ahokas et al. 2012).

OL-KR6 was measured with PFL DIFF before and after the interference test as mentioned before, and there were no notable changes (in the measurement before the interference test) compared to the measurement in 2000. In the PFL measurement done after the interference test, there were some problems during the measurement. This however didn't affect to results of this thesis. The results of these PFL DIFF measurements will be published separately later in a different working report. The preliminary PFL DIFF measurement results before the interference test were utilised when planning the interference test (Section 7.3).

6.1.2 Hydrogeochemistry

The hydrogeochemical results related to the OL-KR6 long-term pumping test are presented in Appendix 1. The red lines on the different tables represent the start of the construction of ONKALO.

Salinity (Cl-concentration) in brackish SO_4 groundwaters was stabilised in 2002–2007. Since then there has been slow, steady dilution. At depth of 97.5–100.5m was change in 2016 and Cl-concentration have stabilized after that. (Posiva 2019)

Development of SO_4 concentration is resembling the development of Cl-concentration, and the evolution of DIC concentration (dissolved inorganic carbon) is opposite to Cl and SO_4 concentrations. This is an indication of an increase in bicarbonate water in relation to SO_4 water and explains the dilution. Small increase of DOC concentration (dissolved organic carbon) could indicate an increase in bicarbonate water. This observation and deduction should consider as uncertain. The increasing DIC concentration at 97.5–100.5 m on 2013 is assumed to be related to the transferring of the extraction pipe for longer distance from OL-KR6. (Posiva 2019)

Also, the DIC concentration indicates the intrusion of bicarbonate water because the DIC concentration of 10–20 mg/L is higher than the initial state of brackish SO_4 groundwater. Isotopes of water (^{18}O) are not sensitive to perceived small changes (Posiva 2019).

On the sampling section 422–425 m, the concentration of SO_4 decreased by approximately 10 % from the 2003 level. In this sampling section, S^{2-} concentration seems to have increased from 2.85 mg/L to 6 mg/L, approximately 110 %. Also, ^{18}O-concentration seems to have been increasing since 2009 (Posiva 2019).

There were no major changes in fracture-specific EC values during the long-term pumping test, but there are small indications of dilution between old and new EC values. These indications support the chemistry results of OL-KR6. During the old EC configuration (Section 5.1.2), it is possible that many of the sampling sections were disturbed by used EC configuration (Posiva 2019).

7 AN INTERFERENCE TEST

An interference test in the OL-KR6 nearby area was done in spring and summer 2019. Planning of the test started in December 2018. The test was done mainly by pumping a specific section of OL-KR6 with a MP pump, and was executed with the modified pumping device presented in Section 7.2.1. The pumping sections of the interference test were selected in collaboration with Pöyry's and Posiva's experts and were based on the 2015 hydrogeological model (Vaittinen et al. 20XX - in prep.), flow-logging data (fracture-specific transmissivities) from PFL measurements and on the results of the long-term pumping test.

The basic principle of the pumping test is described in Section 6.1. Pumping of one part of the drillhole creates a drawdown to the groundwater table near the pumped drillhole (i.e. cone of depression) (Mälkki 1999). When there are several drillholes in the area and hydraulic connections between the drillholes, the drawdown caused by pumping should also be detected from the surrounding drillholes.

In this thesis, the interference test (basically a pumping test on OL-KR6) is meant to cause drawdown to the surrounding area of OL-KR6 (focusing on selected hydrogeological zones). During the test, the GWMS data (Section 5.1.5) will be under more precise monitoring. From GWMS data, it is possible to see the pressure responses caused by drawdown from OL-KR6 pumping.

Drillholes under more precise monitoring are OL-KR2, -KR12, -KR13, -KR19, -KR20 and -KR42 (Figure 9). The distance between OL-KR6 and these drillholes varies between 235 and 505 m.

Figure 9. The drillholes near OL-KR6 under more precise monitoring (red), OL-KR6 (blue). The black colour means that drillhole OL-KR5 has been filled up and monitoring stopped at that drillhole. Map © Posiva.

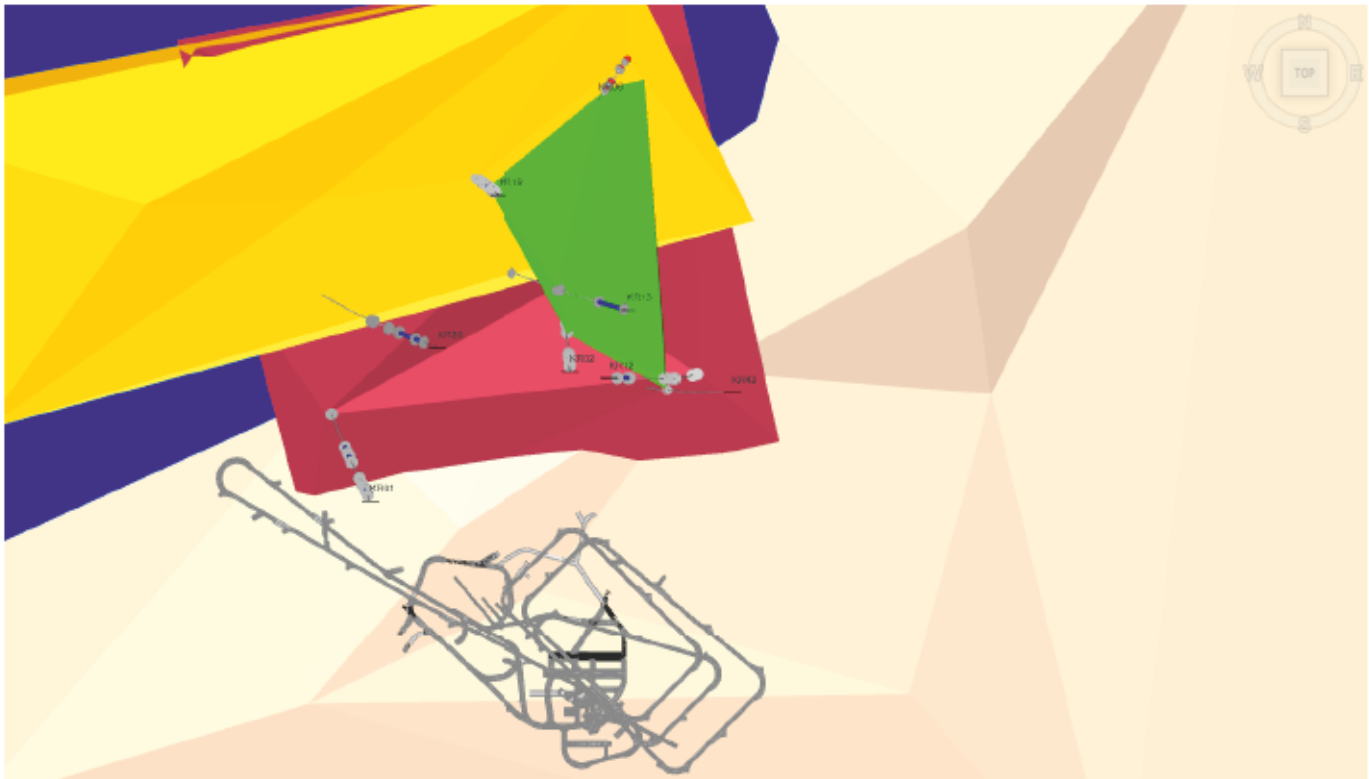

Figure 10. Drillholes included in an interference test and hydrogeological zones in the area. HZL4 is green, HZ001 yellow, HZ099 red, HZ21B blue and HZ21B light brown. A layout of ONKALO is also presented in the figure, which is viewed from above.

One of the aims of this thesis was to verify a hydraulic connection between OL-KR6 and HZ21. The HZ21 connection is uncertain because, during the pumping breaks in the long-term pumping test on OL-KR6, there were no observed connections between OL-KR6 and the HZ21 zone intersections in surrounding drillholes (Reijonen et al. 2015). Another objective was to analyse if there is a connection between OL-KR6 and HZ20A, which was suggested by (Reijonen et al. 2015). Another area of interest was the continuation of the HZL4 zone. One aim was to verify if it reaches OL-KR42. Also of interest is the intersection of the HZ099 zone in OL-KR6. This hydrogeological zone was transposed alongside the geological OL-BFZ099 to OL-KR6 (Vaittinen et al. 20xx. - in prep.).

Uncertainties related to planning an interference test are the effects of the long-term pumping test in OL-KR6 on groundwater flow conditions in the OL-KR6 area. These uncertainties are presented on Section 6.1. Other uncertainties are related to the timetable. It was estimated that within two weeks of the start of pumping on OL-KR6, there should be hydraulic responses in surrounding drillholes, if there is a hydraulic connection between the drillholes. This time value is based on OL-KR6 long-term pumping test data (especially the consequences of the pumping breaks on OL-KR6), experiences of earlier interference tests (e.g. Pentti et al. 2019) and expert estimates. Because the time of this test was limited, pumping at each section lasted two weeks at most.

7.1 Interference test equipment specifications

7.1.1 Equipment overview (pumping)

The interference test on OL-KR6 was done by modified equipment (Figure 11). It consists of some parts of PFL equipment (Section 5.1.2 & 5.1.3) and two inflatable rubberpackers. One utilised component was also a pump container, which was used in an OL-KR29 pumping test years before (Pentti et al. 2018.). The used pump is a normal MP pump (Section 7.2.2).

Rubberpackers are normal ones also used in the multi-packer system in other drillholes. The only difference is that there is a larger lead-through probe through the upper packer (20 mm). Usually the lead-through probes are 8/6 mm, so this time there was add-on equipment above the upperpacker.

The lowest part of the system is the lower rubberpacker (Figure 11) from which there is a flow-through probe (Figure 11.) through the test section to a point above the upper packer. This is done to prevent possible large pressure differences around the test section. There are also 1–2 additional weights (20 kg each) to facilitate the installation of the system in the drillhole.

The lower packer is connected to the upper packer by stainless steel rods. There is also a pressure probe (Figure 11.) for both the packers from above ground. The packers are puffed up with water pumped through the pressure probe.

The upper packer is connected to the SPR sensor (Figure 11) with a stainless-steel rod. The larger sample probe has the aforementioned stainless-steel add-on equipment. It connects a larger diameter sample probe to four small sample probes (diameter 8/6mm), which go through the SPR sensor to the upper part of the system where they are connected to the aforementioned add-on equipment. The other end of the add-on equipment is connected to a larger sample probe (inner diameter 20mm), which is connected to the pump container.

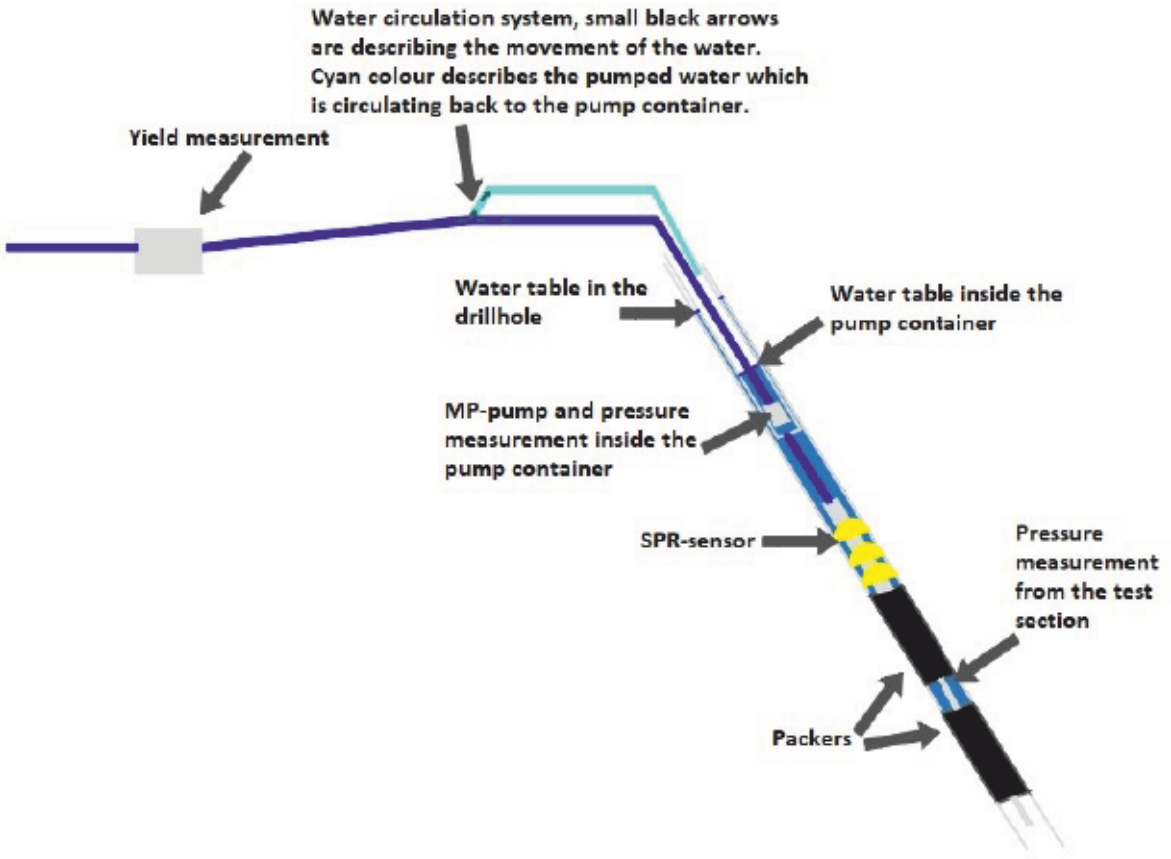

Figure 11. Conceptual visualisation of the interference test equipment. The figure is not to scale. The figure shows measured values (i.e. hydraulic heads of the drillhole, pump container and test section).

Inside the SPR sensor (Figure 11) is a PFL DIFF pressure probe, which measures the sum of atmospheric and hydrostatic pressure inside the test section (absolute pressure) (Pekkanen & Komulainen 20xx – in prep.). Atmospheric pressure is also measured separately. The atmospheric pressure recorded at the site is first subtracted from the absolute pressure measured by the pressure sensor (Pekkanen & Komulainen 20xx – in prep.), then the hydraulic head can be calculated. The calculation of the hydraulic head is presented on Section 7.4.1.

The SPR sensor (Single Point Resistance) is used when installing the investigation equipment to the right depth. Above the SPR sensor there is also a stone collector (in Finnish "kivikuppi"), it is supposed to protect the equipment from debris and rocks) that can be used to prevent the equipment to get stuck in the drillhole. The SPR sensor is

connected to PFL cable through the stone collector. Inside the cable are the electronics used to transfer pressure data from the pressure sensor to the computer located in the PFL trailer (Heikkinen 2019. - personal information).

The pump container is at a depth of 20–40 metres. The lowest part of the pump container is made of stainless steel. The pump container is connected to plastic PEH probes (diameter 63/51 mm), the lowest of which is connected to a pump container with a thread connection and some spiral tape on it. PEH probes are connected to each other by thread connections and inside every junction is a rubber O-ring used to seal it. The PEH probes are each 2 metres long, except the lowest and uppermost, which are 1 metre long. There are a total of 19 2 m-long PEH probes and two 1 m ones. The last probe extends approximately 1 metre above ground.

The MP pump is installed inside the pump container (Figure 7) through PEH probes. The pump is connected to a plastic probe and above ground there are forked valves. This was done to create circulation for some of the pumped water (Figure 7), which was needed because the supposed pumping rate was so low in most of the test sections. Otherwise the water would have ended and the pump would have started to cavitate which would have created problems.

The system is based on the water table in the drillhole being the same as inside the pump container and PEH probes. In this way, the hydraulic heads are also equal in the test section, in the pump container and in the drillhole. On the other hand, in reality there are some differences in the hydraulic head at lower depths because the salinity of the water differs depending of the depth (Section 3.4). Usually, because of this, the hydraulic head is higher in the test section than the freshwater head in the drillhole and pump container.

When pumping is started, the water table (and hydraulic head) decrease dramatically inside the pump container. This creates a pressure difference (hydraulic gradient, Section 3.6) between the test section and pump container. The pressure difference creates suction from the test section to the pump container and the pressure in test section decreases too. This enables a drawdown in the test section.

7.1.2 Equipment overview (overpressure)

The overpressure was utilized in the third pumping (Ch 7.5.3.). Basically the equipment was the same as in the pumping. Still there were some differences. One was the fact that there were no pressure measurement inside the PEH-probes (pump container). The packers used for isolate the test section were same as in the pumping cases. The water table on drillhole as well as the hydraulic head in the test section were measured as in the pumping cases.

Overpressuring is executed by means of a kind of plug (Figure 12.). Plug is inserted to upperparts of pump container. Plug is puffed out in order to isolate the pump container from air. Through the plug there is a hose from which the water is pumped to the pump container. As a consequence the pressure on the pump container starts to increase and after this the pressure will increase also in the test section.

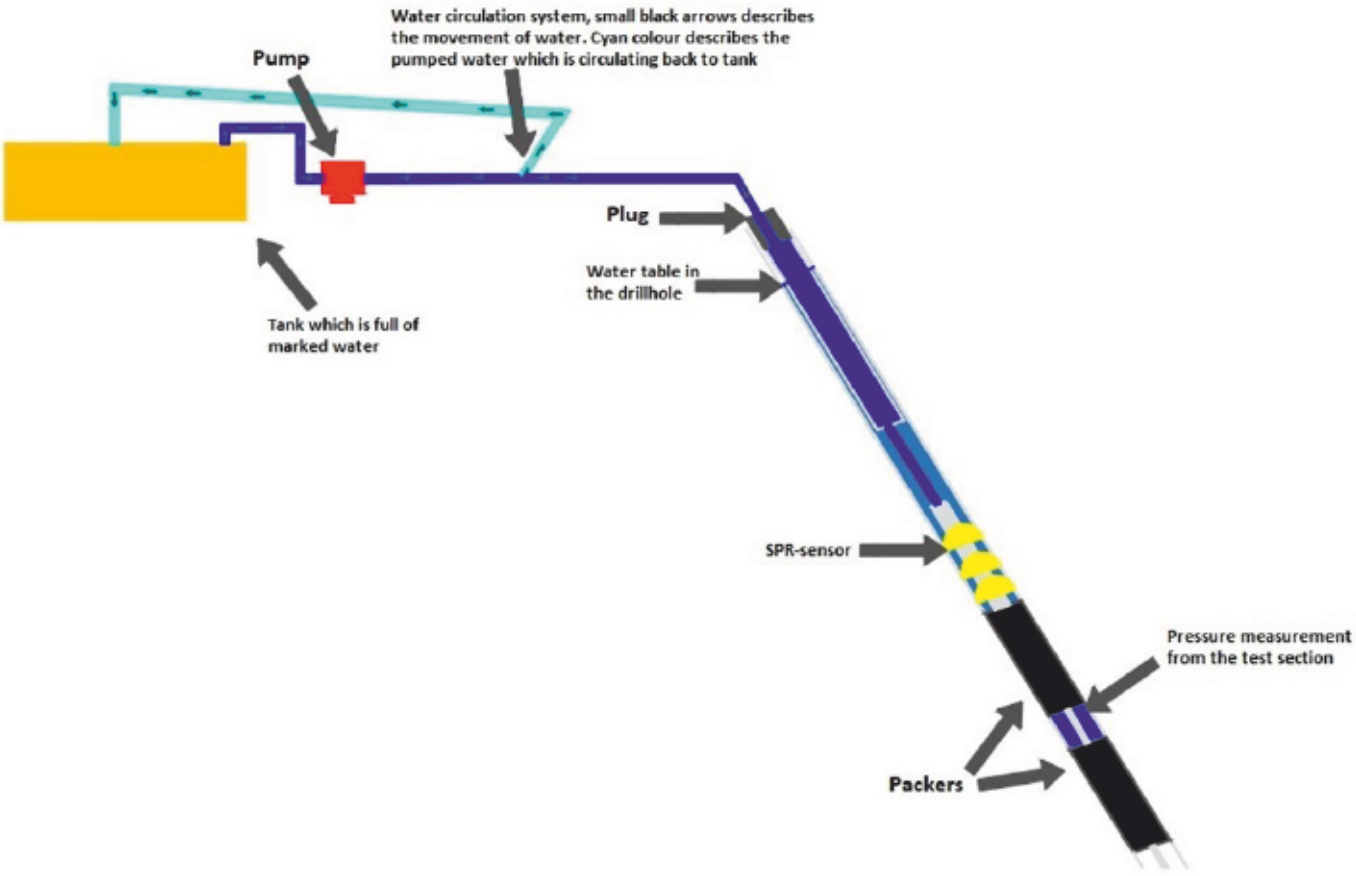

Figure 12. Conceptual visualisation of the interference test (overpressure) equipment. The figure is not to scale. The figure shows measured values (i.e. hydraulic heads of the drillhole and test section

The circulation system (Figure 12) was also utilized in the overpressuring equipment. It was used in order to prevent the increase of pressure which could break the pumpcontainer.

7.1.3 MP pump

The pump used in the interference test was an MP 1 pump designed by Grundfos. It is an electrically driven 2" submersible pump made for purging or sampling contaminated/ polluted groundwater. It is driven by an adjustable BMI/MP 1 converter in the 50 to 400 Hz frequency range and its nominal performance is 1 m^3/h at 75 m head. Nominal flow rate range is 0.1–1 m^3/h (Eijkelkamp 2019).

A converter is used to adjust the frequency of the pump, which adjusts the pump speed, but the yield of the pumped well/drillhole/isolated section should be higher than the pumping rate. If the yield is smaller, the water table may fall below the suction interconnector and air will be sucked into the pump. This reduces the cooling of the motor and the pump can be damaged.

The problem of the used MP1 pump is the fact that it has not been designed for continuous pumping, which could cause some problems if pumping times drag on for longer than planned.

7.2 Planning of the interference test

The planning of the interference test started in December 2018. The process of planning the interference test was gradual as follows:

1. The current hydrogeological model of the OL-KR6 area was studied.
2. The fracture-specific PFL transmissivity values were viewed from OL-KR6 PFL data.
3. Data from 1 and 2 were combined with the OL-KR6 structural model (Vaittinen et al. 20xx) and drillhole lengths for pumping were selected.
4. The precise positions of the inflatable rubber packers were selected based on the geological and geophysical data from Hyperdata software.

5. The amount of pumping needed for 10 m drawdown in OL-KR6 was calculated.
6. Prioritisation with selected drillhole sections was done based on the interest of transmissivities. In reality, because of our equipment specifications we were forced to pump from the lowest test section and proceed to the upper sections.

The exception to point 6 was the first pumping (plan for pumping is presented on figure 13), which was done from a depth of 50 metres. This was done to test that our equipment was working, and because, if there had been some problems with the equipment, possible improvements would have been easier to do while the equipment was closer to the ground surface.

The amount of pumping needed for 10 m drawdown can be calculated as follows (Pekkanen & Komulainen 20xx – in prep.):

$$Q_{s2} = T_{PFL,s} \cdot a \cdot (h_s - h_2), \quad (6)$$

where

- Q_{s2} is predicted flow,
- $T_{PFL,s}$ is transmissivity based on PFL measurements
- a is a constant depending on the flow geometry,
- h_2 is the hydraulic head in the drillhole, and
- h_s is the section head far from the drillhole.

In this case the predicted flow (flow rate out from drillhole = amount of pumping) Q is unknown. $T_{PFL,s}$ is calculated based on PFL measurements and fracture-specific transmissivities are added up from the selected drillhole section. The magnitude of desired drawdown is 10 metres, so the value of h_s- h_2 is 10m.

For cylindrical flow, the parameter *a is:*

$$a = \frac{2\pi}{\ln(R/r_0)}, \quad (7)$$

where

- r_0 is the radius of the drillhole and
- R is the radius of influence, i.e., the zone inside which the effect of pumping is felt

There is very little knowledge of flow geometry, so cylindrical flow without skin zones is assumed (Pekkanen & Komulainen 20xx – in prep.). Cylindrical flow geometry is also justified due to the drillhole being at a constant head (Pekkanen & Komulainen 20xx – in prep.). In this case there are no strong pressure gradients along the drillhole except at its ends (Pekkanen & Komulainen 20xx – in prep.).

Also, the radial distance R to the undisturbed hydraulic head h is not known so it must be assumed (Pekkanen & Komulainen 20xx – in prep.). A value of 500 for the R/r0 quotient can be selected, which corresponds to a radius of influence in the order of 19 m when the diameter of the drillhole is 76mm (Pekkanen & Komulainen 20xx – in prep.) as in OL-KR6's case. In practice, this value of 500 means that parameter α can be assumed to be 1.

Calculated pumping rates for 10 m drawdown at OL-KR6 are shown in Figure 13. If necessary the overpressuring can be utilized instead of pumping. In this case the equipment is basically the same, but instead of pumping the water out from the test section, the marked water is pumped to the test section (Section 7.1.2). This way the created disturbance is opposite compared to pumping.

Figure 13. Calculated pumping rate Q_{s2} for 10 m drawdown at OL-KR6. Formula is presented in equation 4. In the figure is presented projected test sections.

Measurement section	PFL depth of fracture	Tpfl of each fracture (m2/s)	Tpfl of test section (m2/s)	Wanted drawdown (m) (hs-h2)	Qs2 (l/min)
28.9-34.8m	29.4	3.40E-08	1.79E-05	10	10.76
	30.4	1.80E-08			
	30.85	5.90E-09			
	32.8	*7.60E-06*			
	33.6	*1.00E-05*			
	33.9	*2.80E-07*			
48-61m	*48.1*	*1.70E-08*	3.93E-05	10	23.56
	48.8	*4.30E-06*			
	49.1	*1.40E-06*			
	49.5	*7.80E-08*			
	50.4	*9.30E-09*			
	51.1	*8.70E-09*			
	52	*1.50E-08*			
	52.6	*5.0E-06*			
	54.4	*8.5E-08*			
	55.2	*6.8E-06*			
	55.8	*3.0E-08*			
	56.5	*4.70E-07*			
	57	*2.00E-06*			
	59	*1.90E-05*			
	61	5.80E-08			
96.5-102.4m	*99.8*	*5.80E-06*	5.80E-06	10	3.48
122.9-140.6m	*126.2*	1.0E-07	6.95E-06	10	4.17
	128.8	8.3E-07			
	129.8	4.0E-08			
	130.4	7.9E-08			
	136.1	*5.90E-06*			
393.5-400m	*397.2*	*6.00E-06*	6.00E-06	10	3.60
421.5-428m	423.6	1.1E-07	1.10E-07	10	0.07

The uncertainties related to the calculation of T_{PFL}-values and to hydraulic head has been discussed on (Pekkanen & Komulainen 20xx – in prep.). To cut a long story short, it can be said that since the flow geometry and skin effects are basically unknown, PFL transmissivities should be considered as an indication of the order of magnitude of real transmissivity (Pekkanen & Komulainen 20xx – in prep.). Calculated hydraulic heads do not depend on geometrical properties, but only on the ratio of the flows measured at different heads in the drillhole (Pekkanen & Komulainen 20xx – in prep.). For this reason, they should be less sensitive to unknown fracture geometry (Pekkanen & Komulainen 20xx – in prep.). Principle of T_{PFL}-values is presented in section 2.2.1.

7.3 Interpretation

7.3.1 Hydraulic head

The measured hydraulic head from GWMS data is related to the salinity (density) conditions of the groundwater in the bedrock. The hydraulic head (h) in fresh water (constant density) conditions is the sum of two different components: the elevation of the point of measurement (or elevation head) z and pressure head h_p (Ahokas et al. 2008):

$$h = z + h_p \tag{8}$$

Pressure head h_p is the same as the height of the water column in a hose and can be expressed as:

$$h_p = \frac{p}{\rho g} \tag{9}$$

where

- h_p is the pressure head
- p is the pressure water column
- ρ is the density of the water
- g is the acceleration of gravity

Based on this equation, it can be said that pressure head h_p is highly dependent on the density of water (Ahokas et al. 2008). Usually, the density of water varies as a result of the salinity differences and temperature of the water, as mentioned before.

In the Posiva's measurements (GWMS data), the effect of water density on the hydraulic head value is excluded by fresh water filling the measurement hose (Pentti & Vaittinen 2018). In this case, the pressure sensor measures the vertical length of the water above the sensor. When the depth of the pressure sensor in the measurement hose and its' relation to sea level are known, the hydraulic head in m.a.s.l (meters above sea level) can be calculated.

The success of fresh water filling is critical for the aforementioned reasons. If for some reason the fresh water filling is unsuccessful, the measured hydraulic head value will be incorrect.

7.3.2 Hydraulic head based on PFL measurements

The source information for calculating the hydraulic head based on PFL measurements is presented on Section 7.2.1. According to Pekkanen & Komulainen 20xx (in prep.), the hydraulic head (h_{pfl}) at a certain elevation z is calculated as follows:

$$h_{pfl} = \frac{p_{abs} - p_b}{\rho \cdot g} + z, \quad (10)$$

where

- h_{pfl} is the hydraulic head (masl)
- p_{abs} is the absolute pressure (Pa),
- p_b is the barometric (atmospheric) pressure (Pa),
- ρ is the density of water 1,000 kg/m3,
- g is standard gravity 9.80665 m/s2, and
- z is the elevation at the measurement location (masl).

For the calculation of the hydraulic head, it is important that the z-coordinate is exact. An error in this leads to an equal error in the calculated head (Pekkanen & Komulainen 20xx – in prep.). As can be seen from the equation, the density of the water also influences the hydraulic head.

Basically, the difference between equations 9 and 10 is caused by the function of the pressure sensors. The PFL pressure sensor measures a sum of atmospheric pressure (p_b) and absolute pressure (p_{abs}). For this reason, atmospheric pressure should be subtracted from measured absolute pressure in the equation. Calculated hydraulic heads during the pumpings are presented in Appendix 3 and, at OL-KR42, PFL DOPP measurement is presented in Appendix 2.

7.3.3 Hydraulic responses

There are a total of three different kinds of solutions to calculate the hydraulic response of pumping. The solutions are presented by Pentti & Vaittinen (2018). In this thesis these hydraulic response is calculated from corrected GWMS-data. The first is to determine the hydraulic head at the beginning and end of the pumping. When the hydraulic head at the end of pumping is subtracted from the hydraulic head at the beginning, the magnitude of the hydraulic response can be determined.

The second is to determine the minimum head during pumping and to subtract it from the head at the beginning. This way, it is possible to determine the magnitude of the hydraulic response. The third way is to find the maximum hydraulic head during pumping and to calculate the difference between the maximum hydraulic head and the head at the beginning of the pumping (Pentti &Vaittinen 2018). In this Thesis the second solution is utilised.

The hydraulic responses during an interference test were relatively small. For this reason some classification was necessary for visualisation of the hydraulic responses. The responses are classified in this Thesis as weak (< 20 cm), medium (20–40 cm) and strong (> 40 cm). This classification is based on pressure responses detected in OL-KR19 during OL-KR6 long-term pumping test.

Pressure responses from field activities in OL-KR19 are presented in table 4-50 by Pentti & Vaittinen (2018). For this thesis some evaluation was done. It was detected that 20 cm and 40–50 cm are sort of "limits". During breaks of OL-KR6 long-term pumping test in 2015-2016 great amount of hydraulic responses ≤ 20 cm so it was defined as "lower limit". The upper limit was defined as 40 cm because there were less hydraulic responses > 40 cm and on the other hand the major part of the detected and evaluated responses were between 20–40 cm. Presented weak hydraulic responses are included in this thesis only if the times between the OL-KR6 and drawdowns match to each other.

It should be remembered that there are some uncertainities related to hydraulic responses. According to Pentti & Vaittinen (2018) the uncertainities are: location of packed-off sections, transmissivity variation, effects of saline groundwater, near surface fracturing

and open drillholes and long monitoring sections. These uncertainities are discussed further in Pentti & Vaittinen (2018).

7.4 Field work

The field work during the installation of the equipment for the interference test was important in order to ensure reliable results. Part of this thesis was to be involved in activities in the field during the installation of the OL-KR6 equipment and OL-KR42 PFL DOPP equipment. All the installations took approximately 160 hours of work.

The chemical properties (pH-, EC-values) were also measured during the pumping by means of pH and EC gauge (except the first pumping). The measurement was done by taking the pumped water to measure glass. After that the EC-sensor from pH/EC gauge was rinsed with refined water (MQ-water). After that the EC of the water is measured by installing the EC sensor to water. After that the procedure is repeated with pH sensor.

The field work was a continuous learning process because the used equipment was unique and planned especially for this test. For this reason, there were doubts related to the equipment before starting the interference test, mostly concerning the pump container and circulation system. During the field work, things were improved such as the orientation of the pressure probe and the PFL cable during the laying of the pump container. This was important because, if the pressure probe and PFL cable would have got wrapped around the pump container, it had caused the equipment to get stuck in the drillhole.

The field work comprised a major part of the work related to this thesis due to the equipment specifications (Section 7.1.1). When the length of the test section was changed, the whole equipment had to be lifted up from OL-KR6. In this case the length of the test section was changed. When the length of the test section was the same between the pumpings, only the pump container was lifted up. In this case also the whole equipment was lifted up for certain distance along drillhole and equal length (i.e. distance between the test sections; length along the drillhole) was removed from both the pressure hose and the 20 mm hose between the upper packer and the pump container. After that the pump container was connected to 20 mm hose and was installed to next depth.

Figure 14. Installation of the packers in the drillhole during the field work. The figure shows the lower part of the upper packer, pressure probe (blue probe), flow-through probe (white) and stainless-steel rod.

During the installations, two type of tripods were used (bigger and smaller) in order to facilitate the installation procedure. During the OL-KR42 PFL DOPP installations, the PFL dummy equipment (Figure 15) was also used to "clean" the drillhole of rocks and debris and to prevent the equipment from getting stuck in the drillhole.

Figure 15. PFL Dummy installations on OL-KR42 in August 2019. In the upper part is the brush which is supposed to remove the drillhole debris etc. from the drillhole. Fallen off debris is collected to small container and is documented separately in each Dummy run.

7.5 Results

The results of each pumping during the interference test are presented in Appendix 3. Observed hydraulic responses during the pumpings are presented on figure 28. The principle for calculation of different hydraulic responses are presented on section 7.3.3. All of the presented hydraulic head data from GWMS is corrected by subtracting natural effects as presented on section 5.1.5.

Pumping/measurement section	Detected response (drillhole & section)	Head at the start of the event (m.a.s.l)	Minimun head during the event (m.a.s.l)	Calculated hydraulic response	Modelled Zone (Vaittinen et al. 20XX- in prep.)
OL-KR6 (48- 61 m (1. pumping))	OL-KR19 L3	2.89	2.18	0.71	
	OL-KR19 L4	2.63	1.86	0.77	
	OL-KR19 L5	2.63	2.02	0.61	
	OL-KR19 L6	3.51	2.90	0.61	
	OL-KR19 L7	4.14	3.93	0.21	
	OL-KR19 L8	4.17	3.93	0.24	
	OL-KR2 L5	3.65	3.46	0.19	
	OL-KR13 L4	4.39	4.17	0.22	
OL-KR6 (122.9- 140.6 m (4. pumping))	OL-KR19 L3	3.00	2.84	0.16	HZ001 (and old HZ099)
	OL-KR19 L4	2.75	2.56	0.19	
	OL-KR19 L5	2.81	2.70	0.11	
OL-KR6 (96.5- 102.4 m (5. pumping))	OL-KR19 L3	3.10	2.78	0.32	
	OL-KR19 L4	2.72	2.43	0.29	
	OL-KR19 L5	2.80	2.55	0.25	
	OL-KR19 L6	3.63	3.38	0.25	
OL-KR6 (28.9- 34.8 m (6. pumping))	OL-KR19 L3	2.90	2.36	0.54	HZL4
	OL-KR19 L4	2.67	2.07	0.60	
	OL-KR19 L5	2.75	2.26	0.49	
	OL-KR19 L6	3.60	3.22	0.38	
	OL-KR19 L7	4.52	4.42	0.10	
	OL-KR19 L8	4.55	4.42	0.13	
	OL-KR2 L5	4.02	3.78	0.24	
	OL-KR13 L4	4.66	4.45	0.21	
OL-KR42 (PFL DOPP 306.5- 317.4 m)	OL-KR12 L6	5.90	3.45	2.45	HZL4

Figure 16. Calculated hydraulic responses observed during an interference test. Results are based on corrected data. Hydraulic response is calculated by subtracting the minimum head during the event from the head at the start of the event. Values are presented as meters above sea level, m.a.s.l. L means the packer section of the drillhole; the lowest is L1 and number is growing towards ground surface.

7.5.1 The first pumping

The first pumping was done from the depth of 48–61 m. There were a total of 15 hydraulic fractures between the packers. The number of fractures was based on PFL data. The transmissivities of the fractures varied from 8.70E-09 to 1.90E-05. There were no

modelled hydrogeological zone intersections in this section, but there were high transmissivities and it was interesting to see if there were some hydraulic connections to surrounding drillholes.

Pumping was started on 9 April 2019 at 8:10 a.m. The volume of pumping was approximately 30 L/min, which created 12 m drawdown to the hydraulic head in the test section. The calculated pumping rate (Equation 6) for 12 m drawdown is 28.28 L/min. The theory for the difference between the calculated and real pumping rate is given in Section 7.5.9. Leakage of the packers can also affect the pumping rate.

The volume of pumping was controlled during the test. It was 30 L/min until 12 April at 9:30 a.m, then it was reduced to 20 L/min. On 15 April it was reduced to 11.5 L/min, and on 16 April at 8:45 a.m. to 4.7 L/min. On 18 April at 1:30 p.m. it was increased to 13 L/min, and pumping was stopped on 24 April at 8:30 a.m.

However, the fresh water head on the drillhole started to decrease as the pumping continued. This indicates that there was either leakage throug the upper packer or there was a hydraulic connection via bedrock around the upper packer. The water smelt odd as if the pumped water had sulphide in it. This also indicates leakage from the lower packer (like upper packer), because the sulphide-type water occurs at greater depths than 61 m (100–300 m, as said in Section 3.4.).

The responses could be detected from the GWMS data of OL-KR19 (the closest drillhole) and of OL-EP4 (multi-level piezometer 100 metres from OL-KR6). Pumping at OL-KR6 caused drawdown in OL-KR19 in the test sections L3–L8 (Figures 16 &17). These test sections are between the depths of 328 m and 40 m.

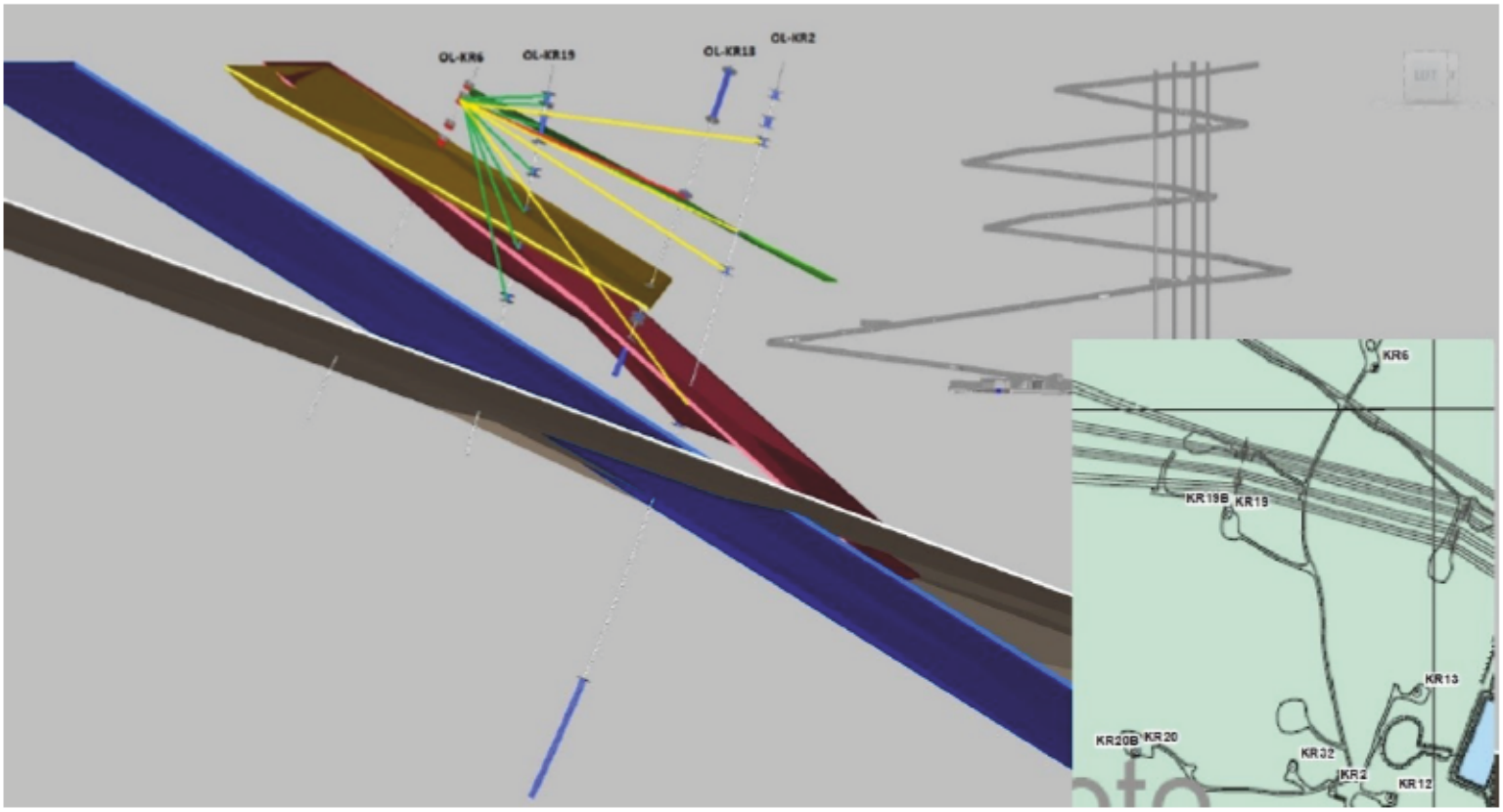

Figure 16. Visualisation of the hydraulic responses during the first pumping. The observed responses were in OL-KR19 sections L3-L8 and OL-EP4. Possible responses were observed at OL-KR2 sections L2, L4–L6 and at OL-KR13 section L4. The figure is not to scale. The hydrogeological zones are same as in Figure 3. Green line is strong (>40cm) and yellow line is medium (20–40cm) hydraulic response.

Because of possible leakage past the packers, there are some uncertainties related to these hydraulic responses. Slight (possible) responses were also detected in OL-KR2 section L5 and OL-KR13 section L4.

A finding from this pumping was that hydraulic responses could be very fast between different observation points. The hydraulic head in the OL-KR19 multi-packer sections started to decrease approximately 3 hours after the pumping started at OL-KR6. The response was fastest in OL-KR19 sections L6–L8. This might indicate that there is a straight hydraulic connection from OL-KR6 (48–61 m) to OL-KR19 sections L6–L8, but

this cannot be confirmed because of (possible) leakage from the packers at OL-KR6. At OL-KR19 L6, the hydraulic head might be responding to changes in pumping rate at OL-KR6, which are not observed as clear and as fast in other packer sections (Figure 17.).

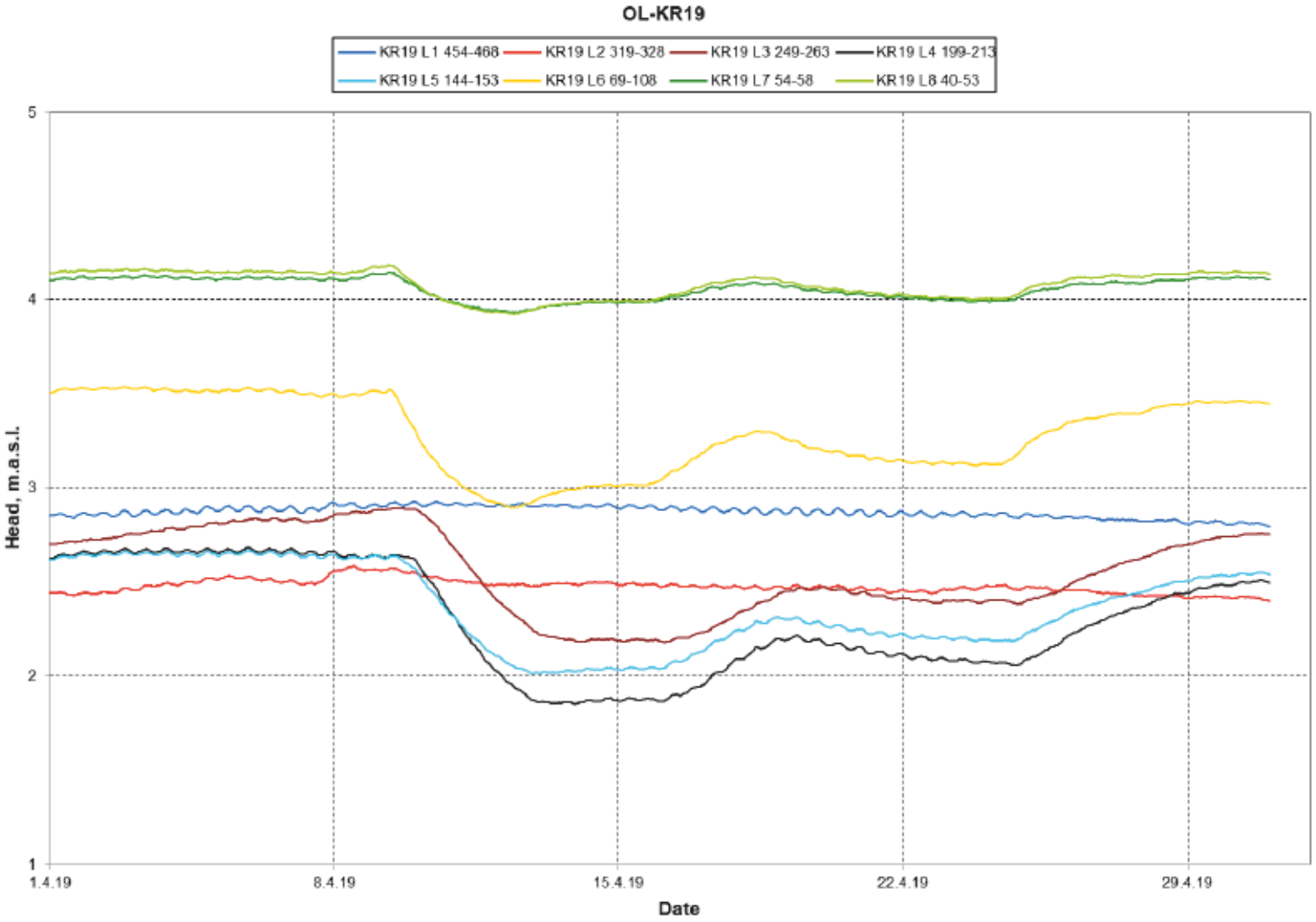

Figure 17. GWMS-data (corrected head) charts from the OL-KR19. Hydraulic responses in sections L3–L8 are obviously seen. Also in section L6 can be seen the response to pumping rate changes in OL-KR6. Little indications like in section L6 can also be seen in sections L7 and L8.

The aforementioned direct hydraulic connection is therefore highly uncertain, but there are still hydraulic connections from OL-KR6 48–61m to OL-KR2 L5, OL-KR13 L4 and OL-KR19 L3–L8. These observations, however, are also uncertain due to possible leakage from packers in OL-KR6 as mentioned before. GWMS data from OL-KR2 and OL-KR13 is presented on Appendix 4.

7.5.2 The second pumping

The second pumping was done from depth of 421.8–428 m. There was only 1 hydraulic fracture between the packers. The transmissivity of the fracture was 1.1E-07 and its depth was 423.6 m according to the PFL measurement. The assumed pumping rate for 10 m drawdown was 0.07 L/min. This section was chosen based on the highest transmissivity, near the modelled HZ21 intersection in OL-KR6. Another reason was technical: there was not enough 20 mm hose (between the pump container and upper packer, see Section 7.1.1) for the equipment to be placed any lower.

The packers were filled on 7 May 2019 at 12:52 p.m. Pumping was started on 8 May at 7:55 a.m. The pumping rate at the beginning of the test was 2 L/min on 8 May at 8:20 a.m. After the desired drawdown was reached, the pumping rate was stabilised at approximately 0.35 L/min. In this case the real pumping rate during the pumping test was approximately five times greater than the calculated pumping rate before the test (0.07 L/min, Figure 13.). The drawdown was approximately 17 m, which was 1.7 times greater than the assumed drawdown. The calculated pumping rate for 17 m drawdown is 0.11 L/min. The theory for the difference between the calculated and real pumping rate is presented on Section 7.5.9.

During the pumping a hydraulic head in the test section (between the packers) rose approximately 1 m, probably due to the more saline water flowing from the fracture to the measurement section (Section 7.3.2, Equation 10). Saline water from the fracture has higher density than drillhole water.

The electrical conductivity measured from the pumped water decreased during the test from 17.7 mS/cm to 16.89 mS/cm, which indicates that there was some fresh water intruding into the pump system. This could be the result of some minor leakage in the pump container or more diluted water flowing to the packer section through the upper packer. The greater pumping rate compared to the calculated pumping rate also indicates minor leakage.

Leakage was, however, so small that it did not affect the success of this pumping test because the drillhole water head did not decrease at all and the desired drawdown in the

measurement section was reached. The stability of the water table at OL-KR6 indicates that there was no leakage by the upper packer. The pumping was stopped on 21 May at 12:45 p.m.

There was some leakage to the pump container, which was proved before the next pumping. When the equipment was moved (Section 7.4), we noticed that one O-ring (Section 7.1.1) was missing from the pump container, which probably caused the small leakage to the pump container. Situation was repaired before next pumping by installing a new O-ring to pump container.

There were no responses in other drillholes during the second pumping. The lowest packer sections of the surrounding drillholes were also disturbed by the start of ONK-PH30 drilling at ONKALO on 13 May 2019. Moreover, PFL DOPP measurement at OL-KR10 during from 29 April to 12 June complicated the interpretation of hydraulic responses. It caused some disturbances in surrounding drillholes.

7.5.3 The third pumping

The third pumping was done at depth of 393.5–400 m. There was only one fracture between the packers. The transmissivity (T_{PFL}) the fracture was 6.00E-06 m^2/s, and its depth was 397.2 m, according to PFL measurement. The assumed pumping rate for 10 m drawdown was 3.60 L/min. This section was chosen due to the modelled HZ21B intersection (Vaittinen et al. 20XX in prep.).

Pumping started on 29 May 2019 at 7:19 a.m. The pumping rate was approximately 1.8 L/min when pumping started. During the test, there were many problems with pumps, which had overheated during the previous pumpings (Figure 18) and also the 20 mm hose from the packers to the pump container was "strangled" because of the pressure difference between the drillhole and inner part of the hose. This was noticed when the equipment was moved for the overpressure test (principle of the operation is presented on (section 7.1.2).

Figure 18. Overheated pump on the third pumping. The normal colour of the MP pump is metallic grey as in the lower parts of the pump. The black contamination on the picture is a mix of iron sulphide and soot. The figure also shows the pressure probe above the MP pump, which measures the hydraulic head inside the pump container.

The aforementioned factors most likely caused the problems for pumps in this test. During the test there were a total of five pump failures. There were probably some problems with the MP pump seal and, if the water table above the pump is high enough, it can cause leakage that may damage the electronics of the pump.

Despite the problems, drawdown of approximately 6 metres was created in the test section. The calculated pumping rate for 6 m drawdown is 2.16 L/min. The real pumping rate between 3 and 10 June was 1.1 L/min. The reason for the difference between the calculated and real pumping rate is presented in Section 7.5.9.

Because of the problems with the pumps, the test was also carried out by using overpressure as hydraulic interference (Figures 12 & 19). A new equipment (7.1.2) was built for this purpose, and overpressurising of the same packer section started on 13 June

2019. Overpressurising was done with marked fresh water (marked with sodium fluorescein, concentration 250 µg/L) between 13 and 20 June. Approximately 20 m^3 of marked water was pumped into the packer section.

Figure 19. The overpressure system at OL-KR6 during 13–20 June. The orange tank is full of marked water that was pumped into OL-KR6.

An approximate 7-meter increase in the hydraulic head of the test section compared to the natural state was created during the overpressurising. The pumping rate was approximately 1.75 L/min. The calculated pumping rate for 0.7 bar (7 metres of water table) overpressure is 2.52 L/min. The theory for the difference between the calculated and real pumping rate is presented in Section 7.5.9. The difference of the hydraulic head of the test section between the lowest and the highest values during the test was approximately 13 metres (1.3 bar).

There were no responses in other drillholes during the third pumping. The test was conducted from 29 May to 20 June, but, because of the problems with the pumps, there were constant pumping breaks until 3 June. During 3–10 June, the pump worked continuously. After the last breakdown on 10 June, it was decided to build the overpressure equipment (between 10 and 13 June).

The disturbance created by pumping and overpressurising maybe should have been longer in order to obtain some hydraulic responses. When creating the opposite disturbance for the groundwater system (drawdown versus overpressure), longer testing times are recommended to be used because of the opposite disturbances interacting in such a way that their effects can be diminished. However, the transmissivity of the fracture was relatively high compared, for example, to the second pumping, which should facilitate the observation of hydraulic responses.

Nevertheless, the pumping rate was approximately 1.1 L/min during pumping. This pumping rate is low and the packer sections at the surrounding drillholes are relatively large (from metres to tens of metres). For this reason, it is possible that even if there are some minor hydraulic connections between OL-KR6 393.5–400 m and surrounding drillholes, the responses are still not shown because of the small volume of flowing groundwater, despite the creation of disturbance in the test section at OL-KR6. Pentti & Vaittinen (2018) discussed that if the yield is only some litres combined to low hydraulic transmissivity, pumpings in such drillholes/drillhole sections cause remarkable changes. In this case, however, the changes in hydraulic gradient are local and for this reason the effects at distance from drillhole could be only minor (Pentti & Vaittinen 2018).

7.5.4 The fourth pumping

The fourth pumping was done from the depth of 122.9–140.6 m. There were a total of 5 fractures between the packers. The transmissivity of the fractures varied from 4.0E-0.8 to 5.9E-06. The depths of fractures were 125.22 m, 128.8 m, 129.8 m, 130.4 m and 135.72 m, according to PFL measurement. The assumed pumping rate for 10 m drawdown was 4.17 L/min. This section was chosen due to the modelled intersection of HZ001 (Vaittinen et al. 20XX - in prep.), and in the previous model (Vaittinen et al. 2011) an intersection of the HZ099 zone was also modelled to the same section.

The fourth pumping started on 10 July 2019 at 8:35 a.m. The pumping was started during the lowering of the pump in the pump container. This was done due to problems during the third pumping. It was assumed that if the pumping was started after the lowering of the pump to a depth of 40 metres and there were approximately 35 metres of water above it, the water would create a 3.5 bar pressure for the pump and there might be some water leakages into the pump's electronic parts (Section 7.5.3). When the pumping was started during the lowering of the pump, the water table above the pump was a maximum of 5 metres. This, however, causes that it is impossible to get the knowledge of watertable inside the pump container, because the pressure probe was installed together with the pump (Figure 10).

The pumping rate during the test was approximately 4 L/min, which created 11 m drawdown to the test section. The calculated pumping rate for 10 m drawdown was 4.17 L/min as mentioned before and for 11 m drawdown, 4.59 L/min. The theory for the difference between the calculated and real pumping rate is presented in Section 7.5.9.

During the pumping, the electrical conductivity of the pumped water increased from 2.83 mS/cm to 9.8mS/cm. The water at the beginning of the fourth pumping was highly diluted because of the overpressure test in the third pumping (Section 7.5.3.). It was also greenish (because of the marked water) approximately one week after the pumping was started. There was sampling on 17 July to analyse the concentration of sodiumfluorescein. Analysing was done at TVO´s laboratory and the concentration of sodiumfluorescein was only 1µg/L. This result combined with the increase of EC indicates that the pumped water was from fractures in the test section. Pumping was stopped on 23 July.

Hydraulic responses during the fourth pumping were observed at OL-KR19 sections L3–L5 (Figures 20 & 21). There were also small changes to the hydraulic head in some other drillholes during the fourth pumping, but the responses were so small that it is almost impossible to tell whether it was due to OL-KR6 pumping or if there was some other reason like natural fluctuation due to the dry summer or some other field activities.

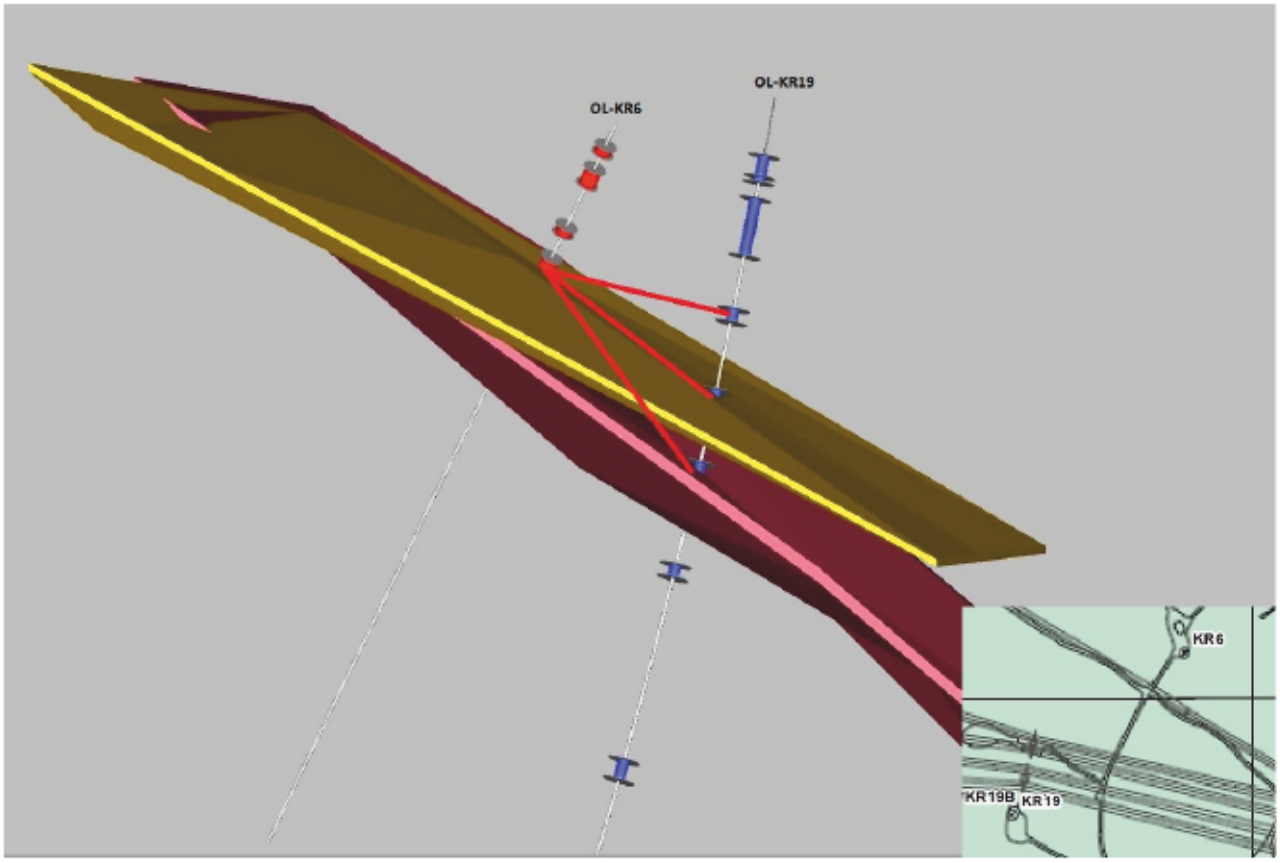

Figure 20. Visualisation of the hydraulic responses during the fourth pumping (view from SW). Hydraulic responses were observed from OL-KR19 sections L3–L5. The figure is not to scale. The responses are classified to be weak (<20 cm) and for this reason the red line has been used. The hydrogeological zones are same as in Figure 4.

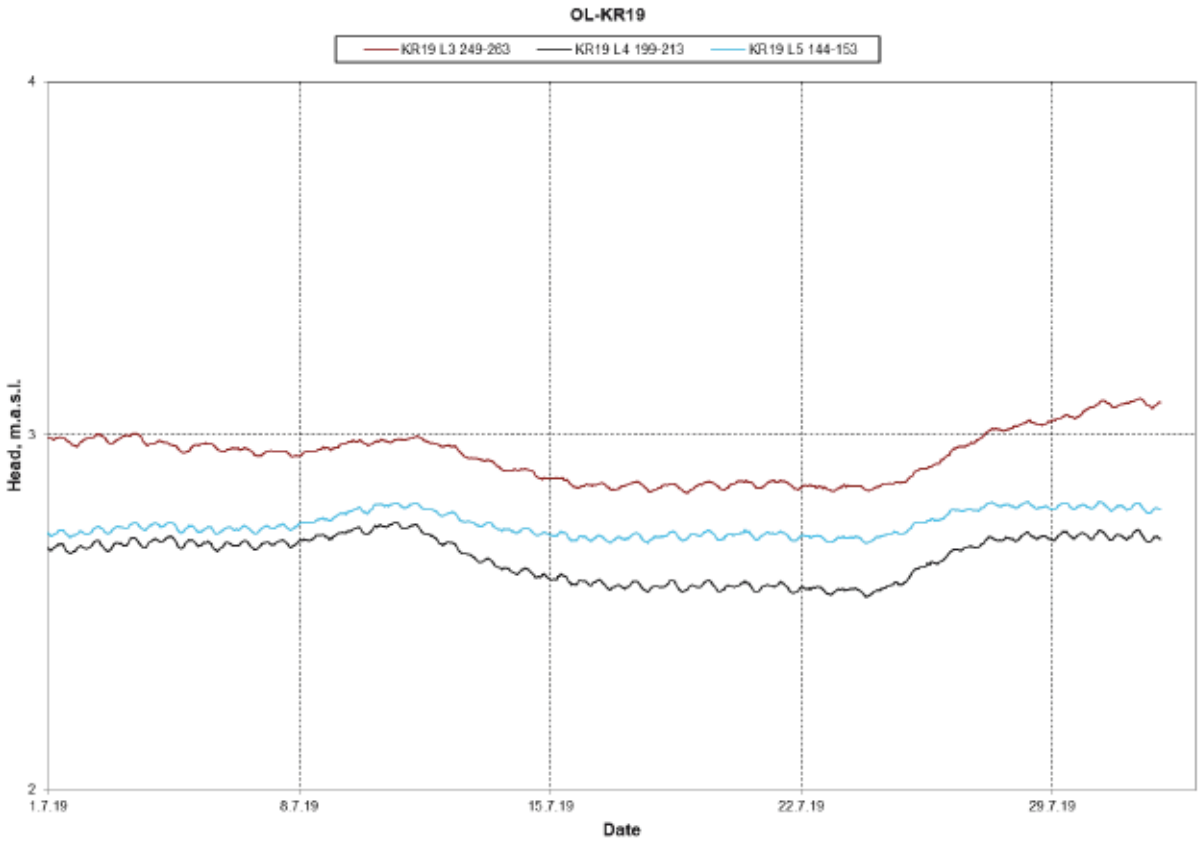

Figure 21. GWMS data chart from OL-KR19 during the fourth pumping. There were slight responses in sections L3–L5. All of the responses were < 20 cm. Those were classified to hydraulic responses due to the fact that the response took place during the OL-KR6 pumping, although the responses were small. Because hydraulic response in section L5 was only 11 cm it should be considered as highly uncertain.

7.5.5 The fifth pumping

The fifth pumping was done from the depth of 96.5–102.4 m. There was only 1 fracture between the packers. The transmissivity of the fracture was 5.8E-06 m^2/s, and its depth was 99.8 m, according to PFL measurement. This section was chosen due to the high transmissivity of the fracture, but there were no modelled zone intersections in this test section.

The assumed pumping rate for 10 m drawdown was 3.48 L/min. The real pumping rate during the test was approximately 4 L/min, which created 15 m drawdown to the packer section. The calculated pumping rate for 15 m drawdown is 5.22 L/min. The reason for the difference between the calculated and real pumping rate is presented in Section 7.5.9, eventhough the difference is quite small.

The fifth pumping started on 1 August 2019 at 9:25 a.m. and lasted until 12 August at 2:14 p.m. The pumping was started as in the fourth pumping during the lowering of the pump to the pump container. This was done due to problems during the third pumping (Section 7.5.4).

During the fifth pumping, there were some problems related to the pressure probe above the pump. It showed that there was enough water above the pump but, as can be seen from the table (Appendix 3), the water level was insufficient, which obstructed the functioning of the pump. This can be seen from the vibration of the line. This did not, however, affect the drawdown between the packers.

The EC value increased from 3.13 mS/cm to approximately 4.4 mS/cm during the pumping. During the earlier sample pumpings at OL-KR6, the EC was 8–8.51 mS/cm, so the water was highly diluted, most likely from the overpressure test during the third set-up (Section 7.3.3). Hydraulic responses during the fifth pumping were at OL-KR19 sections L3–L6 (Figures 22 & 23). This minor change, however, is so small that it is almost impossible to say if it is due to OL-KR6 pumping or just natural fluctuation due to the dry summer.

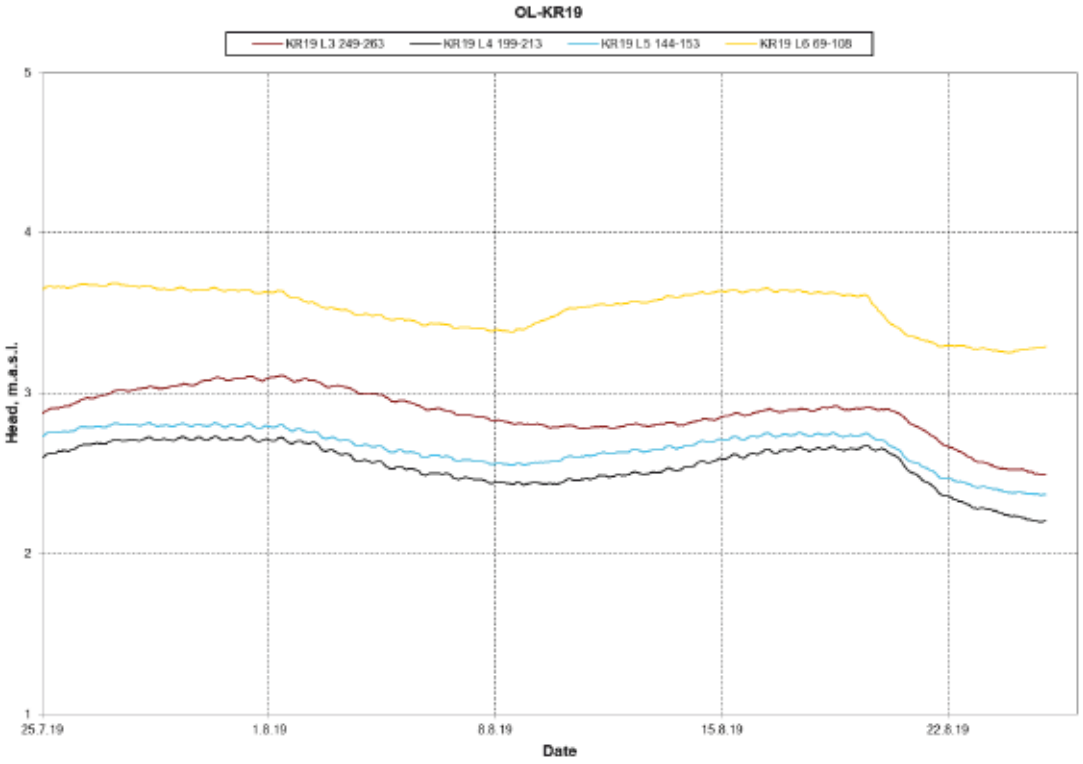

Figure 22. GWMS-data chart from OL-KR19 during the fifth pumping. There were hydraulic responses on sections L3–L6.

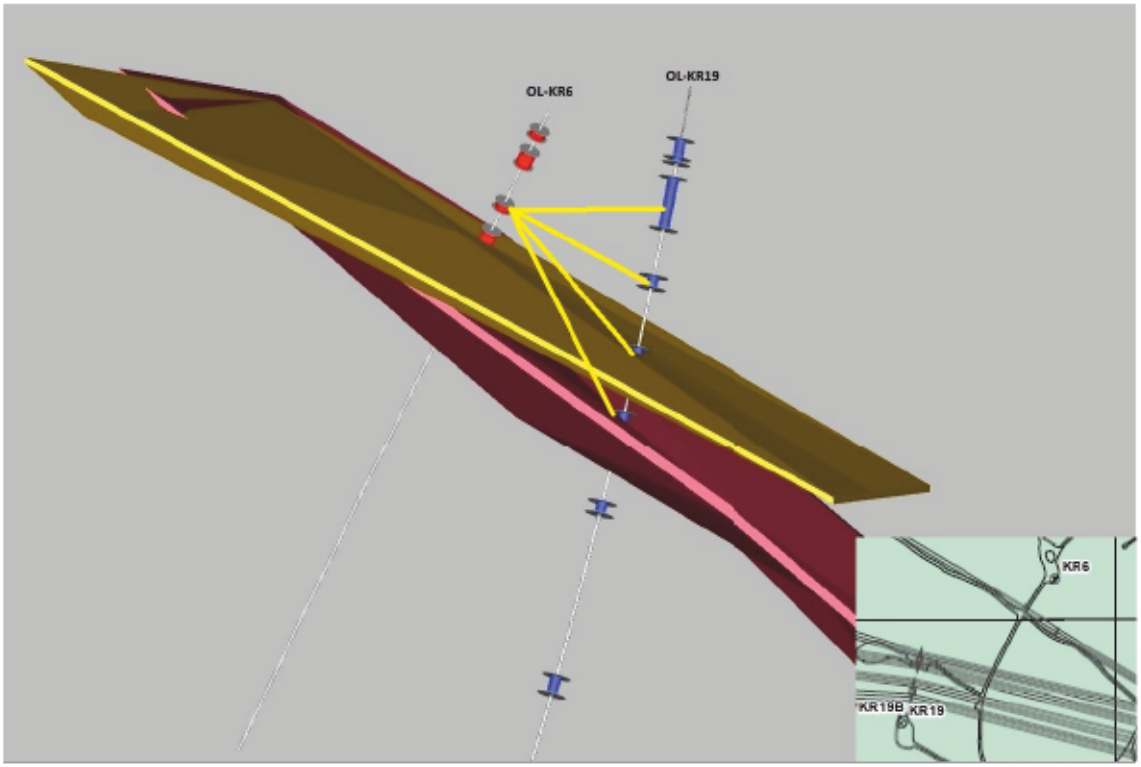

Figure 23. Observed hydraulic responses during the fifth pumping. The responses appeared at OL-KR19 sections L3–L6. Responses were medium (20–40 cm) and therefore yellow colour

describes the responses. The figure is from SW and is not to scale. The hydrogeological zones are same as in Figure 3.

7.5.6 PFL DOPP in OL-KR42

Before the sixth pumping started on OL-KR6, PFL DOPP equipment was installed in OL-KR42 at depth of 306.5–317.4 m. The measured fracture was at depth of 311.2 m. Basic information about the PFL DOPP measurement was presented in Section 5.1.3. Before the installation of PFL DOPP to OL-KR42, the drillhole had to be cleaned with a special PFL dummy device (Section 7.4). This was done three times before the PFL DOPP equipment was installed in OL-KR42.

The packers were inflated on 16 August 10:30. When the packers are inflated, they isolate the measurement section from the drillhole. The packers were emptied on 17 September 2019 at 12:15 p.m.

In my opinion, if the drillhole feeds water to the hydrogeological zone, the pressure on the measurement section decreases. Decrease of the hydraulic head on the measurement section is due to isolation of the section. When the section is isolated from the drillhole, water flows out from the measurement section and there is no compensatory water flowing along the drillhole when the pressure on the measurement section starts to decrease. This phenomenon recurs also in surrounding drillhole sections if there are hydraulic connections. This processes is directed by means of pressure differences.

If there is a strong hydraulic connection to underground openings (e.g. ONKALO), the pressure of the hydrogeological zone should decrease strongly for a long time. If some other drillhole feeds water to the hydrogeological zone, the drillholes hydraulic head should similarly decrease. On the other hand, the hydraulic head at the OL-KR42 measurement section should have only a minor decrease if some other drillhole feds water to the hydrogeological zone.

During the PFL DOPP measurement, the hydraulic head at the measurement section decreased by approximately a total of 4 metres for a week and then stabilised almost completely. The hydraulic head at OL-KR12 section L6 also decreased by 2 metres, right

after the packers at OL-KR42 were deflated. This indicates that there is a direct hydraulic connection between OL-KR42 and OL-KR12 (Figure 24).

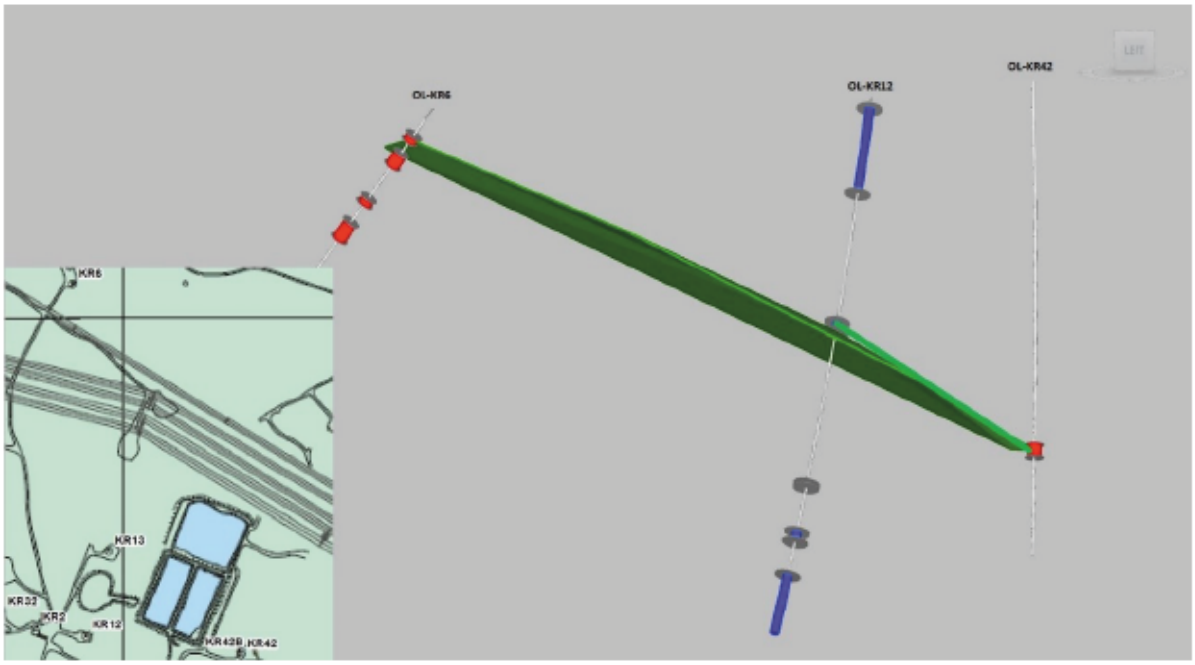

Figure 24. Hydraulic response during the OL-KR42 PFL DOPP measurement. The figure is from the west and is not to scale. The hydrogeological zone in the figure is HZL4 (Vaittinen et al. 20xx - in prep.). The response from OL-KR42 PFL DOPP was strong (>40 cm; green line) and was seen clearly in OL-KR12 section L6.

Earlier studies (e.g. Pentti et al. 2014) discussed that there might be a hydraulic connection from OL-KR42 (fracture 311.2 m) to ONKALO. The hydraulic head decreased by only 4 metres during the OL-KR42 PFL DOPP and, if there were a direct hydraulic connection to ONKALO, the hydraulic head of OL-KR42 should might have decreased more. However, the transmissivity is affecting to created drawdown also. All in all it can be said that, OL-KR42 is within the area of influence of ONKALO. This can be seen from the flow and pressure data of fractures in OL-KR42 (Pentti et al. 2014. table 6-5).

7.5.7 The sixth pumping

The sixth pumping was done from the depth of 28.9–34.8m. There were a total of 6 fractures between the packers. The transmissivity of the fractures varied from 5.9E-09 to 1.00E-05 m^2/s, and their depths were 29.4 m, 30.4 m, 30.85 m, 32.8 m, 33.6 m and 33.9

m, according to PFL measurement. This section was chosen based on the modelled HZL4 intersection (Vaittinen et al. 20XX – in prep.).

The assumed pumping rate for 10 m drawdown was 10.76 L/min. The real pumping rate during the test was approximately 14 L/min, which created approximately 8.5 m drawdown. The calculated pumping rate for 8.5 m drawdown is 9.15 L/min. The theory for the difference between the calculated and real pumping rate is presented in Section 7.5.9.

The sixth pumping started on 19 August at 9:25 a.m. and lasted until 29 August at 8:47 a.m. As in the fourth and the fifth pumping, the pumping was started during the lowering of the pump to the pump container. This was done due to problems during the third pumping (Section 7.5.4).

During the sixth pumping, there was a slight leakage to the pump container or leakage by the upper packer via the bedrock. This can be seen from the table (Appendix 3) where the freshwater head on the drillhole decreased by 2.9 metres immediately after the pumping started. This could be the reason for smaller drawdown than expected in the test section. On the other hand, it could be a reason for a greater pumping rate.

Hydraulic responses during the sixth pumping were at OL-KR19 sections L3–L8 (Figures 25 & 26). Some responses were also observed in OL-KR2 section L5 and OL-KR13 section L4 (Appendix 4). There were also some minor changes in OL-KR13 section L4.

These minor changes, however, are so small that it is almost impossible to say if they were due to OL-KR6 pumping or just natural fluctuation due to the dry summer.

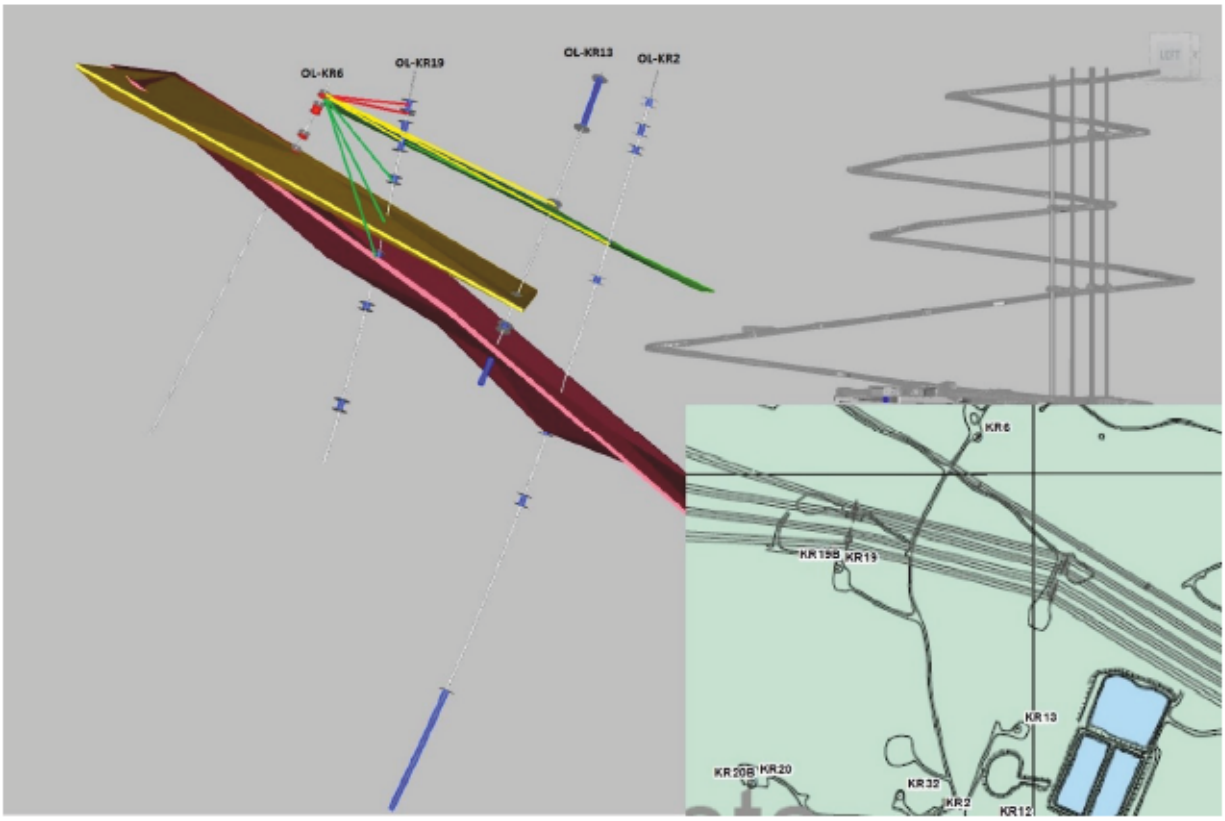

Figure 25. Observed hydraulic responses during the sixth pumping. During OL-KR6 pumping, responses were observed from OL-KR19 sections L3–L8, OL-KR2 section L5 and OL-KR13 section L4. The figure is from SW and is not to scale. The hydraulic responses were strong (green line) in OL-KR19 sections L3–L6, medium (yellow line) in OL-KR19 sections L7–L8 and in OL-KR13 section L4, and weak (red line) in OL-KR2 section L5 based on the classification presented in Section 7.4.3. The hydrogeological zones are same as in Figure 3.

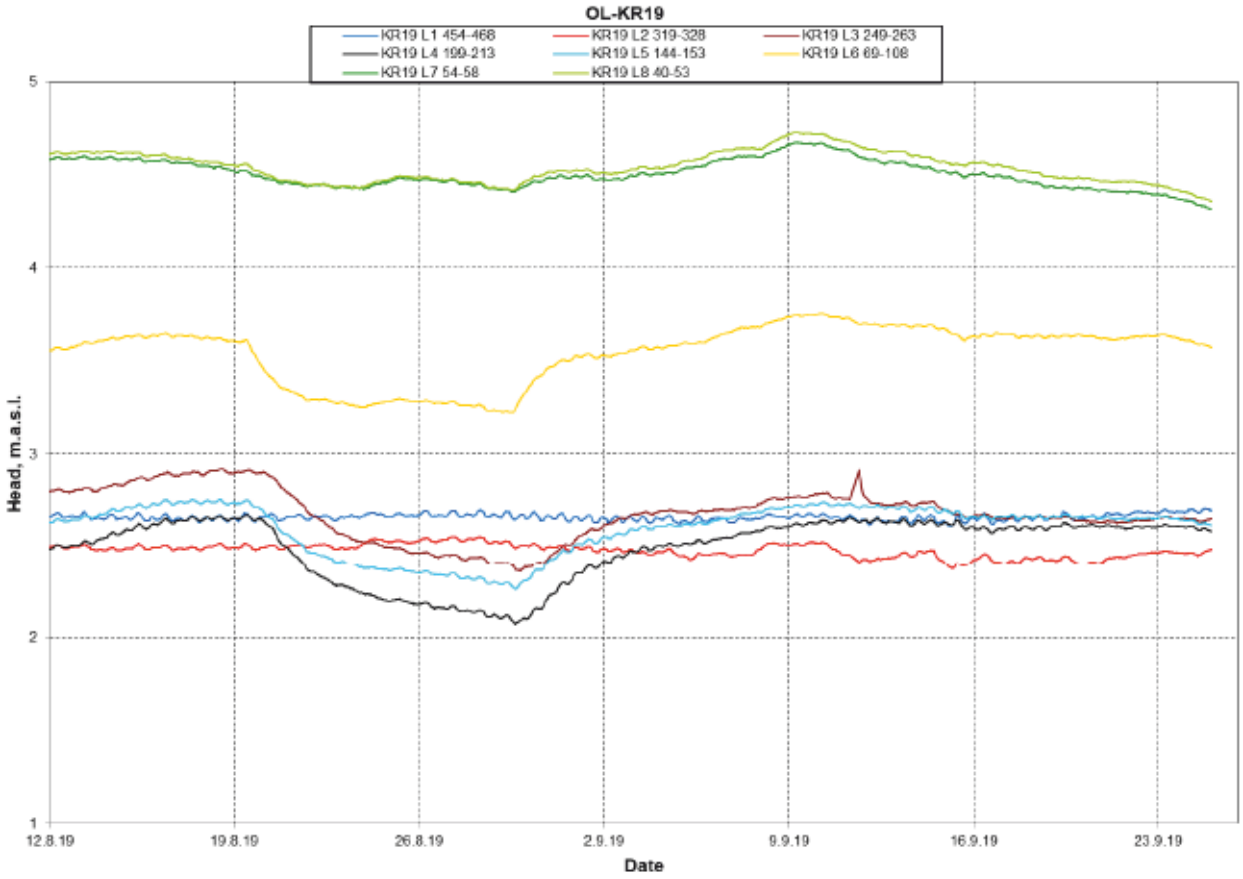

Figure 26. GWMS-data chart from OL-KR19 during the sixth pumping. There were hydraulic responses in sections L3–L8.

7.5.8 Uncertainities of the pumpings

During the pumpings, the only major technical problem was pump breakdowns during the third pumping (Section 7.5.3). Some minor difficulties related to pumpings were observed in the first and sixth pumpings (leakage by upper packer, sections 7.5.1 and 7.5.7). The aforementioned minor difficulties, however, had no notable effect on the success of the pumpings. On the other hand, one problem during the third pumping (Section 7.5.3) was that the 20-mm hose from the packers to the pump container was "strangled", which caused relatively small drawdown during the pumping. This might also have been a result of the overpressuring because the increase in pressure in the test section lasted longer than expected (Appendix 3).

Some other difficulties are related to the excavation of the ONKALO and other field activities in the area. Problems with the OL-KR28 multi-packer system also made the interpretation of the hydraulic responses more difficult. This is due to the fact that OL-

KR28 perforates some of the major hydrogeological zones (HZ19A, -B, -C, HZ20A & -B) (Vaittinen et al. 20XX - in prep.). Hydrogeological zones are packered separately and their hydraulic head is therefore different in every hydrogeological zone. When there are problems with packers the hydraulic head gets disturbed in every HZ zone and the effects (disturbances) are seen in the whole area of each hydrogeological zone.

Another consequence of the multi-packer system was the removal of the packers from OL-KR11 during the interference test, which created uncertainties in the interpretation of the hydraulic responses. Also, the natural decrease of the groundwater table during the summer caused uncertainties in the observations of hydraulic responses in the upper part of the bedrock.

One major (technical) uncertainty related to the interference test is that, due to the lack of space in OL-KR6, there was no possibility for a pressure measurement under the lower packer. This meant that there was no knowledge of whether there were any leakages by the lower packer. The technical problems of monitoring the hydraulic head automatically at OL-EP4 also caused some uncertainties in the results.

At greater depths, there is one element of uncertainty related to the pumping rates presented in section (7.5.3). If the pumping rate is relatively small (e.g. < 0.5 L/min), is it great enough to create a drawdown to longer packer sections (from metres to tens of metres) in observation drillholes, despite the fact that created disturbance (drawdown) should be great enough? This is discussed also in Section 7.5.3.

7.5.9 Discussion and recommendations

The only notable observations during pumpings related to hydrogeological zones were observations in HZL4 zone. Parts of HZL4 (intersections in OL-KR42 and OL-KR12) have a direct hydraulic connection. On the other hand, the sixth pumping at OL-KR6 was observed at every HZL4 intersection, with the exception of OL-KR42 and OL-KR12 L6. However, this observation is uncertain because, when the sixth pumping at OL-KR6 was started, there was still ongoing disturbance in OL-KR42 and OL-KR12 L6.

Moreover, the timetable related to OL-KR42 PFL DOPP measurement should have been modified. The PFL DOPP measurement should have been started two weeks or a month before starting the sixth pumping at OL-KR6 in order to have a steady state at OL-KR42 and OL-KR12 L6. In this case, maybe it would have been possible to observe some hydraulic responses between OL-KR6, OL-KR42 and OL-KR12 (in the whole modelled extent of HZL4).

In future, the pumping times at greater depths in interference tests should be considered more accurately. In this thesis, the pumping times were relatively short and this could be one of the reasons why not all of the expected hydraulic responses were observed. The timetable should be considered depending on which is more important: the number of test sections or the results being aimed for. It should be considered if it is more important to:

1. pump two different test sections for two weeks each, or
2. pump only one test section for four weeks to be "sure" that there are no hydraulic connections.

In this thesis, we chose number 1 in order to gain more results in less time. In retrospect, number 2 could have been a better choice in order to ensure having at least one sure observation rather than two uncertain ones. That said, it was assessed (calculated and based on expert judgement) that the used pumping rates and times should be sufficient for the interference test. In these kinds of investigations certail level of uncertainty always remains.

Also, if there is a need to observe the hydraulic heads of different hydrogeological zones, all the multi-packer systems related to hydrogeological zones under research should be in order. During this test, there were many problems with crucial multi-packer systems (e.g. OL-KR28). The effect of ONKALO (and excavations), Korvensuo reservoir and weather conditions should also be taken into account more accurately than in this thesis.

During almost every pumping, there was a distinction between the calculated and real pumping rate despite the magnitude of drawdown. One reason for this is supposedly because the flow geometry parameter is uncertain (Section 7.2.). For this reason, it could be said that the difference between the calculated pumping rate and the real pumping rate

is related to the uncertainty of the flow geometry, i.e. the effect of the flow geometry parameter (Section 7.2), which should be examined further in order to gain better knowledge for future pumping and interference tests.

The effect of topography can be excluded from this thesis. OL-KR6 is 2.28 m above sea level. The drillholes under closer investigation - OL-KR2, -KR12, -KR13, -KR19, -KR20 and -KR42 - are 5.80–8.80 metres above sea level. Basically, the maximum difference in elevations between OL-KR6 and its surrounding drillholes is therefore 6.62 metres, so the elevation difference will have no substantial effect on the movement of groundwater at least in the deeper sections.

8 DISCUSSION AND CONCLUSIONS

Pumping tests and interference tests have been commonly used tools for investigating groundwater flow conditions, hydraulic connections, etc. on the ground and at ONKALO during the investigations on Olkiluoto Island (e.g. Hansson et al. (2015), Pentti et al. (2019) Reijonen et al. (2015)). Interference tests are a good way to study the groundwater flow properties and hydraulic connections at Olkiluoto where the amount of different kinds of observation points is remarkable. From different observation points, it is possible to get very reliable results for clarifying groundwater observation results.

Table 1. The open questions before an interference test and results gathered from the interference test.

Open question from OL-KR6 long-term pumping test	Result from an interference test
HZ21 intersection on OL-KR6; modelled responses was not seen on the field data	Modelled intersection in OL-KR6 is realistic, during this pumping there were no hydraulic responses in HZ21 (the second pumping; section 7.5.2)
Possible connection to HZ20A system from the depth of 59m from OL-KR6	There were no responses on HZ20A area; Multi-packer equipment problems on OL-KR28 possibly hindered the observations of hydraulic responses (the first pumping, section 7.5.1)
Continuation of HZL4 towards OL-KR42	There was a hydraulic response between OL-KR42 & -12. On the other hand there were hydraulic connections in other HZL4 intersections during OL-KR6 pumping. (PFL DOPP in OL-KR42 and the sixth pumping in OL-KR6, sections 7.5.6 & 7.5.7)
HZ099 intersection in OL-KR6 ("old" vs. new)	During the pumping of old HZ099 intersection point in OL-KR6, there was a hydraulic response in OL-KR19 HZ099 intersection point (the fourth pumping, section 7.5.4)
There were noticed some hydraulic responses outside the HZ zones on the upper parts of the bedrock	Hypothesis of horizontal fracturing in the upper parts of the bedrock (up to 140 m) and there were some indications of interaction between HZ zones and horizontal fractures

The aim of this thesis is presented in Chapter 7 and Table 1. During an interference test, some observations were made. The HZ21 zone is modelled to intersect OL-KR6 at depths of 473.6–477.9 m (Vaittinen et al. 20XX, in prep.). The hydrogeological influence zone of HZ21 is shown to intersect OL-KR6 at depths of 435–492.2m. When planning the interference test, it was noticed that, from the fractures near this depth, the greatest T_{PFL}-

value of 1.1E-07m^2/s was the fracture at depth of 423.6 m. Even though HZ21 was not modelled to this fracture, it was chosen as the second pumping target.

The results from the second pumping are presented in Section 7.5.2 and 7.5.8. There were no observed hydraulic connections from OL-KR6 to the HZ21 zone at the depths of 421.5–428 m. It can be said that based on aforementioned lack of hydraulic responses from pumped depth the modelled intersection of HZ21 in OL-KR6 is realistic. Or at least it intersects OL-KR6 at greater depth than 428 m.

One uncertainty related to this HZ21 connection is whether the pumping time was long enough. Other uncertainty, presented in Sections 7.5.3 & 7.5.8, is whether the pumping rate was too low to detect hydraulic connections in longer packer sections in surrounding drillholes, despite the fact that the created disturbance (drawdown) should have been great enough. Also, the fact that the excavation of ONKALO was ongoing might have caused uncertainties in the observation of hydraulic connections at greater depths.

The results from the third pumping are presented in Section 7.5.3. There were some problems related to function of the pump (see Sections 7.5.3 & 7.5.8). Due to technical problems and opposite disturbance for the groundwater system (drawdown versus overpressure, see Section 7.5.3) there were no hydraulic responses in HZ21B during the third pumping.

A possible connection from OL-KR6 (from a depth of 59 m) to the HZ20A system presented by Reijonen et al. (2015) is highly uncertain. During this interference test, there were no observations of interaction between the OL-KR6 and HZ20A hydrogeological zones. This HZ20A speculation has been "forgotten", because in recent years there have hardly been any observations of this interaction from field activities.

Uncertainties related to the HZ20A connection from OLKR6 relate to problems with the multi-packer equipment on OL-KR28. Technical problems with this equipment are obviously seen in the hydraulic head and in hydrogeological zones HZ20A and HZ19. If there was some hydraulic interaction between OL-KR6 and HZ20A, maybe the hydraulic response would have been concealed by the disturbance caused by OL-KR28. To be sure that the interaction between OL-KR6 and HZ20A does not exist, the first, fourth and fifth

pumpings at OL-KR6 should be repeated when there are no notable disturbances in the HZ20A system.

The current HZ099 intersection was included in the original interference test plan. Due to technical problems during the third pumping, it was left out based on the fact that transmissivity at the depth of the current HZ099 intersection was 1.00E-8 m^2/s. Low transmissivity could cause technical problems for the MP pump as was seen in the third pumping. During the earlier PFL measurements (e.g. Pekkanen 2018), no flow was observed from fracture at a depth of 163.6 m.

The fourth pumping (Section 7.5.4) was from a depth of the "old" HZ099 intersection (Vaittinen et al. 2011) and the current HZ001 (Vaittinen et al. 20XX - in prep.). Hydraulic connections were observed in OL-KR19 sections L3–L5. The modelled intersection of HZ099 on the current model (Vaittinen et al. 20XX - in prep.) is at OL-KR19 section L3, and HZ001 at OL-KR19 section L4. No other hydraulic responses at HZ099 were observed at any other modelled intersections.

Based on the hydrogeological model, a hydraulic response at HZ001 should also have been observed in OL-KR13 section L3 but there was no response. One reason was that the hydraulic head of OL-KR13 sections L3 and L4 started to decrease in mid-June. The downward direction of the hydraulic head lasted until 21 July. After that the groundwater table went below measurement limits so could not have been observed.

These uncertain observations in both zones could be explained by the long distances between OL-KR6 and other intersection points in other drillholes. The long distance combined with the short pumping time (13 days) could explain this observation. As presented before (e.g. Vaittinen et al. 20xx -in prep.), it is known that hydraulic responses diminish as a function of distance. It could still be said that HZ001 on the current model is realistic due to the observation of hydraulic response between OL-KR6 and OL-KR19.

The current intersection of HZ099 on OL-KR6 should be reconsidered due to the hydraulic response at the HZ099 intersection at OL-KR19 L3 during the fourth pumping. The fourth pumping was done at the "old" intersection of HZ099 at OL-KR6. The hydraulic response at OL-KR19 section L5 is also an odd observation.

The extent of HZL4 was one of the targets of this thesis. The results were discussed earlier in Sections 7.5.6, 7.5.7 and 7.5.8. The problem during the sixth pumping related to the fact that there was ongoing disturbance at OL-KR42 and OL-KR12, which could have concealed the hydraulic response from OL-KR6 and OL-KR42 & -12. There are two alternative choices:

1. OL-KR12 and OL-KR42 are connected by a new, not yet modelled, hydrogeological zone separate from HZL4, or
2. OL-KR42 and OL-12 are part of the HZL4 system and the hydraulic response was diminished because of long distance or ongoing disturbance.

Due to the short period of time, it is almost impossible to say which opinion is more correct. The major question is why the OL-KR12 L6 and OL-KR42 hydraulic responses did not appear at other HZL4 intersections, during the three days between the start of PFL DOPP measurement and starting the pumping at OL-KR6. This could be due to the different OL-BFZ zones on the modelled HZL4 i.e. HZL4 zone consists of two different modelled OL-BFZs (Section 4.2.2). However, the hydraulic response appeared at OL-KR19, -KR13 & -KR2 less than a day after starting the pumping at OL-KR6. An unexpected observation was that the sixth pumping at OL-KR6 caused responses at OL-KR19 sections L3–L8. The upper section responses (at OL-KR19) could be caused by leakage by the upperpacker at OL-KR6 (see Section 7.5.7). Also, the lower sections (at OL-KR19) could have been caused by leakage from the lower packer at OL-KR6.

The most important observation resulting from this thesis is that all the pumpings done in the upper part of OL-KR6 (depth of <140 m) were seen in OL-KR19 upper sections less than a day after the pumping was started (Figure 28.). Pumping above 140 metres took place on the first, fourth, fifth and sixth pumpings (Sectionss 7.5.1, 7.5.4, 7.5.5 and 7.5.7).

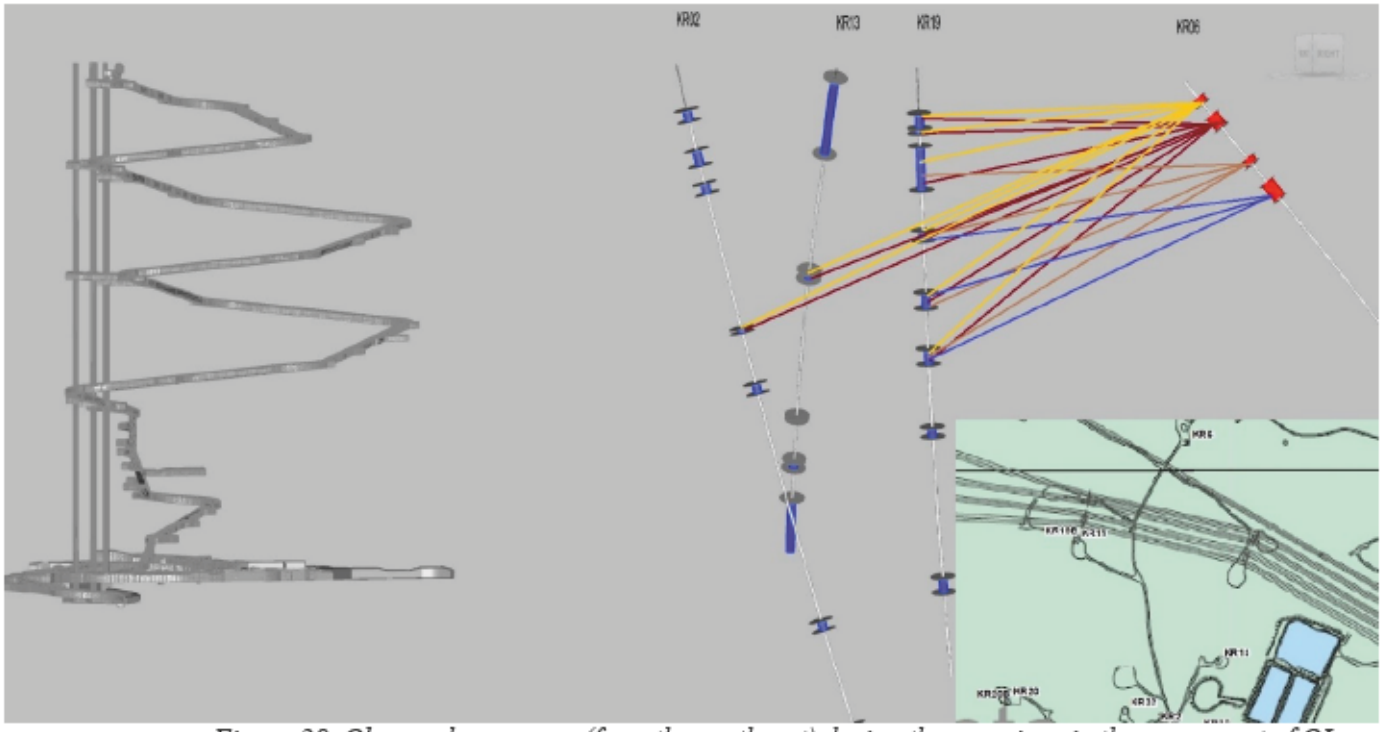

Figure 28. Observed responses (from the southeast) during the pumpings in the upper part of OL-KR6 at depths up to 140m. Observations of the first pumping are red, the fourth pumping blue, the fifth light brown and the sixth yellow. The figure is from SE and is not to scale.

There were slight problems with leakages, for example, from the upper packer (possibly also the lower packer) through the bedrock, which is due to the large number of fractures in the upper part of OL-KR6.

These upper-part hydraulic responses could decrease if the distance between the drillholes is long enough. In addition, the observation of hydraulic responses in the upper part of bedrock is more difficult when the groundwater table is lower in the summer.

These observations (Figure 28.) are not possible without high transmissivities in the upper part of the bedrock, but there should be enough fractures for the creation of flowing routes for groundwater (Section 2.2.1). In this case, the orientation of fractures should be favourable for groundwater to flow in the upper parts of the bedrock. This leads to the hypothesis that there are strong hydraulic connections in the upper parts of the bedrock in the Olkiluoto area caused by continuous horizontal fracturing. If there is no leakage from the lower packer at OL-KR6 (which is impossible to say), the horizontal fracturing could even reach up to approximately 250 metres. The lowest response at OL-KR19

during the sixth pumping was at section L3, which is at depths of 249–263 m and a vertical depth of 250 metres.

This observation appears at least in NTU (Section 3.1) where the planar structural elements are common, and it should be taken into consideration in the next update of the hydrogeological model of the Olkiluoto site.

If the presented hypothesis is correct, it leads to the fact that the infiltration and groundwater flow to the repository level can take more time than was assumed. In this way, the observation of a horizontal fracture network in the upper parts of the bedrock should also be taken into consideration in hydrogeological and hydrogeochemical modelling in the future.

On the other hand, horizontal fracturing could also affect the amount of infiltrated groundwater from Korvensuo reservoir (Sections 2.2.1 and 3.6) or at least the flow paths of infiltrated water. The infiltration process from Korvensuo reservoir has been studied (e.g. Karvonen 2013; Vaittinen et al. 2018), but the results can be assessed further based on these findings.

This horizontal fracturing hypothesis in the upper parts of the bedrock can also affect the safety assessment of the final disposal of spent nuclear fuel. Glacial and permafrost periods can be said to be expected on the future (Posiva 2012c). If there is a "warm-bottom" glacier in the future in the Olkiluoto area, then there will be flowing and high-pressure water under the glacier. Due to the weight of the glacier, melt waters might infiltrate into deep bedrock due to hydraulic gradient differences between areas under glacier and areas with no ice cover (Posiva 2012c). The horizontal fracturing could cause hydraulic dispersion as pressurised groundwater flows alongside the horizontal fractures and does not intrude deeper into the bebrock (according to Posiva (2012c), the impacts of older glacial melt waters are not seen nowadays below 300 metres), at least, not as much as earlier modelled (Posiva 2012c). On the other hand, the geomechanical properties of the bedrock might be different at the time. For example, some of the fractures could be closed due to the weight of the glacier, especially near the ground surface.

This thesis could also help to model and understand the effects of the rock crushing area on Olkiluoto. Oxidation of sulphates is taking place on the ground (Posiva 2012b). This horizontal fracturing can affect to which depth the SO_4 rich water is infiltrating i.e. is the groundwater flowing horizontally after infiltration near surface or is it flowing to deeper horizons. All in all, there are many other features affecting this infiltration: other fracturing, hydrogeological zones, drawdowns caused by construction etc.

For modelling purposes, the continuity of the upper parts of the hydrogeological zones should be reviewed again. Are the upper parts of the hydrogeological zones as part of the horizontal fracturing system or are the hydrogeological zones their own units disconnected from the upper fracture network system? With these observations collected from the interference test, it should be assumed that both the upper parts of the hydrogeological zones and the upper fracture network are in some kind of interaction with each other (Sections 7.5.1, 7.5.4, 7.5.5 and 7.5.7). This assumption is based on the fact that the pumping at the upper parts of OL-KR6 was seen both in the hydrogeological zones and in the horizontal fracturing (e.g. Section 7.5.4). This could also be one reason for the diminishing of the hydraulic response between OL-KR6, -KR12 and -KR42 in the OL-HZL4 zone during the sixth pumping (Section 7.5.7).

The correction factor of the natural fluctuation should perhaps be reviewed. Nowadays, this correction factor is based on natural fluctuation data from the 11 shallow holes and data from five different EP-L4 sections (Pentti 2019) as discussed in Section 5.1.5. It should be considered whether the groundwater system below the horizontal fracturing has a different kind of fluctuation to the upper parts of the bedrock. It has also been discussed by Pentti & Vaittinen (2018) that the time series of natural fluctuation has strong linear correlation to most hydraulic head data from drillholes on Olkiluoto with the exception of the very deepest packer sections.

9 SUMMARY

This thesis presented the planning and execution of an interference test. The observed hydraulic responses during the test were presented and visualised in this thesis. The aim of the thesis was to give suggestions for an update of the hydrogeological model near OL-KR6. The most significant result of this thesis was the hypothesis of a horizontal fracturing in the upper parts of the bedrock, at least in the northern parts of Olkiluoto Island.

The thesis first presented background knowledge of the hydrogeology and geology. After that, basic information of the Olkiluoto site and Posiva's investigation equipment and methods were presented. The long-term pumping test at OL-KR6 (on which the interference test is based) and its results were then discussed.

After that the planning and execution (field work) of the interference test were presented and discussed, then discussion of the results of the test were presented and, based on the results, suggestions for an update of the hydrogeological model were presented. This thesis did not take into account the costs of this kind of interference test.

The hypothesis of the horizontal fracture network was based on observations during the first, fourth, fifth and sixth pumping. The continuation of the hydrogeological zones in the area of the fracture network was discussed. The conclusion was that the hydrogeological zones are integrated into the horizontal fracture network in the upper parts of the bedrock.

It was noticed that the hydrogeological model of OL-KR6 is valid in the case of the hydrogeological zones. Suggestions for improvement of the hydrogeological model include consideration of whether the horizontal fracturing should be incorporated into the model and, on the other hand, whether the separation of HZL4 into two different parts should be considered.

HZL4 separation would be useful because of the distribution of hydraulic responses at HZL4. Possible separation of hydrogeological zone HZL4 would be done based on the

fact that the hydraulic response from OL-KR42 PFL DOPP measurement was observed only at OL-KR12 section L6 and, on the other hand, the hydraulic responses of OL-KR6 sixth pumping were observed in the other parts of the HZL4 zone.

REFERENCES

Aaltonen, I (ed.), Engström, J., Front, K., Gehör, S., Kosunen, P., Kärki, A., Paananen, M., Paulamäki, S. & Mattila, J. 2016. Geology of Olkiluoto. Posiva-report 2016-16. 398p. ISBN: 978-951-652-244-2

Aaltonen, I (ed.), Lahti, M., Engström, J., Mattila, J., Paananen, M., Paulamäki, S., Gehör, S., Kärki, A., Ahokas, T., Torvela, T. & Front, K. 2010. Geological model of the Olkiluoto Site - version 2.0. Working report 2010-70. Posiva Oy, Eurajoki, Finland. 580p.

Ahokas, H., Pöllänen, J., Rouhiainen, P. & Kuusela-Lahtinen, A. 2012. Quality Review of transmissivity data from Olkiluoto Site – Drillholes OL-KR1 – KR57. Working report 2012-99. Posiva Oy, Eurajoki, Finland. 392p.

Ahokas, H., Tammisto, E. & Lehtimäki, T. 2008. Baseline head in Olkiluoto. Working report 2008-69. Posiva Oy, Eurajoki, Finland. 191p.

Ahokas, H., Vaittinen, T., Tammisto, E. & Nummela, J. 2007. Modelling of hydro-zones for the layout planning and numerical flow model 2006. Part 1. Working Report 2007-01. Posiva Oy, Eurajoki, Finland. 212p.

Alhonmäki-Aalonen, S. 1999. Installation of multi-packer systems into boreholes at Olkiluotoon Olkiluoto between 1997-1998 (In Finnish with an English abstract). Posiva Oy, Helsinki, Finland. Working Report 99-49. 33p.

Davis, S. N. 1964. The chemistry of saline waters. In: Krieger, R.A. - Discussion. Groundwater, vol 2(1), 51.

Domenico, P. A. & Schwartz, F. W. 1990. Physical and chemical hydrogeology. New York: Wiley. 824p. ISBN 0-471-50744-X

Eijkelkamp. 2019. Manual grundfos MP 1 and Redi-Flo2 pump. published 07/2019 (referenced on 14.10.2019), available from:

https://www.eijkelkamp.com/download.php?file=M1227E_Grundfos_MP_1_and_RediFlo2_pump_c698.pdf

Fitts, Charles R. 2012. Groundwater Science. 2nd ed. Academic Press. 692. ISBN 978-0-12-384705-8

Hansson, K., Ludvigson, J-E., Nordqvist, R., Ragvald, J. & Andersson, P. 2015. Analysis of Detailed Hydraulic Interference Tests between Boreholes ONK-PP262 and ONK-PP274. Working report 2014-48. Posiva Oy, Eurajoki, Finland. 176p.

Hartley, L., Appeleyard, P., Baxter, S., Mosley, K., Williams, T. & Fox, A. 2018. Demonstration Area Discrete Fracture Network Modelling at Olkiluoto. Working report 2017-31. Posiva Oy, Eurajoki, Finland. 312 p.

Heikkinen, P. 2019. Personal information during the field work.

Hiscock, K.M. 2005. Hydrogeology: Principles and practice. Blackwell Science Ltd. 389p. ISBN: 978-0-632-05763-4.

Karvonen, T. 2013. Olkiluoto surface and near-surface hydrogeological modelling. Update 2012 including salt transport modelling. Posiva Oy, Eurajoki, Finland. Working Report 2013-22. 228p.

Komulainen, J. 2014. Flow Measurements and Hydraulic Interference Tests at the Olkiluoto Site in Eurajoki, Drillholes OL-KR14, OL-KR30, OL-PP66, OL-PP67, OL-PP68 and OL-PP69. Posiva Oy, Eurajoki, Finland. Working Report 2014-42. 262p.

Lahdenperä, A-M., Palmén, J. & Hellä, P. 2005. Summary of overburden studies at Olkiluoto with an emphasis on geosphere-biosphere interface. Posiva Oy, Eurajoki, Finland. Working Report 2005-11. 85 p.

Mälkki, E. 1999. Pohjavesi ja pohjaveden ympäristö. Tammi. Helsinki. 304 p (in Finnish)

Mönkkönen, H., Somervuori, P., Ranta-aho, S. & Pehkonen-Ollila A-R. 2017. Overburden Database and Stratigraphy Model at Olkiluoto Island and Nearby Sea Area. Working report 2017-27. Posiva Oy, Eurajoki, Finland. 111p.

Nurmi, P., Hurstinen, J., Lehtinen, M., A., Rämö, T., Hurskainen, J. 1998. Suomen kallioperä: 3000 vuosimiljoonaa. Suomen Geologinen Seura ry. Helsinki. 375 s.

Pastina, B. & Hellä, P. 2010. Models and Data Report 2010. Posiva Oy, Eurajoki, Finland. Posiva Report 2010-01. 478 p.

Pekkanen, J. 2018. Flow and Electrical Conductivity Measurements During Long-Term Pumping of Drillhole OL-KR6 at Olkiluoto, Results from November 2015 and September 2016 Measurements. Posiva Oy, Eurajoki, Finland. Working report 2017-17. 62p.

Pekkanen, J. & Komulainen, J. 201X Monitoring Measurements with the Difference Flow Method in Drillholes OL-KR10, -KR12, -KR28, -KR42, -KR46 and with the Transverse Flow Method in Drillholes OL-KR31, -KR33, -KR35, -KR36 and -KR42 during the Year 2017. Pöyry Finland Oy. Posiva Working report 201x-xx. - in preparation.

Pekkanen, J., Ripatti, K & Komulainen, J. 2016. Monitoring Measurements with the Difference Flow Method in Drillholes OL-KR40, -KR55 and -PP56 and with the Transverse Flow Method in Drillholes OL-KR31, -KR33, -KR35 and -KR36 during the Year 2013. Posiva Oy, Eurajoki, Finland. Working report 2014-70. 266p.

Pentti, E. 2019. Havaintojen tulkinnat, Posivalaisten perehdytys hydrologisen monitoroinnin menetelmiin -powerpoint show.

Pentti, E., Pulkkinen, P. & Ripatti, K. 2018. Pumping test in drillhole OL-KR29 in Summer 2016. Posiva Oy, Eurajoki, Finland. Working report 2017.48. 36p.

Pentti, E., Pöllänen, J., Komulainen, J. & Ripatti, K. 2014. Monitoring Measurements with the Difference Flow Method in Drillholes OL-KR32, -KR33, -KR42 and ONK-KR13, and with the Transverse Flow Method in Drillholes OL-KR31, -KR33, -KR35 and

-KR36 During the Year 2012. Posiva Oy, Eurajoki, Finland. Working report 2013-30. 224p.

Pentti, E. & Vaittinen, T. 2018. Compilation and analysis of hydrogeological responses to field activities in Olkiluoto during 2015-2016. Posiva Oy, Eurajoki, Finland. Working report 2018-27. 303 p.

Pentti, E., Vaittinen, T., Pekkanen, J. & Karvonen, T., 2019. Pumping tests in drillholes OL-KR49, -KR50, and -KR56 at Olkiluoto in 2012–2014. Posiva Oy, Eurajoki, Finland. Working report 2018-32. 212p.

Penttinen, T., Lamminmäki, T., Pitkänen, P. Loimula, K., Partamies, S., Ahokas, T. & Lahdenperä A. 2017. Results of monitoring at Olkiluoto in 2012 – Hydrogeochemistry. Posiva Oy, Eurajoki, Finland. Working report 2013-44. 282p.

Penttinen, T., Partamies, S., Lahdenperä A-M., Lamminmäki, T., Lehtinen, A. & Sireeni, S. 2013. Results of monitoring at Olkiluoto in 2010 – Hydrogeochemistry. Posiva Oy, Eurajoki, Finland. Working report 2011-44. 366p.

Penttinen, T., Partamies, S., Lahdenperä, A-M., Pitkänen, P., Ahokas, T., & Kasa, S. 2011. Results of monitoring at Olkiluoto in 2010 – Hydrogeochemistry. Posiva Oy, Eurajoki, Finland. Working report 2010-44. 296p.

Posiva. 2012a. Monitoring at Olkiluoto - a programme for the period before repository operation. Posiva Oy, Eurajoki, Finland. 188p. Posiva 2012-01. ISBN 978-951-652-182-7.

Posiva. 2012b. Olkiluoto Site Description 2011. Posiva Oy, Eurajoki, Finland. Posiva 2011-02. 1029 p. ISBN 978-951-652-179-7

Posiva. 2012c. Safety Case for the Disposal of Spent nuclear fuel at Olkiluoto - Performance assessment 2012. Posiva Oy, Eurajoki, Finland. Posiva 2012-04. 520p. Part of Posiva Oy's Safety Case "TURVA-2012" report portfolio. ISBN 978-951-652-185-8

Posiva. 2018. Kennoston ja pumpunohjausyksikön asennus ja käyttö. Eurajoki, Finland, Posiva Oy. Posiva work instruction POS-023606. 22p.

Posiva. 2019. OL-KR6 pumppauskokeen lopetus -powerpoint. Warvi-group meeting 01/2019. Posiva's internal memo. (POS-028205)

Reijonen, H (ed), Ahokas, H., Lamminmäki, T., Partamies, S., Pitkänen, P., Lehtinen, A. & Karvonen, T. 2015. OL-KR6 long-term pumping test - Summary report draft 2013. 130p. Posiva's internal report. (PRJ-008721).

Rämä, T. 2011. Numerical modeling of the hydrogeological effects of ONKALOin 2009. Posiva Oy, Eurajoki, Finland. Posiva working report 2011-30. 32p.

Salonen, V-P., Eronen, M. & Saarnisto, M. 2002. Käytännön maaperägeologia. Turku: Kirja-Aurora. 237 p. ISBN 951-29-2247-9.

STUK. 1987. Nuclear Energy Act 11.12.1987/990. available from: https://www.stuklex.fi/en/ls/19870990, referenced on 25.9.2019.

Vaittinen, T., Ahokas, H., Nummela, J. & Paulamäki, P. Hydrogeological structure model of the Olkiluoto site - update in 2010. 2011. Posiva Oy, Eurajoki, Finland. Working report 2011-65. 330p.

Vaittinen, T., Ahokas, H., Nummela, J., Pentti, E., & Paulamäki, S. 2017. Hydrogeological structure model of the Olkiluoto site in 2015. - in preparation. Posiva report 20xx-xx, Posiva Oy, Eurajoki, Finland. xx p (PRJ-007352)

Vaittinen, T., Hurmerinta, E., Komulainen, J., Nummela, J., Pentti, E., Tammisto, E., Turku, E. & Karvonen, T. 2018. Results of Monitoring at Olkiluoto in 2017, Hydrology and Hydrogeology. Posiva Oy, Eurajoki, Finland. Working report 2018-43. 712p.

Vaittinen, T., Hurmerinta, E., Nummela, J., Pentti, E., Tammisto, E., Turku, J. & Karvonen, T. 2019. Results of Monitoring at Olkiluoto in 2018 - Hydrology and Hydrogeology. Posiva Oy, Eurajoki, Finland. Working report 2019-43. 642 p.

Van Camp., M. & Vauterin., P. 2005. Tsoft: graphical and interactive software for the analysis of time series and Earth tides, Computers & Geosciences, Volume 31, Issue 5, 2005, p. 631-640, ISSN 0098-3004. available from: https://doi.org/10.1016/j.cageo.2004.11.015 (http://www.sciencedirect.com/science/article/pii/S0098300404002456)

Voipio, S., Tammisto, E., Lehtimäki, T. & Ahokas, H. 2004. Summary of long-term hydrological monitoring at the Olkiluoto site. Posiva Oy, Eurajoki, Finland. Working report 2003-42. 188p.

Vuorio, M., Lamminmäki, T., Pitkänen, P., Penttinen, T., Komulainen, J., Loimula, K., Wendling, L., Partamies, S. & Ahokas, T. 2018. Results of Monitoring at Olkiluoto in 2016 Hydrogeochemistry. Posiva Oy, Eurajoki, Finland. Working report 2017-44. 400p.

Öhberg, A. 2006. Investigation equipment and methods used by Posiva Oy. Posiva Oy, Eurajoki, Finland. Working report 2006-81. 115 p.

http://www.gtk.fi/geologia/luonnonvarat/pohjavesi/, referenced on 12.1.2019

https://kartta.paikkatietoikkuna.fi/?lang=fi, referenced on 20.11.2019

APPENDICES

Appendix 1. Hydrogeochemical results of the long-term pumping test on OL-KR6.

Tables Saline

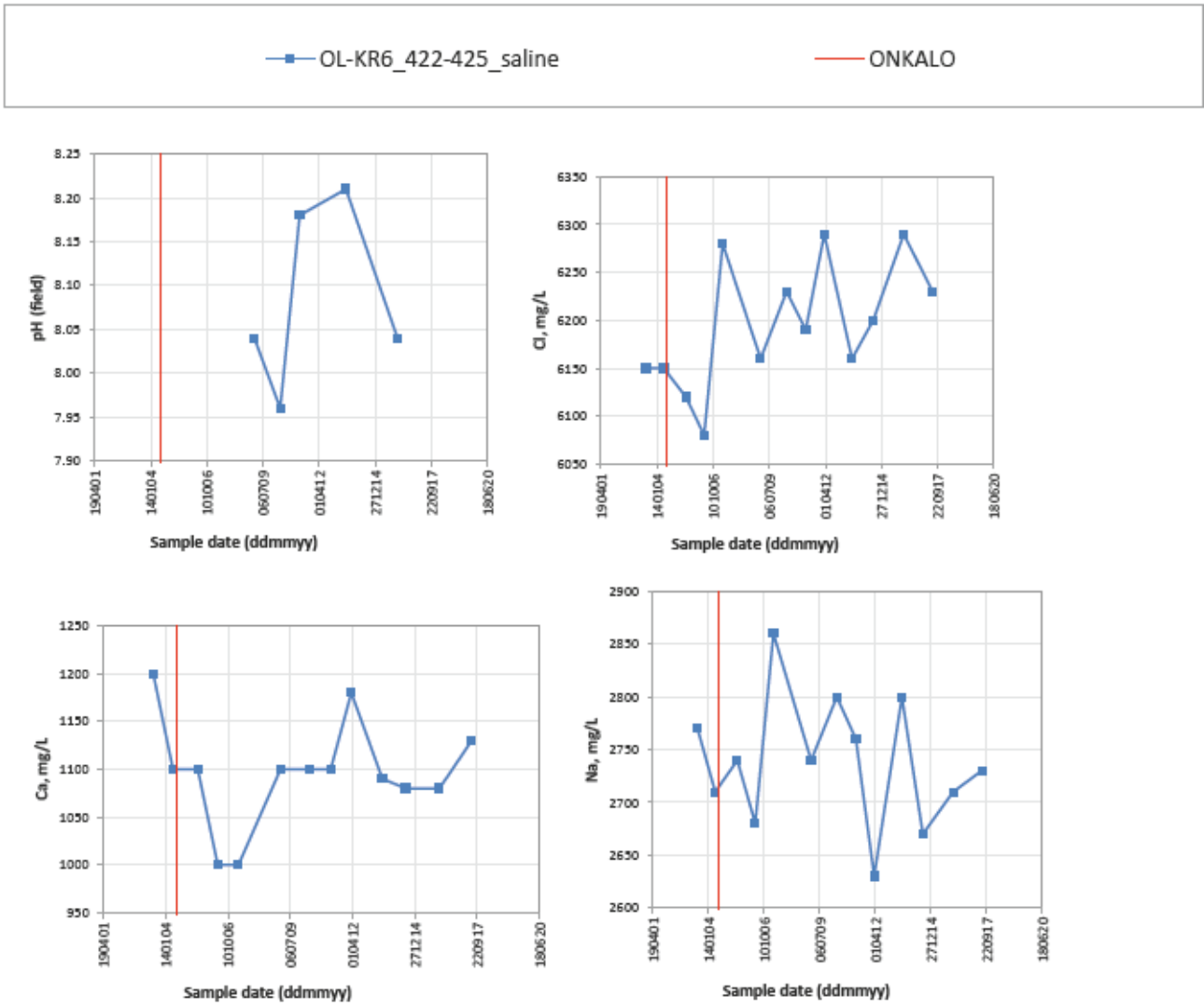

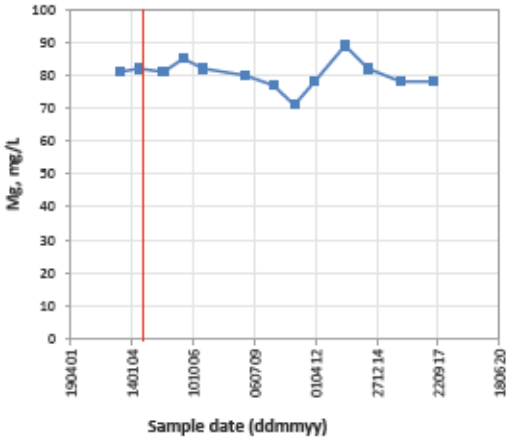
Mg, mg/L
Sample date (ddmmyy)
190401
140104
101006
060709
010412
271214
220917
180620

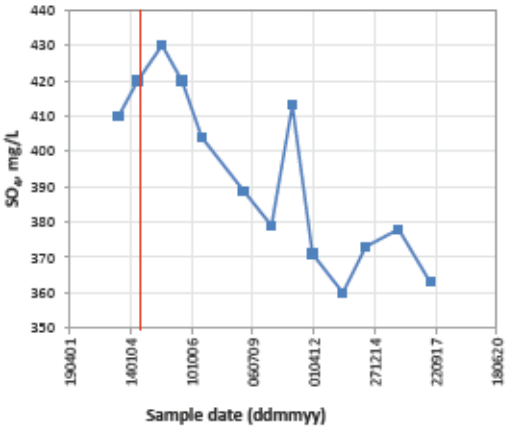
SO_4, mg/L
Sample date (ddmmyy)
190401
140104
101006
060709
010412
271214
220917
180620

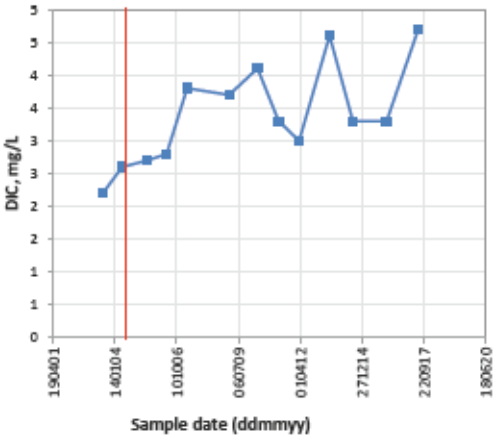
DIC, mg/L
Sample date (ddmmyy)
190401
140104
101006
060709
010412
271214
220917
180620

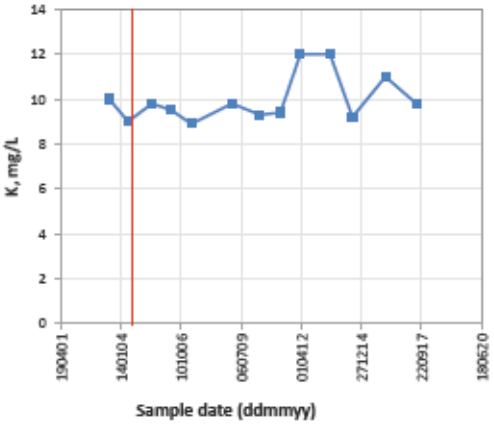
K, mg/L
Sample date (ddmmyy)
190401
140104
101006
060709
010412
271214
220917
180620

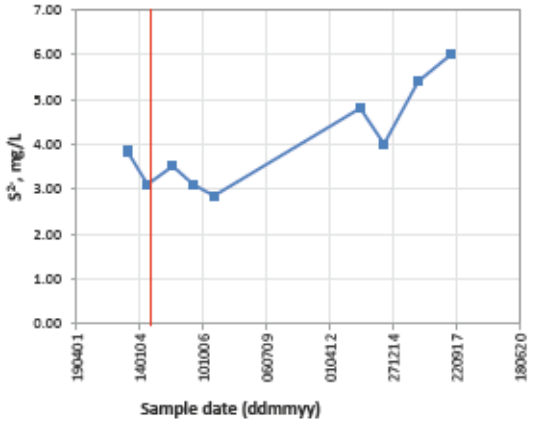
S^{2-}, mg/L
Sample date (ddmmyy)
190401
140104
101006
060709
010412
271214
220917
180620

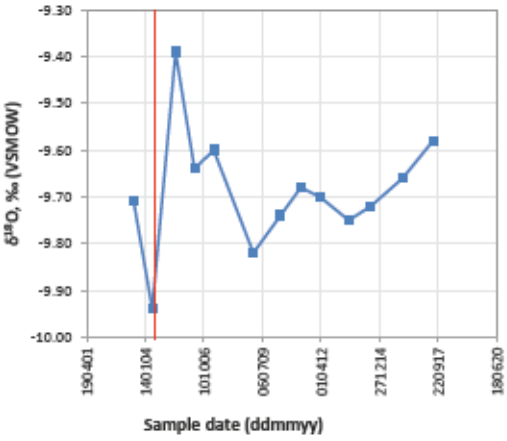
$\delta^{18}O$, ‰ (VSMOW)
Sample date (ddmmyy)
190401
140104
101006
060709
010412
271214
220917
180620

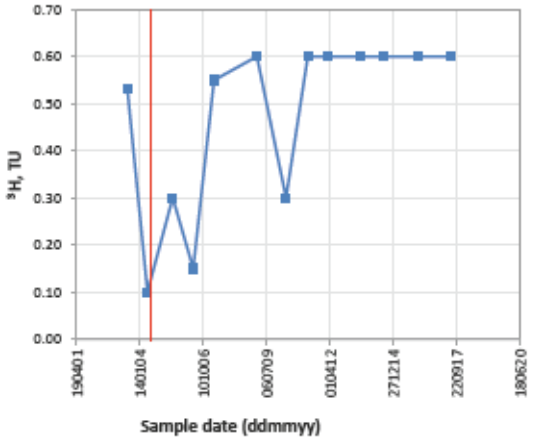

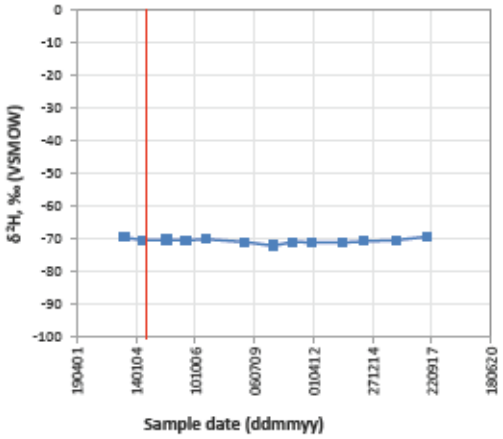

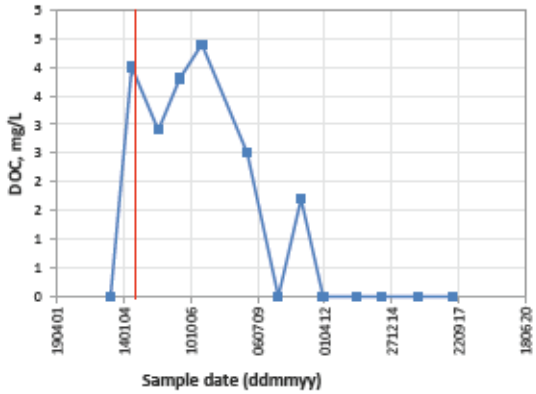

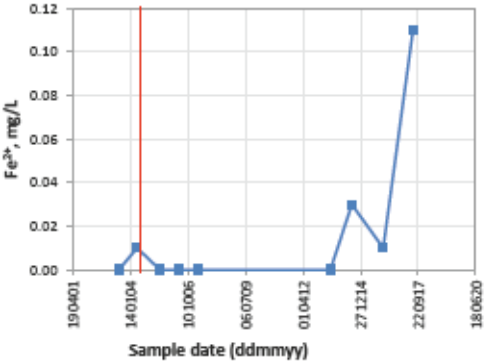

Tables brackish SO4 & Cl

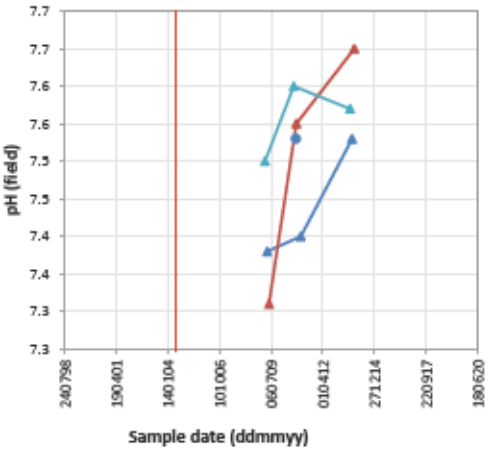

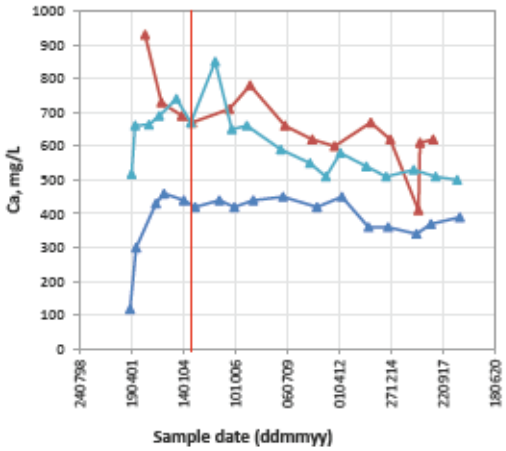

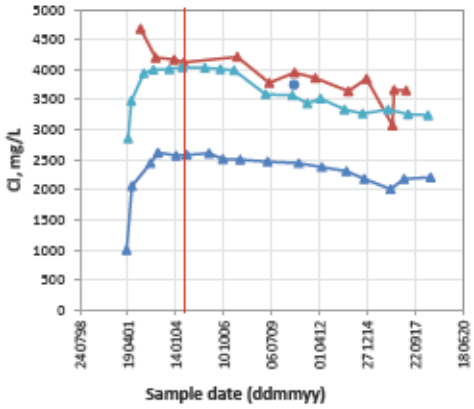
Cl, mg/L
5000
4500
4000
3500
3000
2500
2000
1500
1000
500
0
240798
190401
140104
101006
060709
010412
271214
220917
180620
Sample date (ddmmyy)

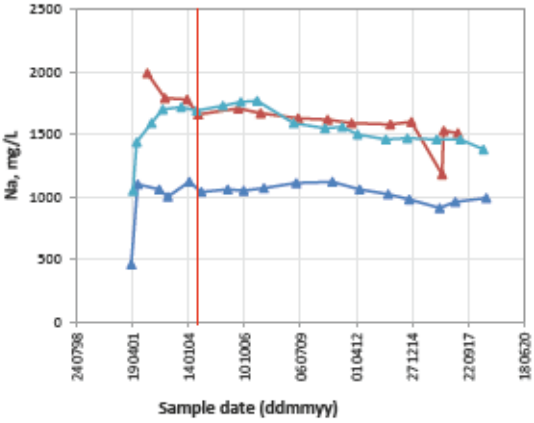
Na, mg/L
2500
2000
1500
1000
500
0
240798
190401
140104
101006
060709
010412
271214
220917
180620
Sample date (ddmmyy)

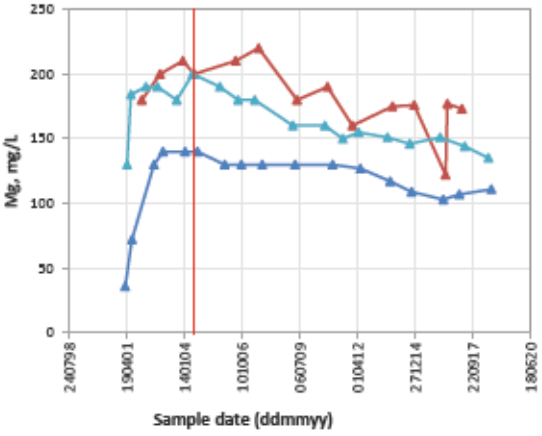
Mg, mg/L
250
200
150
100
50
0
240798
190401
140104
101006
060709
010412
271214
220917
180620
Sample date (ddmmyy)

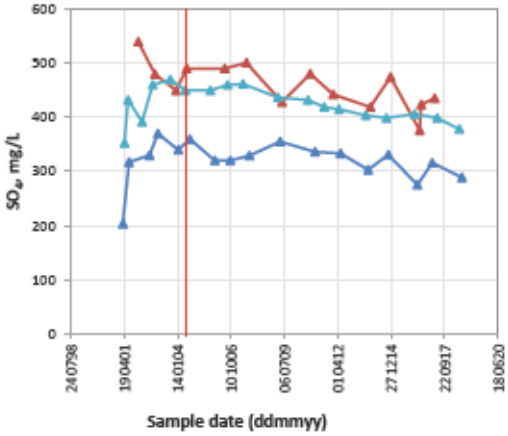
SO4, mg/L
600
500
400
300
200
100
0
240798
190401
140104
101006
060709
010412
271214
220917
180620
Sample date (ddmmyy)

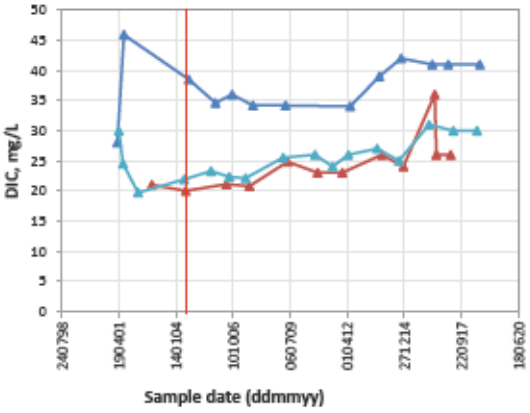
DIC, mg/L
50
45
40
35
30
25
20
15
10
5
0
240798
190401
140104
101006
060709
010412
271214
220917
180620
Sample date (ddmmyy)

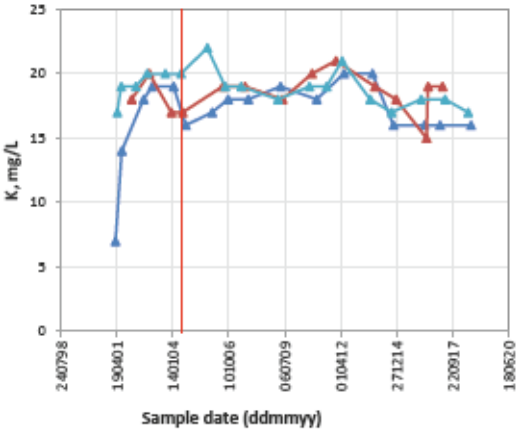
K, mg/L
25
20
15
10
5
0
240798
190401
140104
101006
060709
010412
271214
220917
180620
Sample date (ddmmyy)

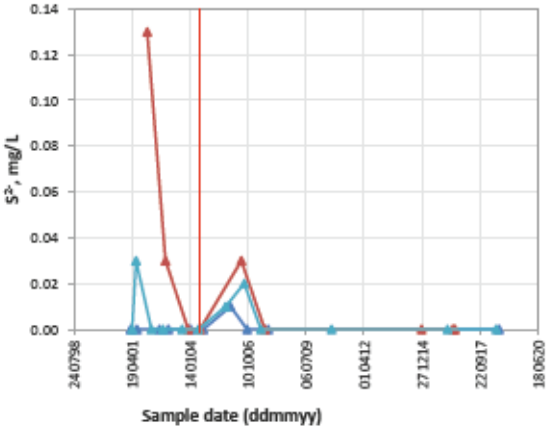
S2-, mg/L
0.14
0.12
0.10
0.08
0.06
0.04
0.02
0.00
240798
190401
140104
101006
060709
010412
271214
220917
180620
Sample date (ddmmyy)

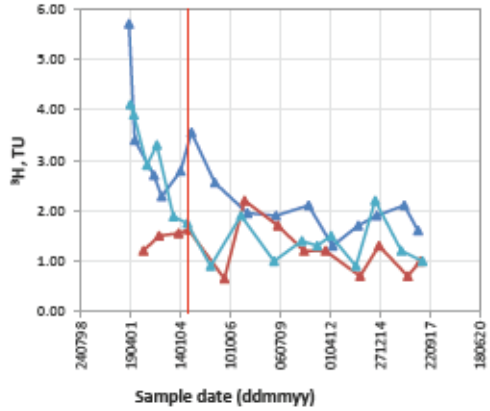
3H, TU
6.00
5.00
4.00
3.00
2.00
1.00
0.00
240798
190401
140104
101006
060709
010412
271214
220917
180620
Sample date (ddmmyy)

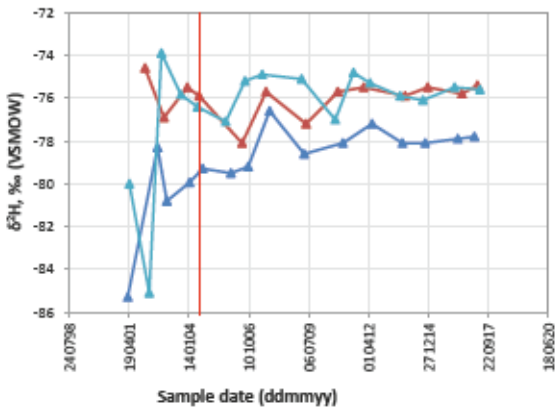

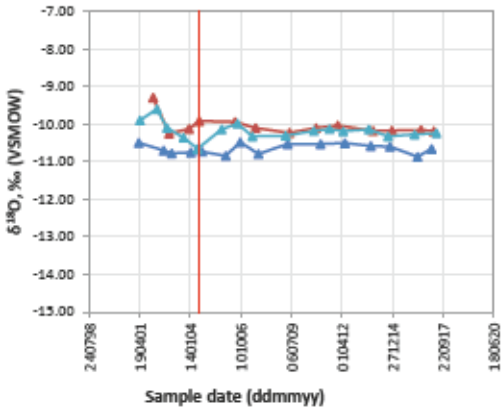

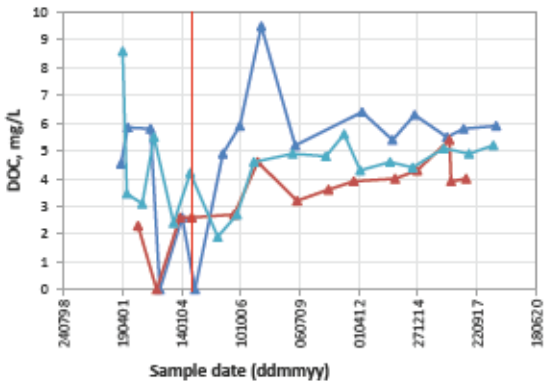

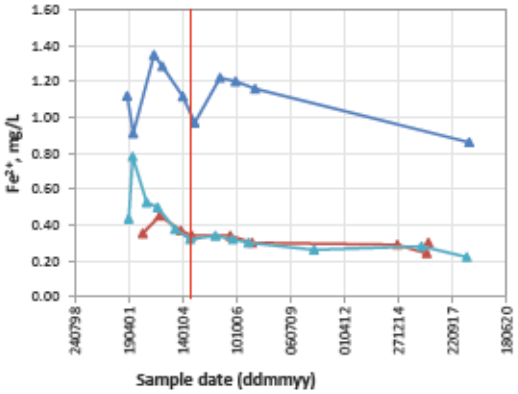

Tables freshBrackish HCO3

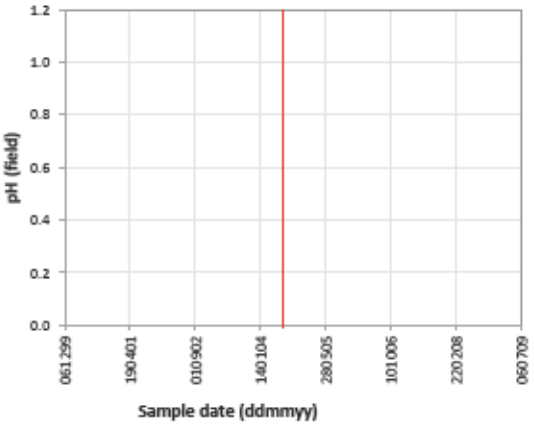

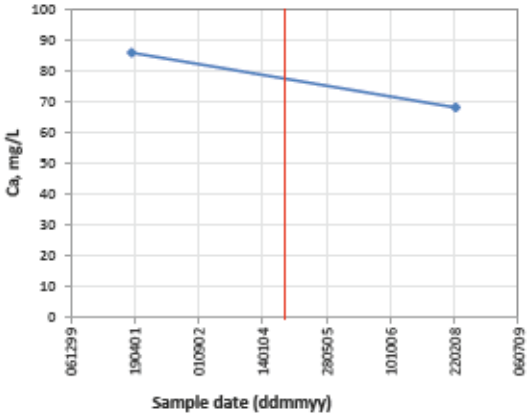

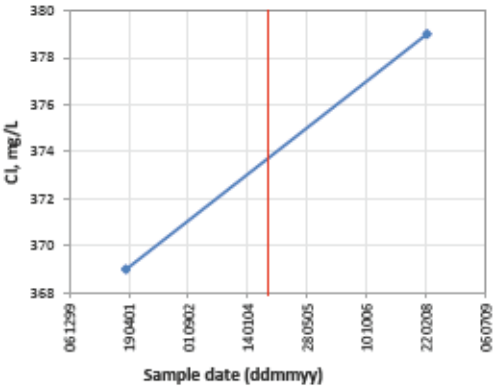
Cl, mg/L
380
378
376
374
372
370
368
061299
190401
010902
140104
280505
101006
220208
060709
Sample date (ddmmyy)

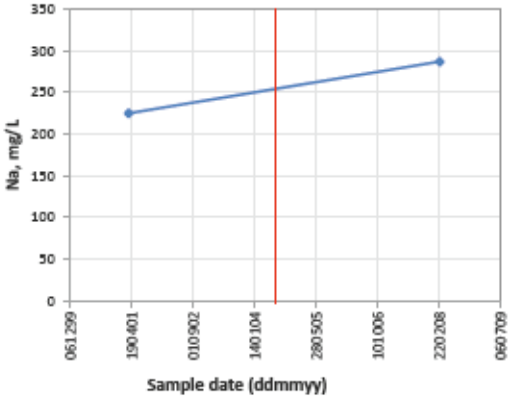
Na, mg/L
350
300
250
200
150
100
50
0
061299
190401
010902
140104
280505
101006
220208
060709
Sample date (ddmmyy)

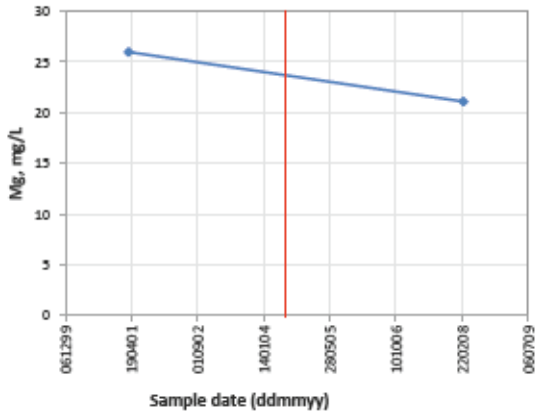
Mg, mg/L
30
25
20
15
10
5
0
061299
190401
010902
140104
280505
101006
220208
060709
Sample date (ddmmyy)

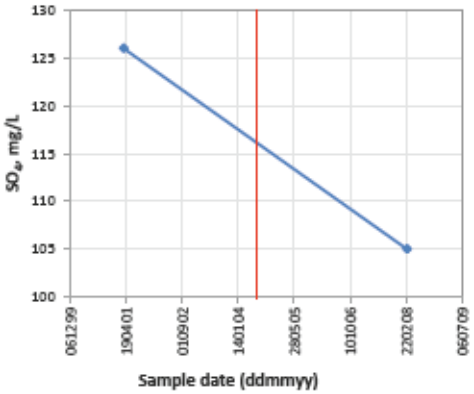
SO4, mg/L
130
125
120
115
110
105
100
061299
190401
010902
140104
280505
101006
220208
060709
Sample date (ddmmyy)

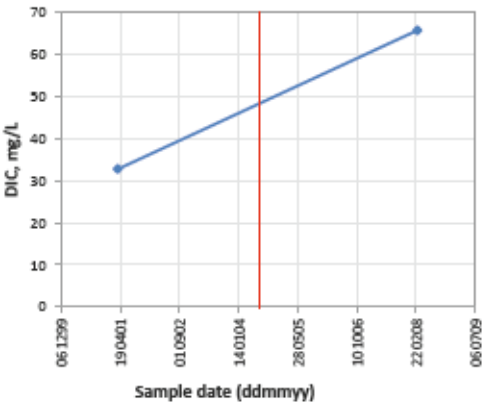
DIC, mg/L
70
60
50
40
30
20
10
0
061299
190401
010902
140104
280505
101006
220208
060709
Sample date (ddmmyy)

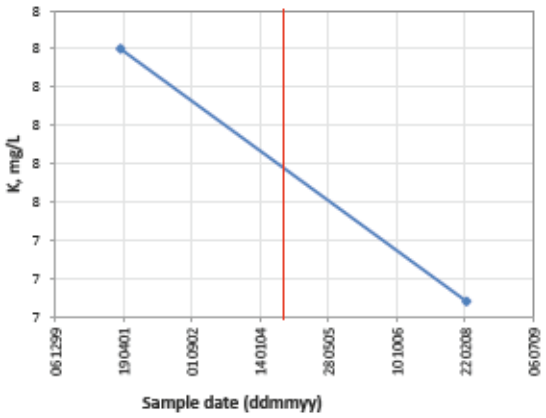
K, mg/L
061299
190401
010902
140104
280505
101006
220208
060709
Sample date (ddmmyy)

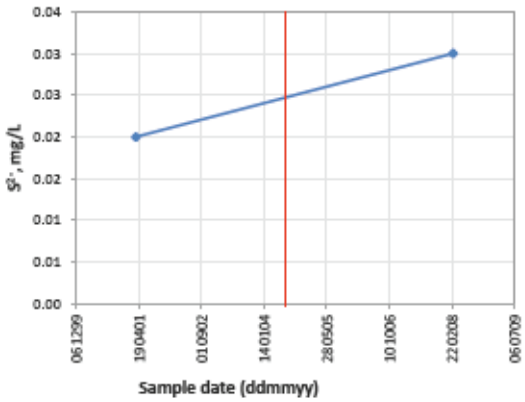
S2-, mg/L
0.04
0.03
0.03
0.02
0.02
0.01
0.01
0.00
061299
190401
010902
140104
280505
101006
220208
060709
Sample date (ddmmyy)

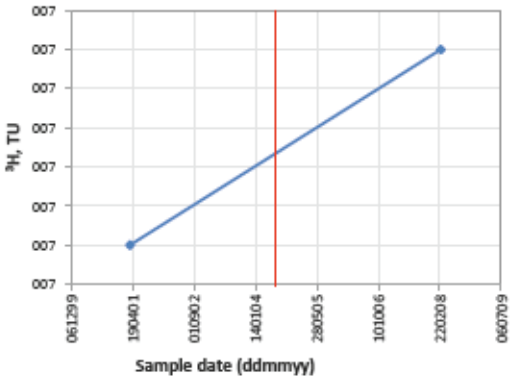
3H, TU
007
007
007
007
007
007
007
061299
190401
010902
140104
280505
101006
220208
060709
Sample date (ddmmyy)

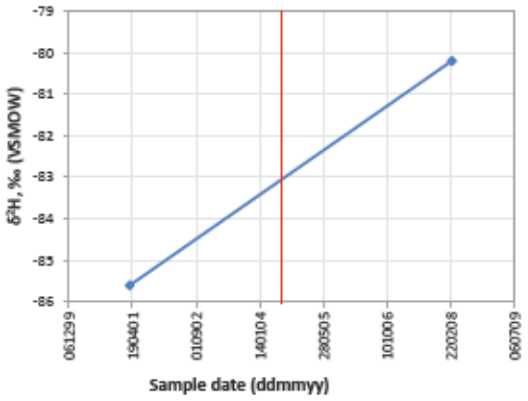
δ²H, ‰ (VSMOW)
-79
-80
-81
-82
-83
-84
-85
-86
061299
190401
010902
140104
280505
101006
220208
060709
Sample date (ddmmyy)

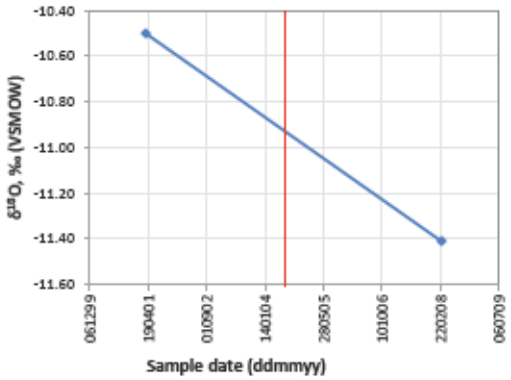
δ¹⁸O, ‰ (VSMOW)
-10.40
-10.60
-10.80
-11.00
-11.20
-11.40
-11.60
061299
190401
010902
140104
280505
101006
220208
060709
Sample date (ddmmyy)

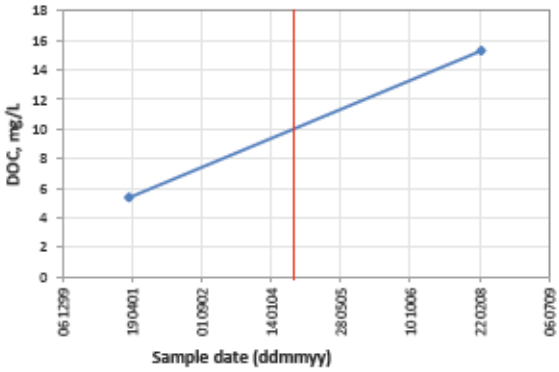
DOC, mg/L
18
16
14
12
10
8
6
4
2
0
061299
190401
010902
140104
280505
101006
220208
060709
Sample date (ddmmyy)

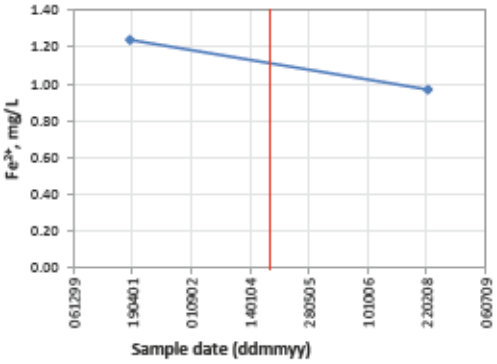
Fe²⁺, mg/L
1.40
1.20
1.00
0.80
0.60
0.40
0.20
0.00
061299
190401
010902
140104
280505
101006
220208
060709
Sample date (ddmmyy)

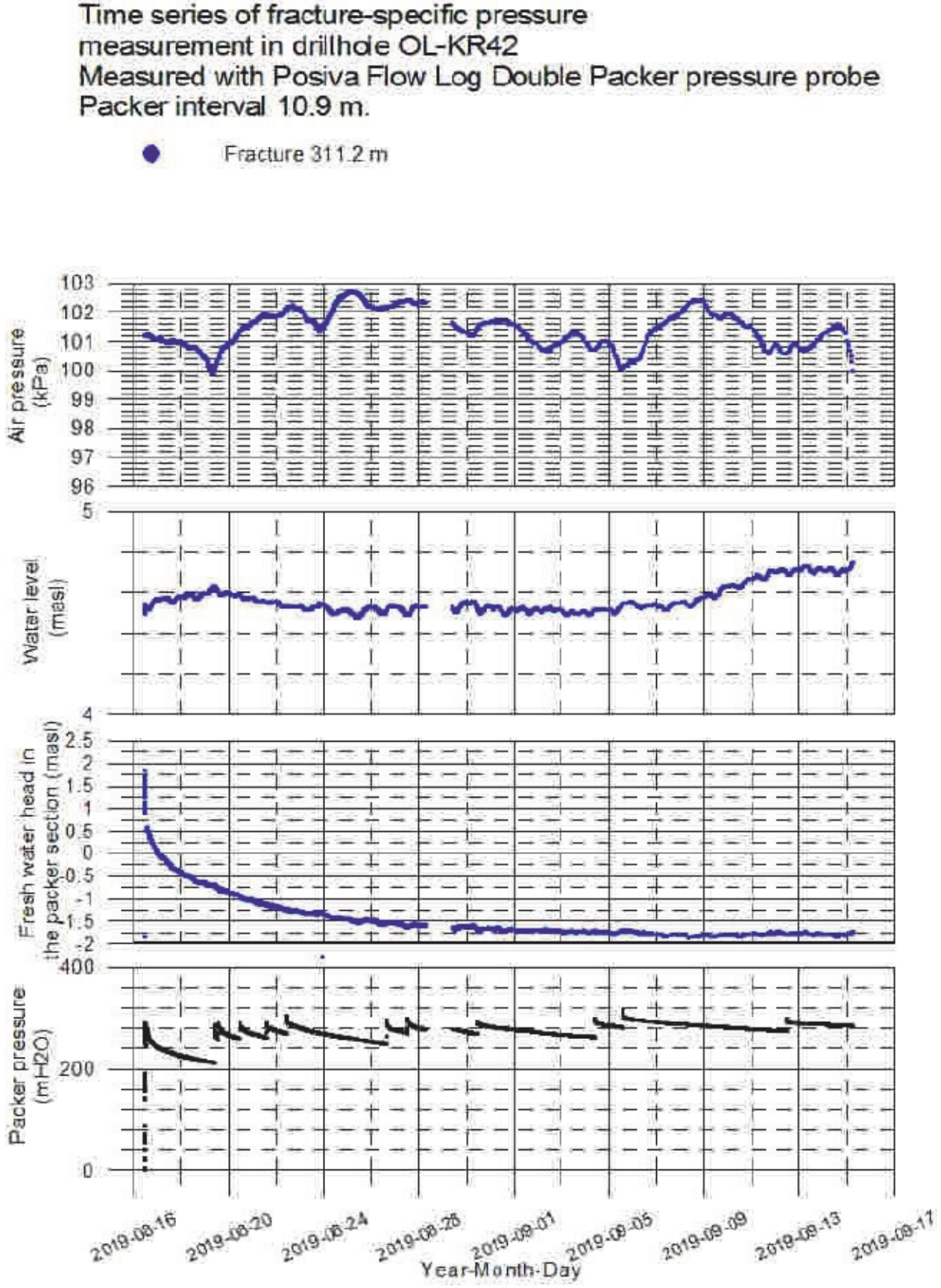
Time series of fracture-specific pressure
measurement in drillhole OL-KR42
Measured with Posiva Flow Log Double Packer pressure probe
Packer interval 10.9 m.
Fracture 311.2 m
Air pressure (kPa)
Water level (masl)
Fresh water head in the packer section (masl)
Packer pressure (mH2O)
2019-08-16
2019-08-20
2019-08-24
2019-08-28
2019-09-01
2019-09-05
2019-09-09
2019-09-13
2019-09-17
Year-Month-Day

Appendix 3. The results of the interference test. Blue line on tables represents hydraulic head (m.a.s.l) in the drillhole at OL-KR6, red line represents hydraulic head in the test section at OL-KR6, and green line represents hydraulic head inside the pump container. The hydraulic head values are presented as m.a.s.l. values.

The first pumping 9.–24.4.

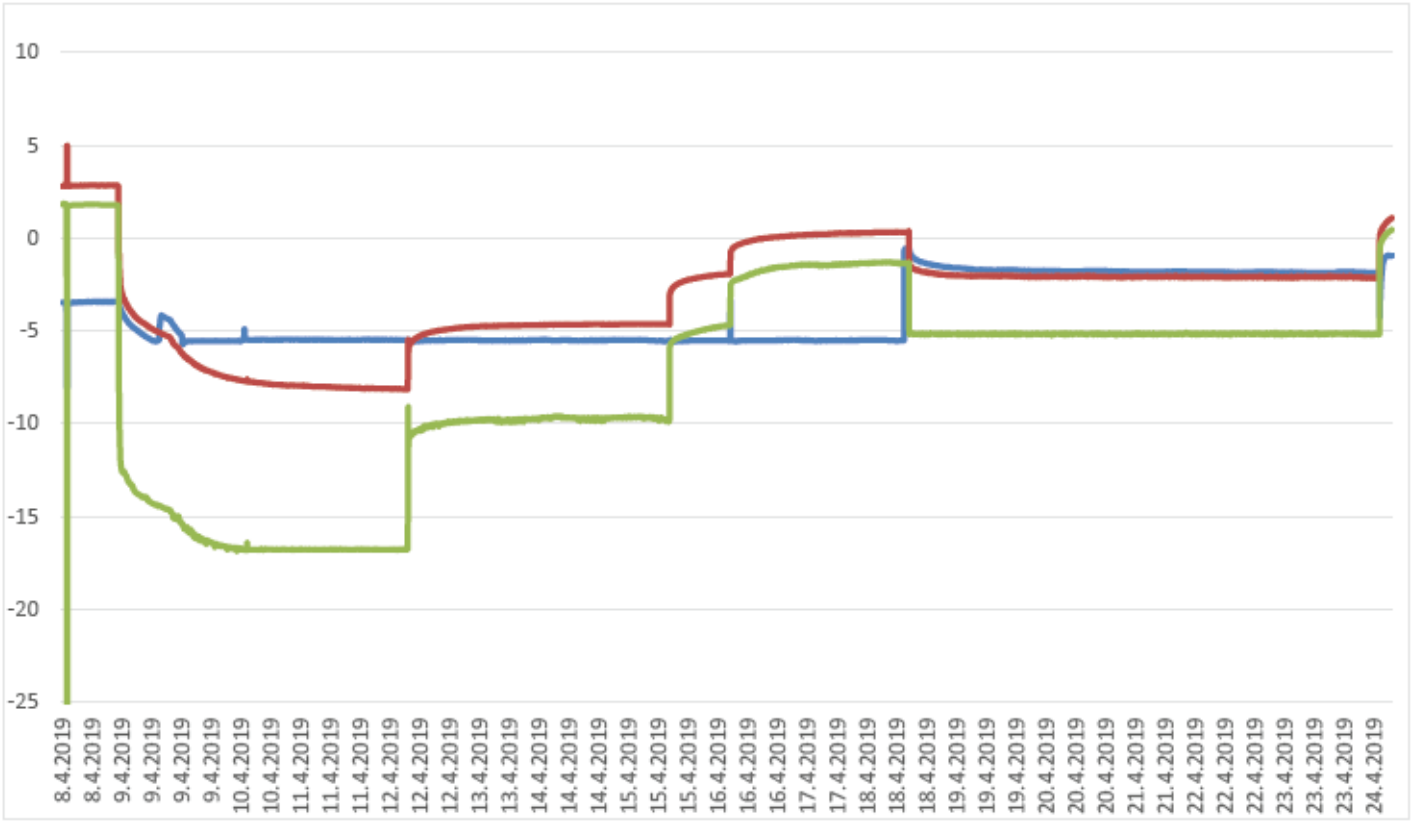

The second pumping 8.–21.5.

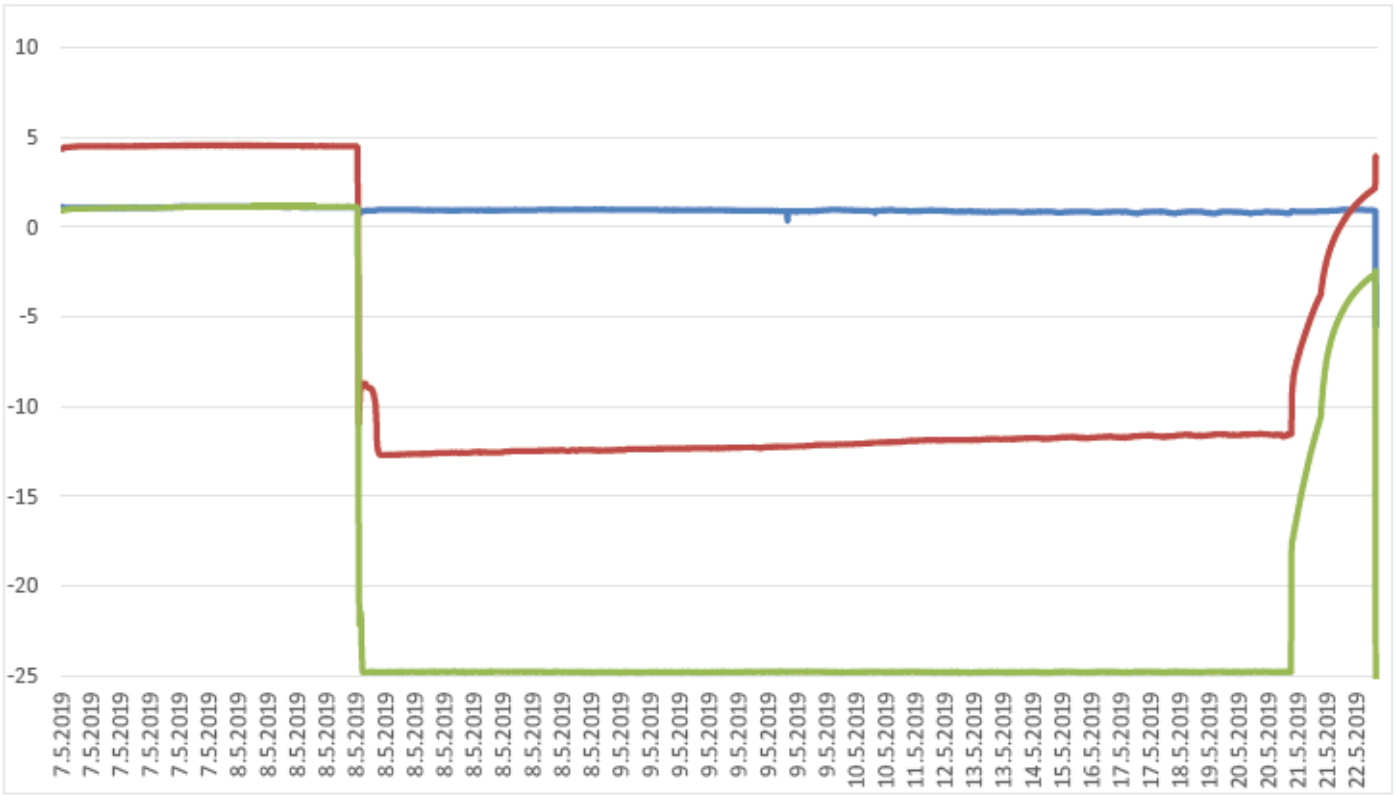

The third pumping 29.5.–20.6.

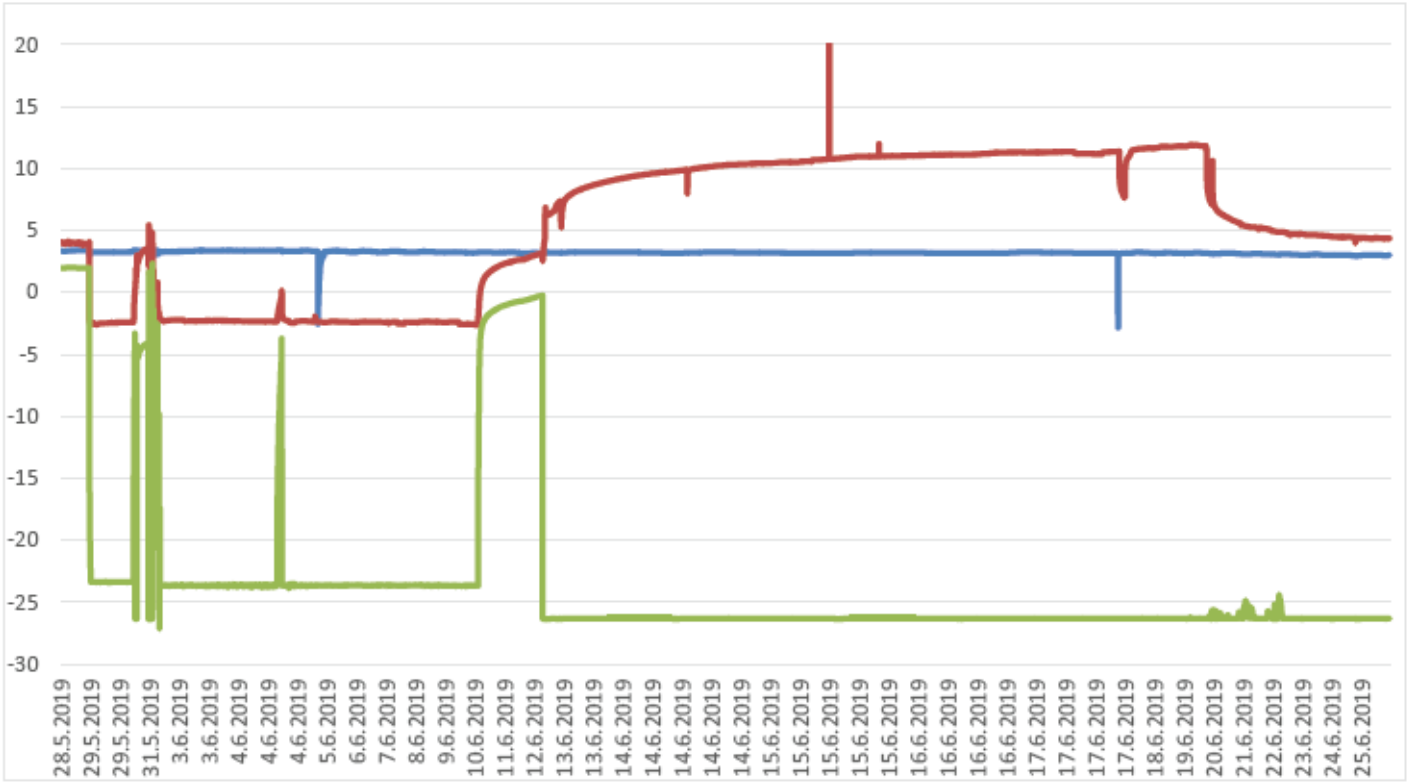

The fourth pumping 10.–23.7. The hydraulic head value (greenline) is incorrect in early stages of pumping due to the fact that the pumping was started during the laying of the pump in the pump container (Section 7.5.4).

The fifth pumping 1.–12.8. The hydraulic head value (greenline) is incorrect in early stages of pumping due to the fact that the pumping was started during the laying of the pump in the pump container (Section 7.5.5).

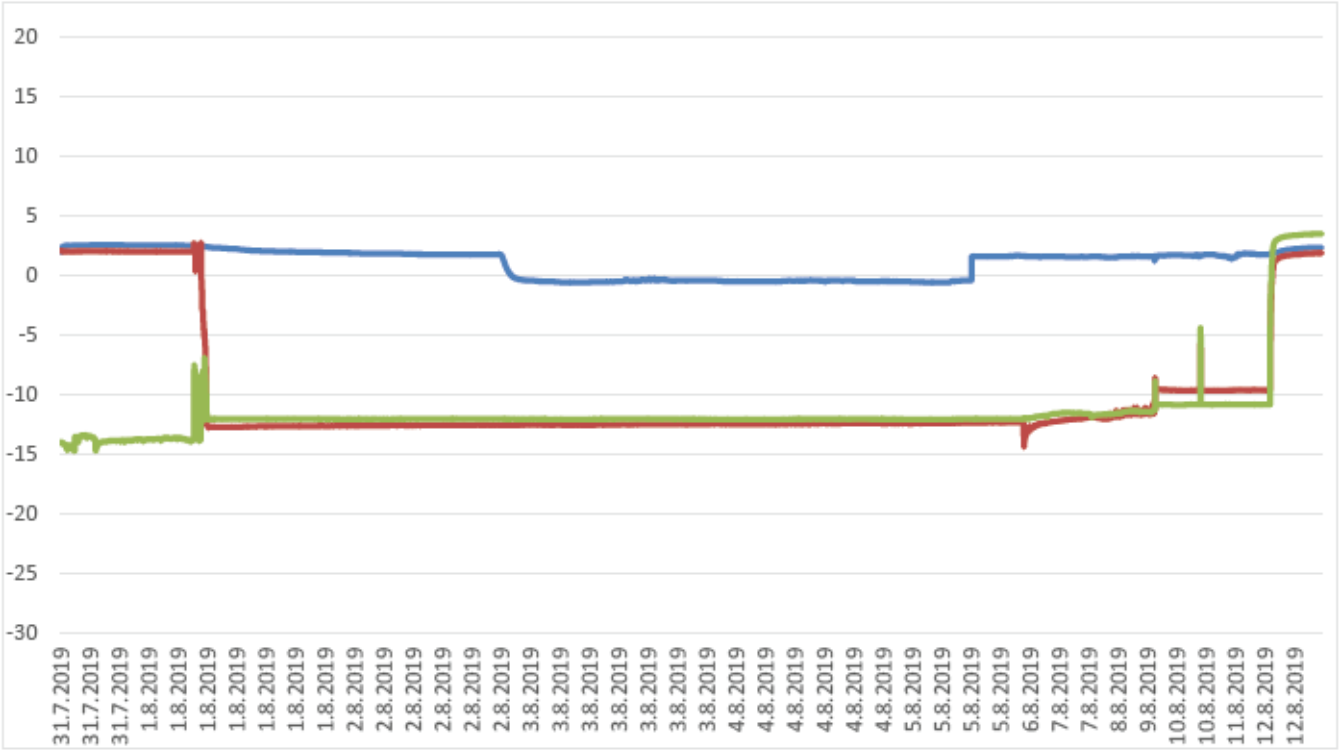

The sixth pumping 19.–29.8. The hydraulic head value (greenline) is incorrect in early stages of pumping due to the fact that the pumping was started during the laying of the pump in the pump container (Section 7.5.7).

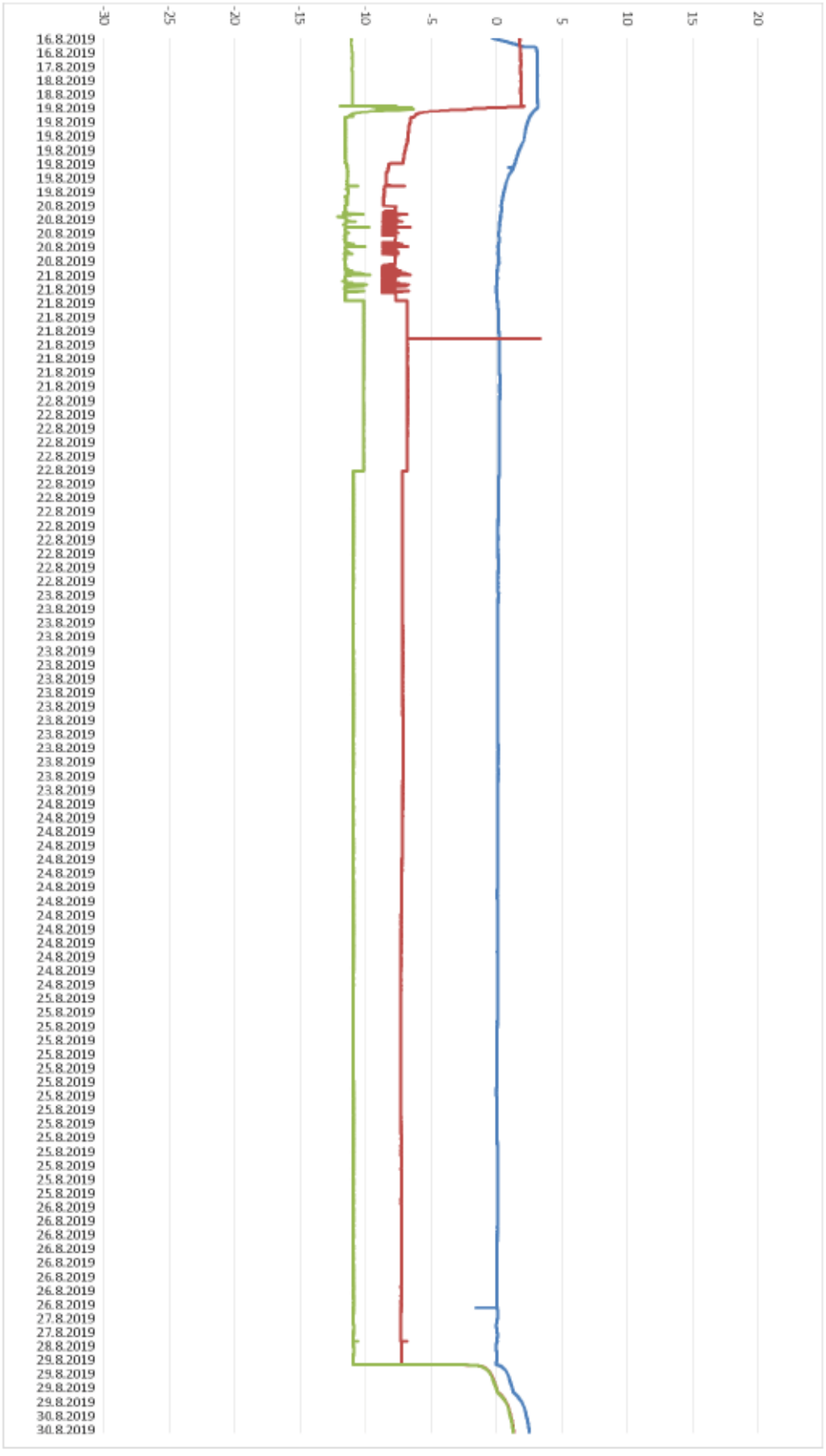

Appendix 4. GWMS-data from the drillholes which were under close monitoring during an interference test. It should be noticed that the pumping times are inserted to pictures by hands, for this reason they should consider as approximate. They are in the figures for ease the understanding.

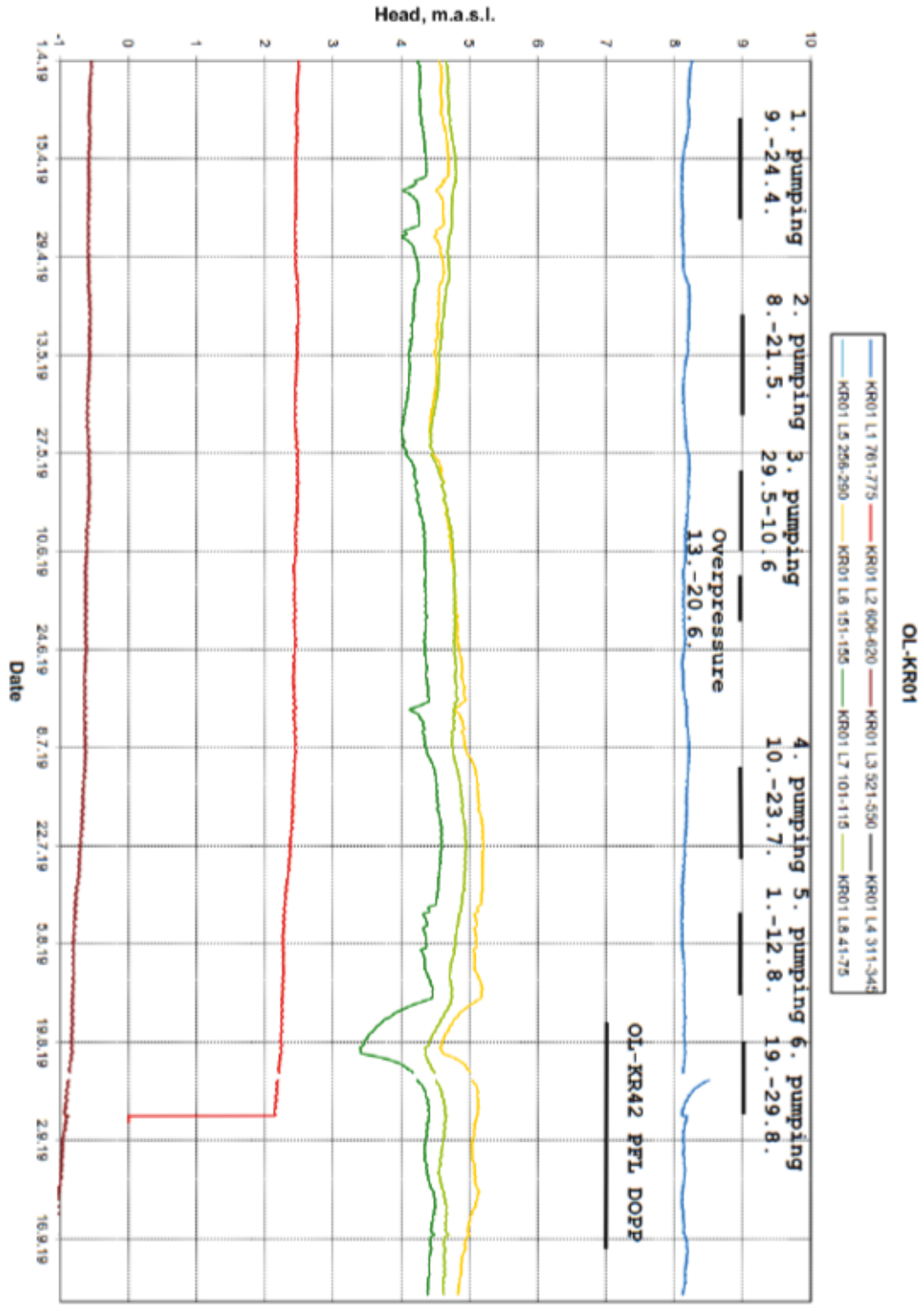

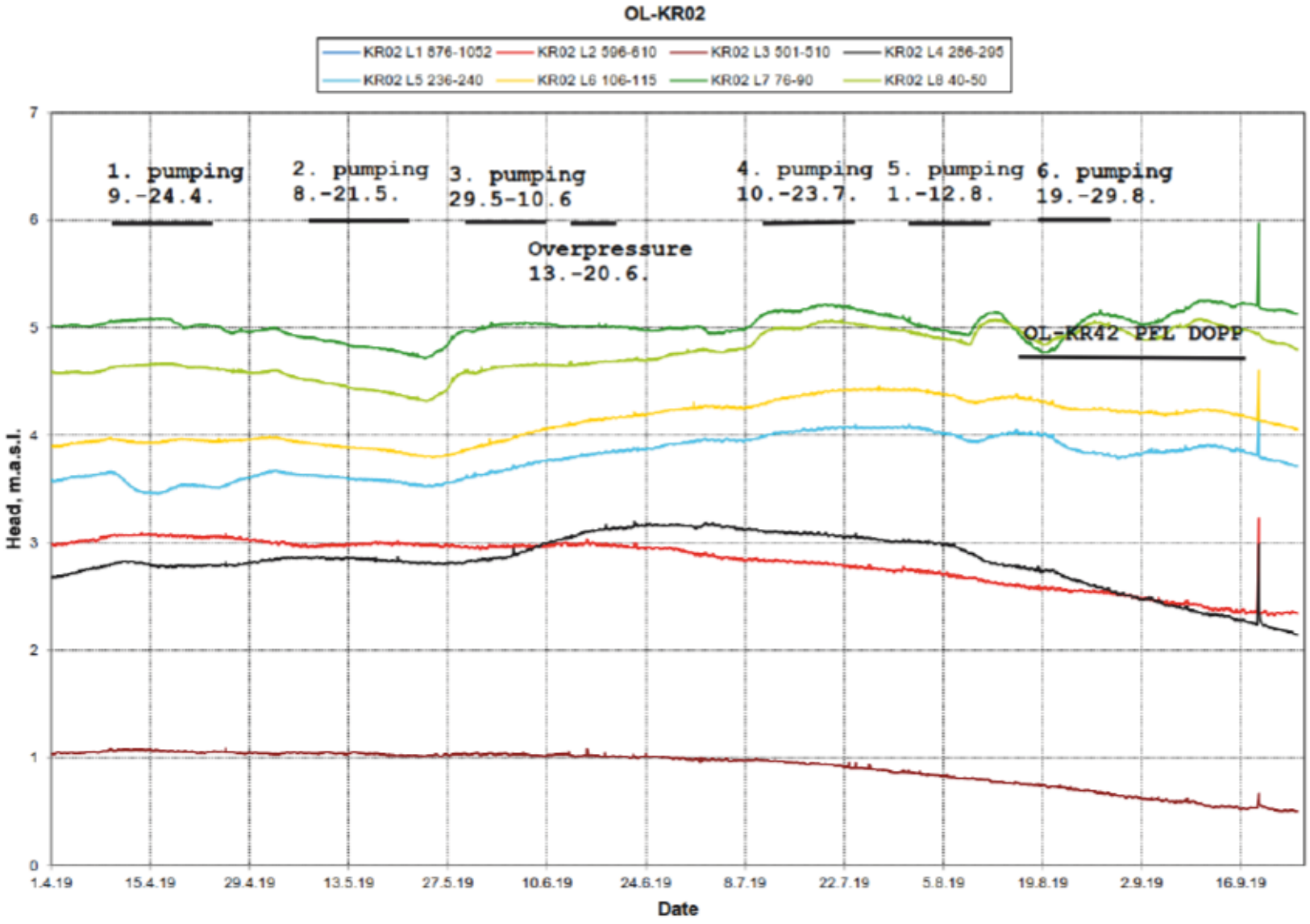
OL-KR02
KR02 L1 876-1052
KR02 L2 596-610
KR02 L3 501-510
KR02 L4 286-295
KR02 L5 236-240
KR02 L6 106-115
KR02 L7 76-90
KR02 L8 40-50
1. pumping 9.-24.4.
2. pumping 8.-21.5.
3. pumping 29.5-10.6
Overpressure 13.-20.6.
4. pumping 10.-23.7.
5. pumping 1.-12.8.
6. pumping 19.-29.8.
OL-KR42 PFL DOPP
Head, m.a.s.l.
Date
1.4.19
15.4.19
29.4.19
13.5.19
27.5.19
10.6.19
24.6.19
8.7.19
22.7.19
5.8.19
19.8.19
2.9.19
16.9.19

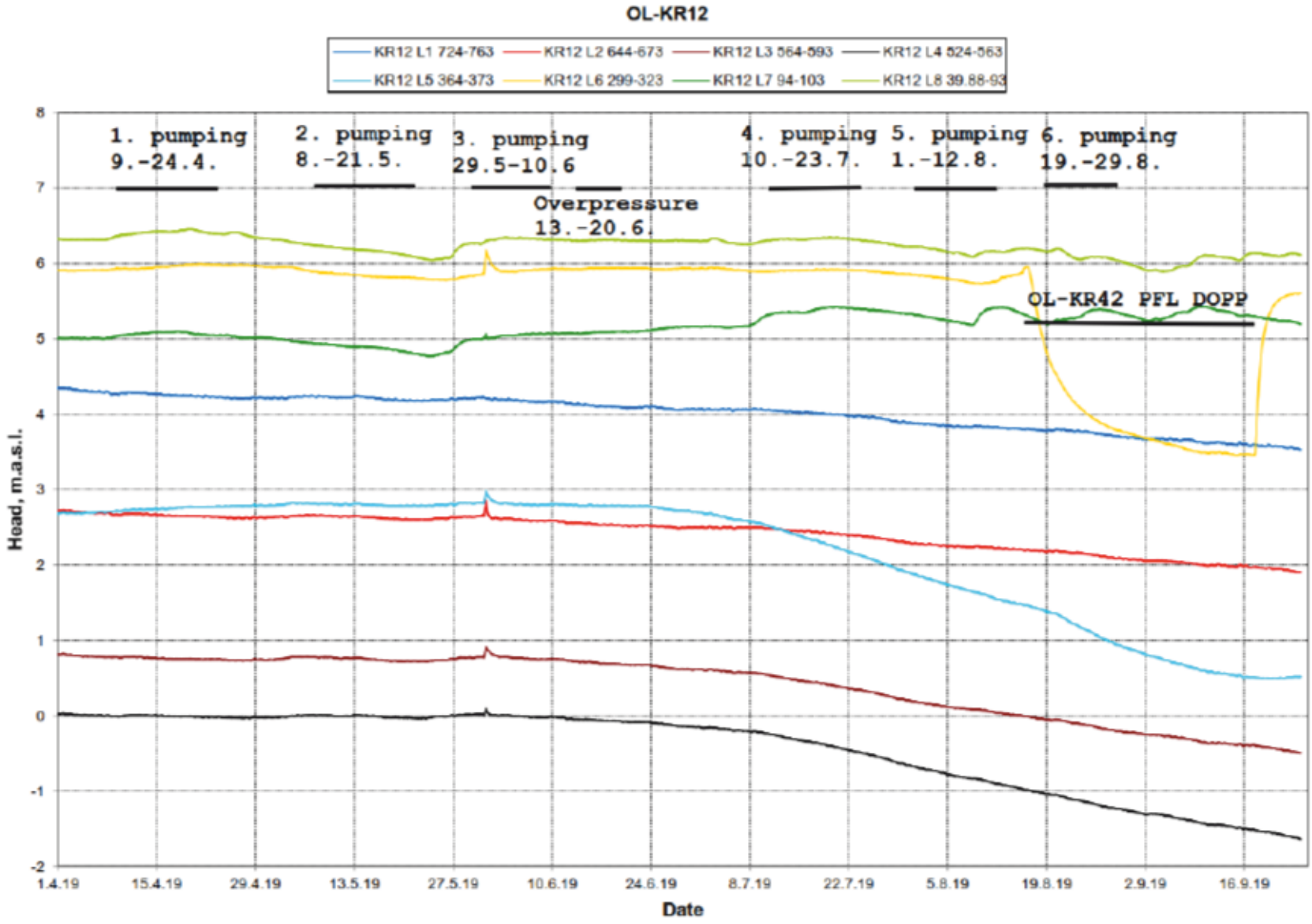
OL-KR12
KR12 L1 724-763
KR12 L2 644-673
KR12 L3 564-593
KR12 L4 524-563
KR12 L5 364-373
KR12 L6 299-323
KR12 L7 94-103
KR12 L8 39.88-93
1. pumping 9.-24.4.
2. pumping 8.-21.5.
3. pumping 29.5-10.6
4. pumping 10.-23.7.
5. pumping 1.-12.8.
6. pumping 19.-29.8.
Overpressure 13.-20.6.
OL-KR42 PFL DOPP
Head, m.a.s.l.
Date
1.4.19
15.4.19
29.4.19
13.5.19
27.5.19
10.6.19
24.6.19
8.7.19
22.7.19
5.8.19
19.8.19
2.9.19
16.9.19

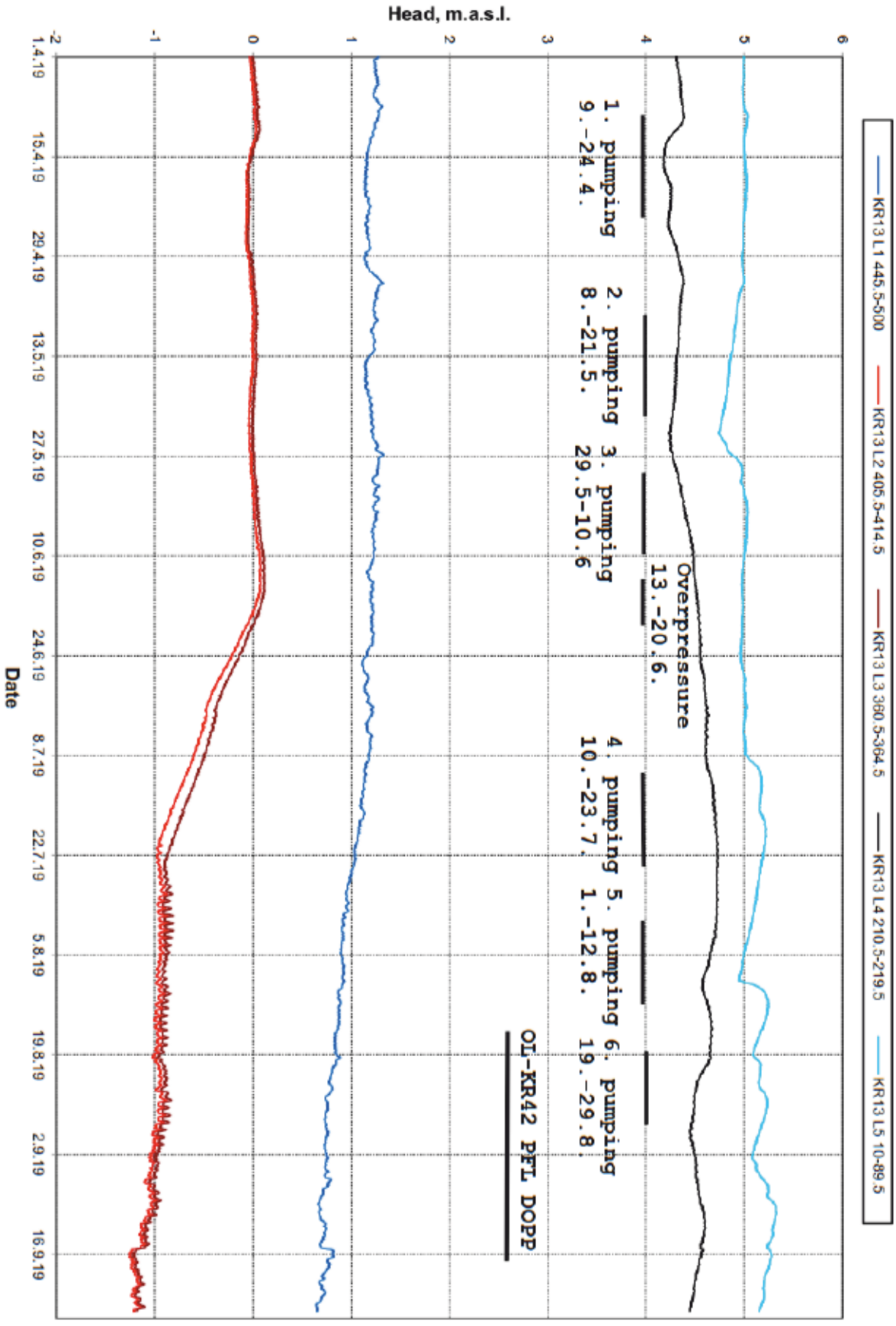
OL-KR13
KR13 L1 445.5-500
KR13 L2 405.5-414.5
KR13 L3 360.5-364.5
KR13 L4 210.5-219.5
KR13 L5 10-89.5
Head, m.a.s.l.
Date
Overpressure
13.-20.6.
1. pumping
9.-24.4.
2. pumping
8.-21.5.
3. pumping
29.5-10.6
4. pumping
10.-23.7.
5. pumping
1.-12.8.
6. pumping
19.-29.8.
OL-KR42 PFL DOPP

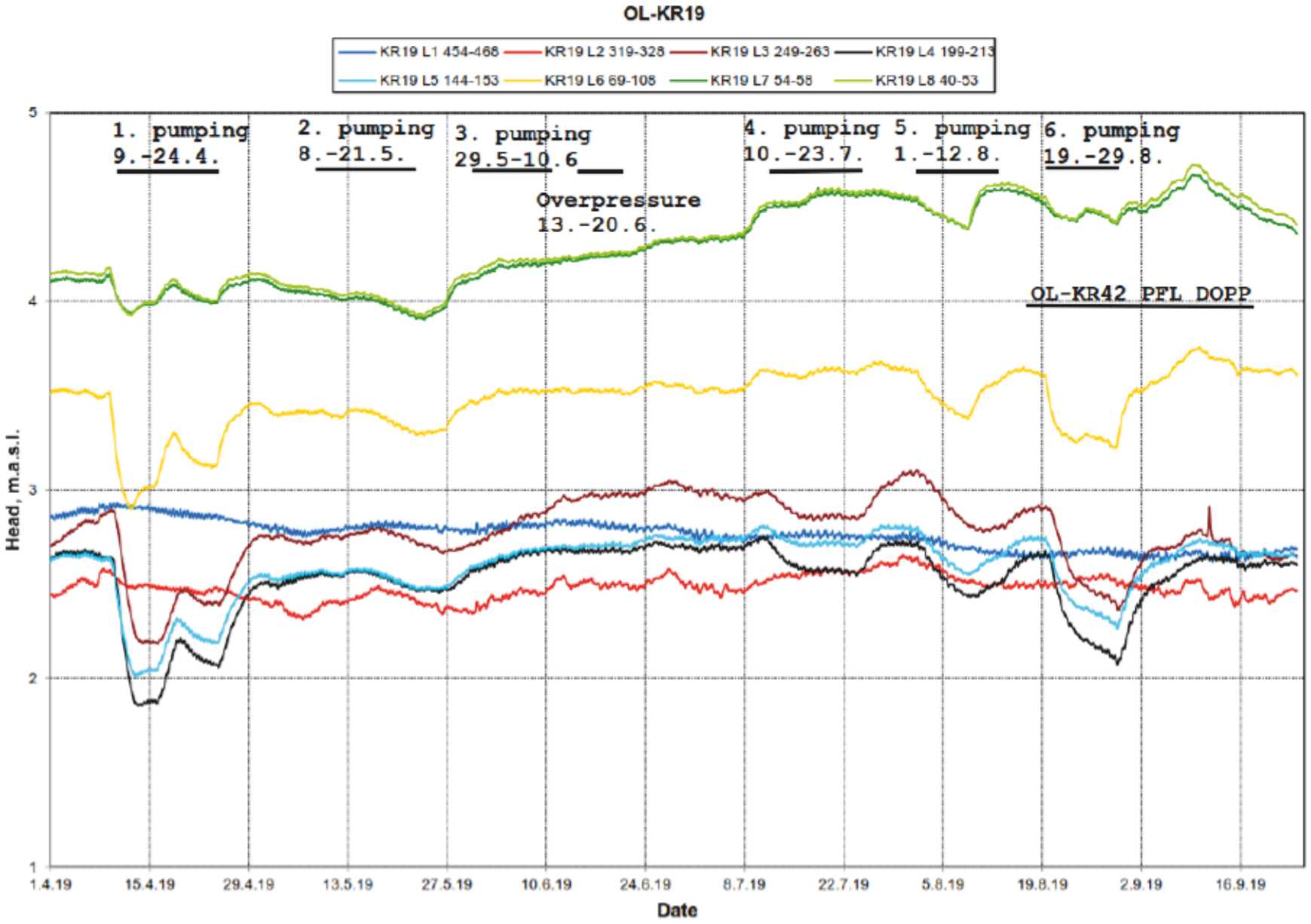
OL-KR19
KR19 L1 454-468
KR19 L2 319-328
KR19 L3 249-263
KR19 L4 199-213
KR19 L5 144-153
KR19 L6 69-108
KR19 L7 54-58
KR19 L8 40-53
1. pumping 9.-24.4.
2. pumping 8.-21.5.
3. pumping 29.5-10.6
Overpressure 13.-20.6.
4. pumping 10.-23.7.
5. pumping 1.-12.8.
6. pumping 19.-29.8.
OL-KR42 PFL DOPP
Head, m.a.s.l.
5
4
3
2
1
1.4.19
15.4.19
29.4.19
13.5.19
27.5.19
10.6.19
24.6.19
8.7.19
22.7.19
5.8.19
19.8.19
2.9.19
16.9.19
Date

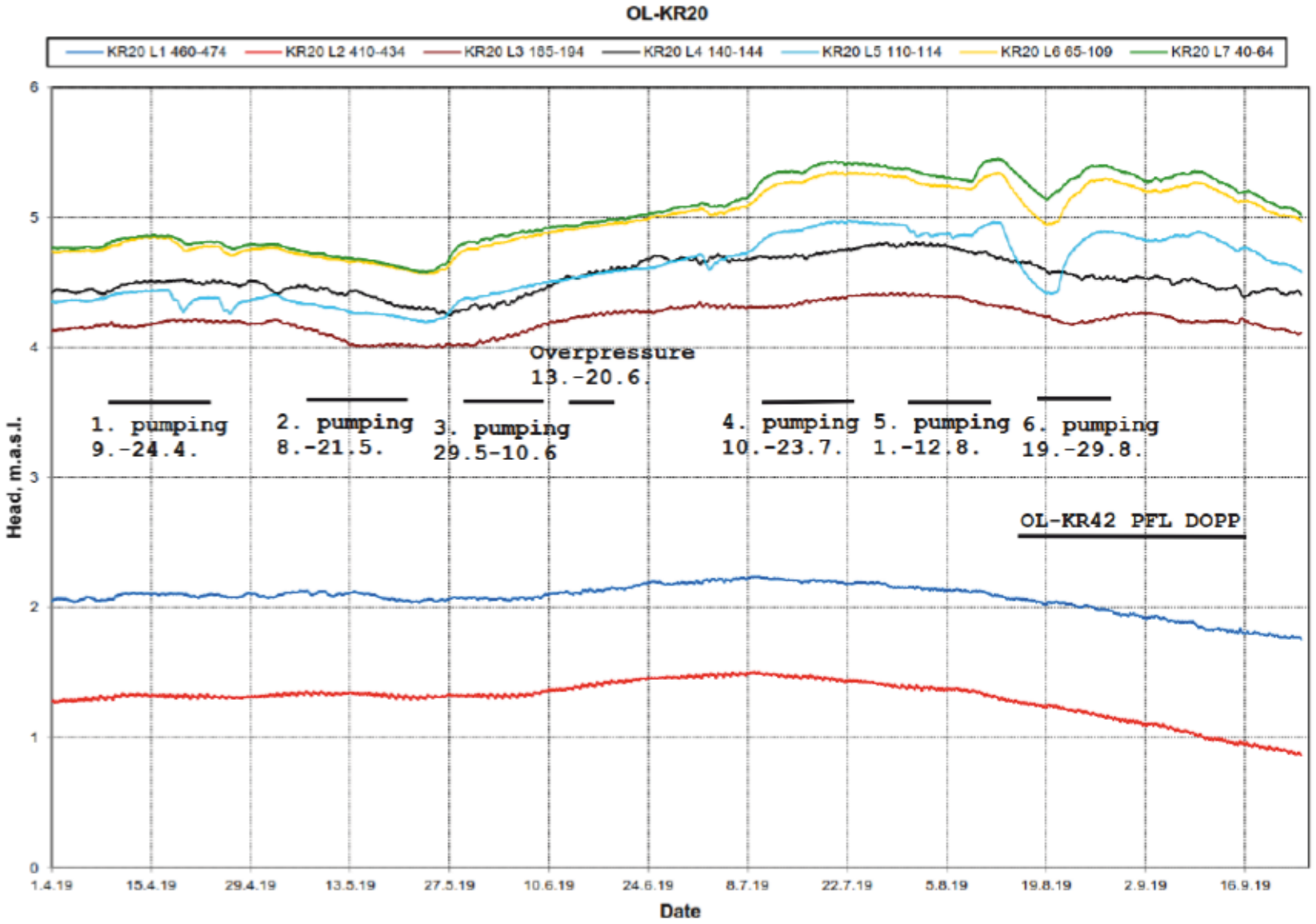
OL-KR20
KR20 L1 460-474
KR20 L2 410-434
KR20 L3 185-194
KR20 L4 140-144
KR20 L5 110-114
KR20 L6 65-109
KR20 L7 40-64
Head, m.a.s.l.
Date
1.4.19
15.4.19
29.4.19
13.5.19
27.5.19
10.6.19
24.6.19
8.7.19
22.7.19
5.8.19
19.8.19
2.9.19
16.9.19
Overpressure
13.-20.6.
1. pumping
9.-24.4.
2. pumping
8.-21.5.
3. pumping
29.5-10.6
4. pumping
10.-23.7.
5. pumping
1.-12.8.
6. pumping
19.-29.8.
OL-KR42 PFL DOPP